

1-1-2014

Thermal And Cooling Systems Modeling Of Powertrain For A Plug -In Parallel-Through-The-Road Hybrid Electric Vehicle

Mengjia Cao
Wayne State University,

Follow this and additional works at: http://digitalcommons.wayne.edu/oa_theses

 Part of the [Mechanical Engineering Commons](#)

Recommended Citation

Cao, Mengjia, "Thermal And Cooling Systems Modeling Of Powertrain For A Plug -In Parallel-Through-The-Road Hybrid Electric Vehicle" (2014). *Wayne State University Theses*. Paper 290.

This Open Access Thesis is brought to you for free and open access by DigitalCommons@WayneState. It has been accepted for inclusion in Wayne State University Theses by an authorized administrator of DigitalCommons@WayneState.

**THERMAL AND COOLING SYSTEMS MODELING OF POWERTRAIN FOR A PLUG
-IN PARALLEL-THROUGH-THE-ROAD HYBRID ELECTRIC VEHICLE**

by

Mengjia Cao

THESIS

Submitted to the Graduate School

of Wayne State University,

Detroit, Michigan

in partial fulfillment of the requirements

for the degree of

MASTER OF SCIENCE

2014

MAJOR: ELECTRIC-DRIVE VEHICLE

ENGINEERING

Approved By:

Advisor

Date

DEDICATION

It is dedicated to Mengjia Cao when she was a child, and also to the grown-up from whom this child grew, this is her dream come true.

ACKNOWLEDGEMENTS

I owe my deepest gratitude to my advisor Professor Jerry Ku for his generous guidance and patience in my academic growth, who leads me to EcoCAR2 competition. Last two years is a life-changing journey, I would like to proudly proclaim that Electric-drive vehicle Engineering Master Program couples with EcoCAR2 competition is the best education I've ever had, for not only the knowledge, methodology and skill I've learned but also the wideness of horizon and revolution of mind, which will be the most priceless treasure and continues to benefit my life in the further.

I also would like to extend my special thanks to my program manager Idan Kovent and lead engineer Kevin Snyder, as well as fellow EcoCAR2 team members and friends I made out of the competition, their warrior spirit and endless passion for engineering through the project had set great example for me and make me so happy with my dedication to the engineering career.

Lastly, my important debt is to my significant one Shuai Zhang, he always cherished my dreams as carefully as his own.

TABLE OF CONTENTS

| | |
|------------------------------------------------------------|------|
| Dedication..... | ii |
| Acknowledgment..... | iii |
| List of Figures..... | viii |
| List of Tables..... | xi |
| List of Abbreviations..... | xii |
| Chapter 1. BACKGROUND AND OVERVIEW..... | 1 |
| 1.1 EcoCAR2 Competition | 1 |
| 1.2 Motivation | 2 |
| 1.3 Model-based Design..... | 4 |
| 1.4 Literature Review | 5 |
| Chapter 2. OVER-ALL VEHICLE MODELING | 9 |
| 2.1 WSU PTTR Hybrid Vehicle | 9 |
| 2.2 Vehicle Plant Model..... | 10 |
| 2.2.1 Engine Model..... | 12 |
| 2.2.2 ESS Model | 14 |
| 2.2.3 Electric Motor & MCU Model | 15 |
| 2.2.4 Vehicle Model..... | 16 |
| 2.3 Vehicle Supervisor Controller..... | 19 |
| 2.3.1 Vehicle Operation Mode..... | 20 |
| 2.3.2 Fault Detection and Mitigation Control Strategy..... | 22 |

| | | |
|--------------------------------------------------------------------------|------------------------------------------------|----|
| 2.4 | Component Model Library and Initial File | 24 |
| 2.5 | GUI as Analysis Tool..... | 25 |
| 2.6 | Thermal Model Organization..... | 27 |
| Chapter 3. PTTR HYBRID VEHICLE SYSTEM COOLING LOOPS | | 29 |
| 3.1 | Cooling Loop Design | 29 |
| 3.2 | Cooling Component Sizing | 31 |
| 3.2.1 | Determine Heat Generation Rate | 32 |
| 3.2.2 | Calculate Radiator Performance | 34 |
| 3.2.3 | Design ESS Chill Plate | 35 |
| 3.2.3 | Cooling System Pressure Drop..... | 38 |
| 3.2 | Cooling Loop Configuration | 42 |
| CHAPTER 4. COMPONENT AND SUB-SYSTEM THERMAL PLANT MODEL DEVELOPMENT..... | | 46 |
| 4.1 | Heat Source Component..... | 47 |
| 4.1.1 | Convection Heat Transfer Model..... | 49 |
| 4.2 | Heat Sink Component | 50 |
| 4.2.1 | Radiator..... | 50 |
| 4.2.2 | Oil-to-water Heat Exchanger | 59 |
| 4.3 | Fluid Delivery Component..... | 62 |
| 4.3.1 | Coolant Pipe..... | 62 |

| | | |
|------------------------------------------------------|-------------------------------------------|-----|
| 4.3.2 | Thermostat | 63 |
| 4.3.3 | Cooling Pump | 64 |
| 4.3.4 | Cooling Fan..... | 65 |
| 4.3.5 | Thermal Properties..... | 65 |
| CHAPTER 5. THERMAL CONTROL STRATEGY DEVELOPMENT..... | | 68 |
| 5.1 | Thermal Manager Development..... | 68 |
| 5.1.1 | Control Work Flow for Engine Loop..... | 72 |
| 5.1.2 | Control Work Flow for ESS Loop..... | 73 |
| 5.1.2 | Control Work Flow for Motor/MCU Loop..... | 74 |
| 5.1.3 | Control Work Flow for AC system..... | 78 |
| 5.1.4 | Over-all Fan Control Logic..... | 79 |
| 5.2 | Thermal Manager Bench Testing..... | 81 |
| CHAPTER 6. RESULTS AND DISCUSSIONS..... | | 88 |
| 6.1 | Thermal Model Integration | 88 |
| 6.2 | Simulation Results..... | 89 |
| 6.3 | Conclusion..... | 94 |
| 6.4 | Future Work | 96 |
| APPENDIX A. A Complete Cooling Components List | | 97 |
| APPENDIX B. Pumps Performance Characteristics | | 101 |
| REFERENCES | | 104 |

| | |
|---------------------------------|-----|
| ABSTRACT..... | 107 |
| AUTOBIOGRAPHICAL STATEMENT..... | 108 |

LIST OF FIGURES

| | |
|-------------------------------------------------------------------|----|
| Figure 2-1. The WSU PTTR Vehicle Architecture | 10 |
| Figure 2-2. Electric Motor Plant Model..... | 12 |
| Figure 2-3. Typical engine fuel consumption data | 13 |
| Figure 2-4. PTTR Hybrid Vehicle Plant Model..... | 18 |
| Figure 2-5. Hierarchical Control in HEV | 19 |
| Figure 2-6. Analysis Tool-Setup GUI..... | 25 |
| Figure 2-7. Analysis Tool-Analysis GUI..... | 26 |
| Figure 2-8. Thermal Model Organization..... | 28 |
| Figure 3-1. Vehicle Cooling System Architecture | 29 |
| Figure 3-2. Heat Generation Rate under US06_City Drive Cycle..... | 33 |
| Figure 3-3. Battery Chill Plate Design Calculator | 36 |
| Figure 3-4. Battery Chill Plate | 38 |
| Figure 3-5. System Resistance of ESS Loop | 39 |
| Figure 3-6. Total Pressure Drop of ESS Cooling Loop | 40 |
| Figure 3-7. System Resistance of Motor/MCU Loop..... | 41 |
| Figure 3-8. Total Pressure Drop of Motor/MCU Cooling Loop..... | 42 |
| Figure 3-9. ESS Cooling Loop Configuration | 43 |
| Figure 3-10. Motor/MCU Cooling Loop Configuration..... | 45 |
| Figure 4-1. The Heat Flow Diagram..... | 46 |
| Figure 4-2. Unederhood Air Velocity..... | 50 |
| Figure 4-3. Schematic of Radiator | 51 |
| Figure 4-4. Finned Flat Tube Geometry | 52 |

| | |
|------------------------------------------------------------------------------------------|----|
| Figure 4-5. Heat Transfer Characteristic and Friction Factor for Finned Flat Tubes | 52 |
| Figure 4-6. Heat Transfer Characteristic and Friction Factor for Coolant | 55 |
| Figure 4-7. The Radiator Model | 57 |
| Figure 4-8. The Radiator Model Performance | 59 |
| Figure 4-9. Schematic of Oil-to-Water Heat Exchanger | 60 |
| Figure 4-10. The Oil-to-water Heat Exchanger Model Performance | 61 |
| Figure 5-1. Communication Architecture | 68 |
| Figure 5-2. The Functional Diagram of Thermal Manager | 69 |
| Figure 5-3. Control Work Flow of Engine in ECM..... | 73 |
| Figure 5-4. Control Work Flow of ESS in Thermal Manager | 74 |
| Figure 5-5. Control Work Flow of Motor in Thermal Manager | 76 |
| Figure 5-6. Control Work Flow of MCU in Thermal Manager | 77 |
| Figure 5-7. Control Work Flow of AC system in Thermal Manager | 79 |
| Figure 5-8. Over-all Fan Control | 80 |
| Figure 5-9. Thermal Manager Block | 82 |
| Figure 5-10. Simulated Component Temperature Performance under Highway Condition | 83 |
| Figure 5-11. Results Comparison under Highway Condition..... | 84 |
| Figure 5-12. Simulated Component Temperature Performance under Mode Switch Condition . | 85 |
| Figure 5-13. Results Comparison under Mode Switch Condition..... | 86 |
| Figure 6-1. Thermal Manager Model..... | 88 |
| Figure 6-2. ESS Plant Model | 89 |
| Figure 6-3. EcoCAR2 4-cycle Drive Schedule (2 times) | 90 |
| Figure 6-4. Powertrain Operation Condition under EcoCAR2 4-cycle Schedule | 92 |

Figure 6-5. Thermal Performance under EcoCAR2 4-cycle Schedule..... 93

Figure 6-6. Thermal Performance under grade load condition..... 94

LIST OF TABLES

| | |
|---------------------------------------------------------------------------------|----|
| Table 2-1. Vehicle Operation Mode | 22 |
| Table 2-2. Fault Levels and Required Action | 23 |
| Table 3-1. Component Target Temperature..... | 30 |
| Table 3-2. The Average Heat Generation Rate for Each Drive Cycle..... | 33 |
| Table 3-3. The Calculated Radiator Capacity..... | 35 |
| Table 4-1. Specification for Finned Flat Tubes Heat Exchanger Core..... | 53 |
| Table 4-2. The Radiator Working Conditions under Study | 57 |
| Table 4-3. The Oil-to-water Heat Exchanger Working Conditions under Study | 60 |
| Table 4-4. Standard Plastic Pipes Specification | 62 |
| Table 4-5. Pump Power Consumption | 64 |
| Table 4-6. Fan System Status..... | 65 |
| Table 4-7. Lumped Component Thermal Properties | 66 |
| Table 4-8. Ambient Air Thermal Properties | 66 |
| Table 4-9. Oil Coolant Thermal Properties | 67 |
| Table 4-10. Water Coolant Thermal Properties | 67 |
| Table 5-1. The Used Signals of Thermal Model..... | 69 |
| Table 5-2. The Temperature Threshold Set Points | 72 |
| Table 6-1. Driving Condition..... | 90 |
| Table 6-2. Peak Temperature under Grade Load Condition..... | 95 |

LIST OF ABBREVIATIONS

| | |
|-----------|-----------------------------------------------------------|
| A | Area, m^2 |
| C | Heat Capacity Rate, W/K |
| C_p | Specific Heat, J/kg·K |
| D | Diameter, m |
| \dot{E} | Rate of Energy, W |
| F | Force, N |
| f | Friction Factor |
| G | Mass Velocity, $kg/s \cdot m^2$ |
| h | Convection Heat Transfer Coefficient, $W/m^2 \cdot K$ |
| I | Current, A |
| j_H | Colburn j factor for the heat transfer |
| k | Thermal Conductivity, $W/m \cdot K$ |
| L | Length, m |
| LHV | Lower Heating Value |
| m | Mass, kg |
| \dot{m} | Mass Flow Rate, kg/s |
| N | Number |
| Nu | Nusselt Number |
| P | Pressure, kPa or Power, W |
| Pr | Prandtl Number |
| q | Heat Transfer Rate, W |
| Q | Volumetric Flow Rate, m^3/s |
| R | Electrical Resistance, Ohm or Thermal Resistance m^2K/W |
| Re | Reynolds Number |
| S | Spacing, m |
| SOC | State Of Charge |
| T | Temperature, $^{\circ}C$ |
| t | Thickness, m or Time, s |
| U | Overall Heat Transfer Coefficient, $W/m^2 \cdot K$ |
| V | Velocity, m/s |

Greek Letters

| | |
|---------------|----------------------------|
| ω | Angular Speed, rad/s |
| ε | Effectiveness |
| η | Efficiency |
| μ | Viscosity, kg/s·m |
| ρ | Density, kg/m ³ |
| τ | N·m |

Subscripts

| | |
|-------------|-----------------------|
| <i>Al</i> | Aluminum |
| <i>areo</i> | Aerodynamic |
| <i>avg</i> | Average |
| <i>cap</i> | Capacity |
| <i>chem</i> | Chemistry |
| <i>chg</i> | Charge |
| <i>clt</i> | Coolant |
| <i>comp</i> | Component |
| <i>cont</i> | Continue |
| <i>conv</i> | Convection |
| <i>cr</i> | Cross Section |
| <i>Cu</i> | Copper |
| <i>D</i> | Diameter |
| <i>die</i> | Dielectric layer |
| <i>dis</i> | Discharge |
| <i>eng</i> | Engine |
| <i>ess</i> | Energy Storage System |
| <i>exh</i> | Exhaust |
| <i>f</i> | Fin |
| <i>ff</i> | Free Flow |
| <i>fr</i> | Frontal |
| <i>fw</i> | Front Wheel |
| <i>gen</i> | Generation |
| <i>grad</i> | Gradient |
| <i>h</i> | Hydraulic |
| <i>hx</i> | Heat Exchanger |
| <i>i</i> | Inlet |
| <i>init</i> | Initial |
| <i>L</i> | Loss |
| <i>max</i> | Maximum |
| <i>mech</i> | Mechanical |
| <i>min</i> | Minimum |

mot
o
p
pre
r
rad
rw
s
veh
wat

Motor
Outlet or Overall
Perimeter
Previous
Ratio
Radiator
Rear Wheel
Surface
Vehicle
Water

CHAPTER 1. BACKGROUND AND OVERVIEW

1.1 EcoCAR2 Competition

The 2011-2014 EcoCAR2: Plugging In to the Future Competition is sponsored by U.S. Department of Energy (DOE) and General Motors (GM). 15 participating universities across North America were put into a time and technology race for the honor of best hybridized vehicle with highest efficiency and lowest emissions while avoiding compromising performance, safety and consumer acceptability. A 2013 Chevrolet Malibu, donated by GM, is designated as the integration platform for the team's advanced vehicle design.

In order to offer an unparalleled hands-on, real-world experience to the student engineers participating in the competition, EcoCAR2 Vehicle Development Process (VDP) modeled after GM's VDP is adopted. The VDP serves as a roadmap for the engineering process of designing, building and refining the vehicles. It ensures the engineering tools are used for analysis and verification before hardware build that teams are not rushing to design conclusions.

Wayne State University (WSU) EcoCAR2 team adheres to the core concept throughout the project. In the first year of EcoCAR2, the team received \$25,000 in seed money to begin developing its vehicle designs. Year One is an essential foundation for establishing a successful vehicle by emphasizing the use of math-based design tools like Argonne's Autonomie and Mathwork's Matlab, also the development of software-in-the-loop (SIL) and hardware-in-the-loop (HIL) simulation techniques. After researching, comparing and selecting Hybrid Electric Vehicle (HEV) architectures that met the competition and team goals, WSU EcoCAR 2 team finally designed its own Parallel through the Road (PTTR) architecture based on decision matrix and utilized a crowd-sourcing format to select the powertrain components that will integrate into

the vehicle [1]. The team had completed the first year of EcoCAR 2 and earned the key to a new 2013 Chevrolet Malibu.

During the second and third years of the competition, students build the vehicle and continue to refine, test, and improve vehicle operation to reach a 99% production-ready state. At the end of Years Two and Three, the re-engineered student vehicle prototype competes in a week-long competition of engineering tests. These tests are similar to the tests GM conducts to determine a prototype's readiness for production. The Greenhouse gas, Regulated Emissions, and Energy in Transportation (GREET) model, developed at Argonne National Laboratory, is used to assess a well to wheel analysis of the greenhouse gas impacts of each technology approach the teams select. The team had successfully brought a drivable vehicle to the Year Two final competition at GM proving ground in Yuma, Arizona and obtained satisfactory achievements.

1.2 Motivation

The internal combustion engine (ICE) vehicles offer good performance and long operation range. They are also very easy to refuel, which make it still the most prevailing choice for today's customer. However, its disadvantages of poor fuel economy and environmental issues have always been complained by the public. Electric Vehicle (EV) on the other hand demonstrates several solid edges on conventional ICE vehicle. The most attractive merit of EV must belong to zero gasoline consumption and zero tailpipe emissions, also the speed-torque characteristic of electric motor is much closer to ideal profile compare with engine. However, even though EV can offer environmental benefits and great efficiency, what stop EV from mass commercialization still remain enormous challenges: the limited range, the deficiency of facilities, the extended recharge time and the excessive up-front cost, etc.

The gap between the ideal and the present reality calls in the presence of HEV, which utilizes the best features of the two powertrain to complement their individual shortcomings. The United States now is the largest HEV market around the world, according to sales numbers provided by HybridCars.com, approximately 2,600,000 units of hybrid electric automobiles and SUVs have been sold by December 2012. The notable development of HEV continues and will continue to serve as the emerging engine of economic growth and magnet of research investment.

The history of vehicle thermal management can be traced back to 19th century when patents related to ICE cooling can be found. Over more than a century the thermal management technologies have developed and changed with the trend of automotive industry and customer demand.

Today the vehicle power source is not only limited to ICE any more, the ever-increasing interest in HEV since its first introduction in the United States in 1999 leads the vehicle propulsion configuration moving towards more electrically dominant system. The adoption of electric-drive system such as electric motor, power electronics and Energy Storage System (ESS) brings additional cooling requirements because they can experience significant thermal loading as well. Additionally, the optimal operation temperature of each component is different, meaning that each component needs individual cooling system for different coolant temperature and flow rate. A cooling system may contain many components like coolant pumps, heat exchangers, fans and thermostat. Given that cooling system of conventional ICE is already packaged compactly under the hood, the situation leads to the question of how to efficiently utilize the cooling effect of each system by integrating or sharing. Besides, the conventional thermal control strategy is impacted as well because of the dual powertrain. In popular concept, HEV is able to operate in 3

modes: the ICE-drive mode, the motor-drive mode and the hybrid mode, the primary power source also known as the heat source switches according to operation mode and driving condition. Therefore, a more comprehensive thermal management method must be developed to accommodate new changes.

The motivation of this paper is to study the methodologies of thermal management for hybrid architecture. The optimization of hybrid powertrain must account for thermal effect because it plays a crucial part in safety considerations as well as offers real potential in improvement of efficiency. Emphasis is placed on creating a framework for systematically approaching the HEV thermal modeling and control based on Mathworks Simulink so as to predict the thermal behavior of major components of HEV and ensure their operation is within optimal range. The simple but fairly accurate thermal model will be specialized for real-time vehicle level testing without heavy computational work like numerical modeling or additional commercial software package to simulate the thermal behavior of HEV.

1.3 Model-based Design

HEV is a complex of various electrical and mechanical components and subsystems. It contains more electric components than conventional vehicle, such as ESS, electric motor, power electronics as well as their corresponding control system-Electric Control Unit (ECU)-it is like the “brain” of the component which controls all the functions by reading signal from sensor and interprets its needs. Beyond that, the conventional mechanical components like ICE, transmission and brake still remain. Prototyping and testing HEV can be very expensive, iterative and time-consuming using the conventional design process, on account of the dynamic interactions among various components and the multidisciplinary nature. It is difficult to define

the design parameters properly to meet safety, performance and efficiency target while maintaining reasonable price to customer market[2].

The trend in the automotive industry has been towards model-based design approach, it allows the components to be tested in a virtual environment where re-test, re-design and re-validation can be done inexpensively prior to hardware build. Furthermore, this design tool is capable of providing a modeling environment that can promote parallel and integrated development of both the component and its ECU, this is critical in HEV design because it meet the challenge to predict the interaction among various components or subsystems even though the complexity of component and its dependence on ECU rise. The model-based design can be generally divided into 4 steps: 1) building component plant model, 2) developing control strategy and synthesizing a controller for the plant model, 3) simulating the plant model and controller, 4) verifying and optimizing. The modeling and simulation tool makes it possible to design the model with functional characteristics and optimize the proposed model through real-time testing and verification before the final vehicle hardware test.

1.4 Literature Review

The thermal management for HEV powertrain system seems to remain a relatively under-developed field. The hybrid system adds another dimension to the variety of vehicle architecture. HEVs can be generally classified into 4 categories but not limit to them: series hybrid, parallel hybrid, series-parallel hybrid and complex hybrid. The derivations based on the major categories are many and various, each architecture has its own special needs and requires distinctive thermal design, and therefore there is no universal thermal management solution for HEV.

Park [3] demonstrated a comprehensive model of vehicle thermal management system for a heavy duty series hybrid electric vehicle by using numerical simulations. He divided the entire thermal model into 3 categories by its function: the heat source components, the heat sink components and the fluid delivery components and discussed the modeling method of each component. The thermal model and the vehicle powertrain model are integrated to predict thermal response under different architecture design and various vehicle driving conditions. He argued the temperature fluctuation of the powertrain component is aggravated by the interaction between the components sharing a cooling loop, thus technical consideration on the operation group is necessary and critical.

Lang and Kitanoski [4] presented a parallel hybrid vehicle uses ICE and two electric drives, which features three different cooling circuits. The sophisticated simulation technique by means of co-simulation of the mechanical, electrical and thermal system is applied. The simulation software veDYNA was used for the vehicle dynamics and the driver model. A supplementary Mathworks Simulink model was developed to simulate the hybrid power train and the electrical system. The thermal system was simulated with the software KULI. With such a co-operative model, the temperatures of the individual components can be investigated under different loads and ambient conditions.

Besides the works dedicated to the system-level thermal management based on over-all vehicle model, there are some studies that focus on modeling and simulation of individual cooling system for specific component as well.

Pesaran [5] proposed a battery thermal model for HEV using lumped capacitance thermal approach in the ADVISOR simulation tool. The model can predict the temperature changes in a vehicle's battery according to the drive cycle and air cooling flow rate. Also, in his other study

[6] he discussed such topics as active cooling versus passive cooling, liquid cooling versus air cooling for thermal management of batteries in EVs and HEVs, he argued that passive cooling systems (only the ambient environment is used) works properly only when ambient air have a mild temperature ($10^{\circ}\text{C}\sim 35^{\circ}\text{C}$). Outside of these conditions, active components such as evaporators and coolant are needed. For large battery pack, liquid cooling is preferable to provide efficient heat removal.

Hu and Lin [7] presented a battery cooling system for EV/HEV using a Foster network, the model can be coupled with a battery electrical circuit model to predict accurate battery temperature. The parameters in the Foster network, including capacitance and resistance, were extracted from computational fluid dynamics (CFD) results. It is shown in their study that the Foster network approach gave equivalent solution as the CFD but was able to offer shorter run time.

Saxena [8] showed the analytical model and simulation results of cooling system including radiator, fan and pump for electric motor and its power electronics. The model was generated and analyzed in software KULI. Different cooling system layouts were compared to obtain best performance. He concluded that by implementing radiator fan and pump flow variation according to coolant temperature, significant amount of power can be saved.

Beside the above works dedicated to the cooling system for EV/HEV powertrain, there are also methodologies in the modeling of conventional ICE cooling system that can be adopted in HEV thermal management.

In their work Yoo and Simpson [9] demonstrated a relatively simple engine coolant temperature model for the diagnosis of the engine cooling system. The proposed model utilized

available information within the production ECU to compute coolant temperature thus diagnostic algorithm can be verified.

Arici and Johnson [10] developed Vehicle Engine Cooling System Simulation (VECSS) computer code to simulate the operation of the response of the cooling circuit, oil circuit, and the engine compartment air flow when the VECSS is operated using driving cycle data of vehicle speed, engine speed, and fuel flow rate for a given ambient temperature, pressure and relative humidity. Extensive test data for a 12.7 L diesel engine that would be used in validation of the updated VECSS was gathered and analyzed. The simulation results computed by the software program were validated with test data and showed good agreement.

In their work Cortona and Onder [11], Jawad and Zellner [12] and Wagner and Ghone [13] discussed that variable speed electric pump allows for ECU-based control for ICE can offer significant improvements over the conventional mechanically driven pump. It is shown that the application of electric pump can reduce parasitic power consumption, make further improvement on the fuel economy, reduce mechanical wear during cold start, increase the overall effectiveness of the cooling system and eliminate overheating problems.

The previous work had greatly inspired the development of the proposed study. However, it requires intensive numerical computations often involving commercial software applications that are incompatible with real-time control needs. In this study, emphasis is placed on a simple but fairly accurate thermal model based on Mathworks Simulink, specialized for real-time vehicle level testing. The objective is to develop a modeling framework and methodologies for hybrid powertrain thermal and control development.

CHAPTER 2. OVER-ALL VEHICLE MODELING

2.1 WSU PTTR Hybrid Vehicle

WSU EcoCAR2 team finally selected PTTR hybrid architecture among three initial options offered. The decision was made based on 4 iterations of analysis and selection process, in consideration of design constrains and team's resource and experience [1]. The selected architecture is shown in Figure 2-1.

As the nature of PTTR architecture, the Front Wheel Drive (FWD) and Rear Wheel Drive (RWD) are mechanically and electrically independent. The battery can be recharged by regenerative braking, by recovering excessive power produced by engine when driving, or wall-charging. Power is only transferred by the road surface when vehicle is in motion, when vehicle is at standstill the battery can't be recharged. However, PTTR is capable of offering great flexibility to switch between 2 powertrains and even 4-wheel drive. In addition, the advantage of conventional ICE is successfully retained, such as high efficiency during highway cruising.

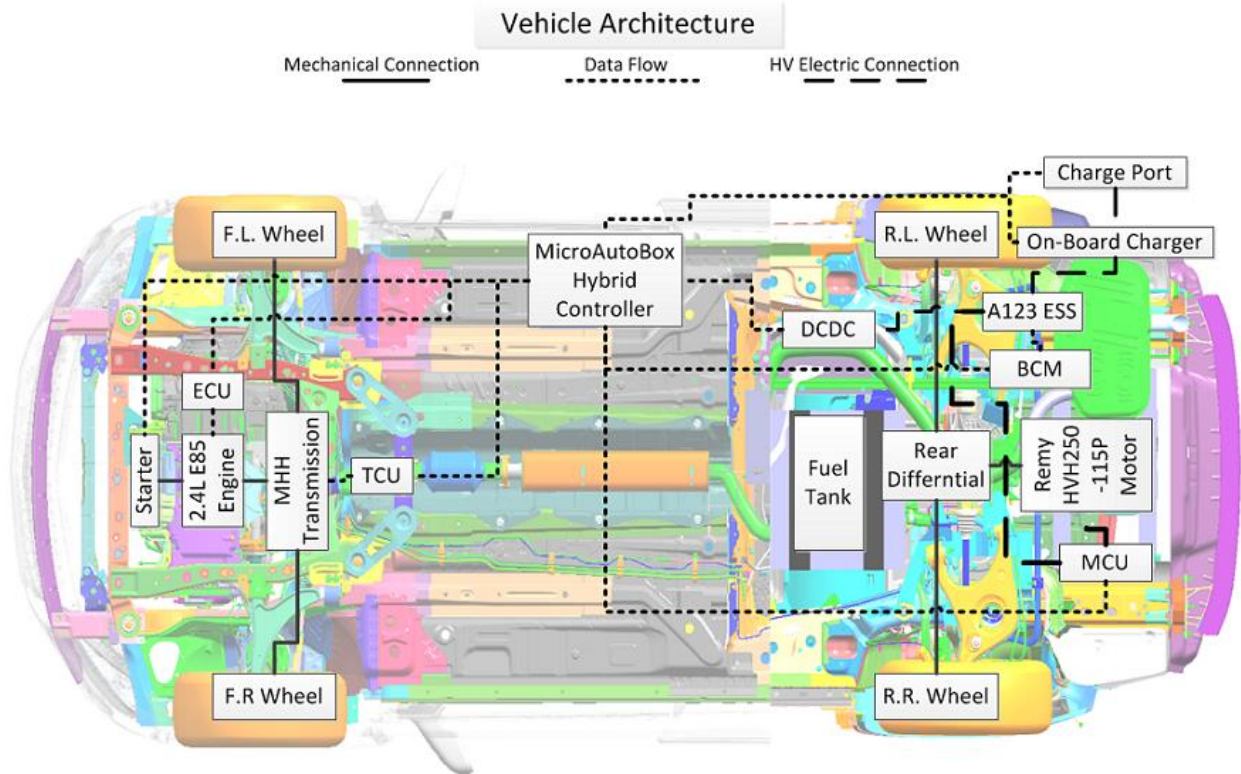


Figure 2-1. The WSU PTTR Vehicle Architecture

The stock 2013 Chevrolet Malibu is a mid-sized conventional sedan with a FWD powertrain propelled by ICE. The PTTR conversion design requires adding a RWD powertrain while keeping the conventional FWD. For the second power source a 150-kW electric motor is selected, along with it a 20-kWh lithium-ion battery park, which can provide 30-40 miles of pure electric range. Also, Motor Controller Unit (MCU) as an inverter and motor operation controller is selected accordingly. Lastly the stock 2.4L gasoline engine is replaced by a 2.4L flex fuel engine running on E85, which is an alternative blend fuel of 85% ethanol and 15% gasoline.

2.2 Vehicle Plant Model

The vehicle plant models configured in Mathworks Simulink environment are created by team leader Idan Kovent [14] for SIL and HIL development. The plant models are designed to

react and respond similarly as their hardware counterparts, interacting with simulator to emulate the actual component behavior.

The plant model is made up of component model and its corresponding local software ECU. The component model is based on equations that model the physics of a component to compute outputs from provided inputs, or on the performance maps provided by the component supplier when applicable. Note that physical realm and controls/software realm are separated. Take electric motor plant model in Figure 2-2 for example, the local ECU is MCU, marked as “Soft MCU” in the blue blocks. It can be seen that motor current, the physical performance is calculated by power divided by voltage in plant model. The control algorithm and non-physical calculation like torque limit are done in MCU. The electric motor model has MCU that reads its sensors, communicates with other controllers and sends commands to be executed by the actuators in that model. For example, MCU receives torque demand from the supervisory controller, it decides the limited torque command based on torque demand from supervisory controller and current motor speed from plant model, and finally commands the actuator to produce that torque.

The following section will discuss each major component plant model in detail.

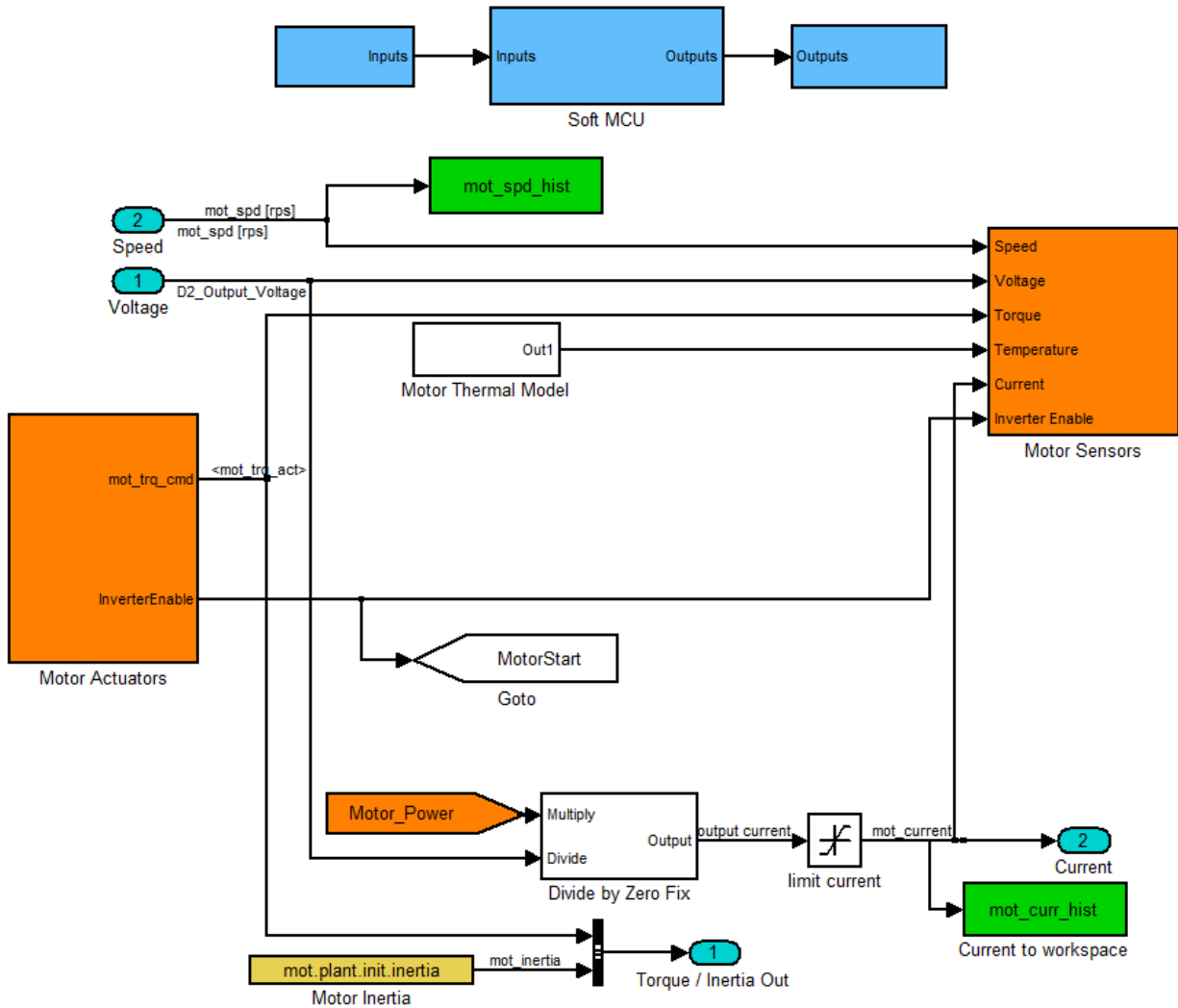


Figure 2-2. Electric Motor Plant Model

2.2.1 Engine Model

The engine model consists of the plant model and soft Engine Control Module (ECM). The main function of engine plant model is to compute fuel consumption, modeled by interpolating data from a 2D look-up map based on the engine speed and engine torque. Figure 2-3 shows a performance map for typical engine fuel consumption.

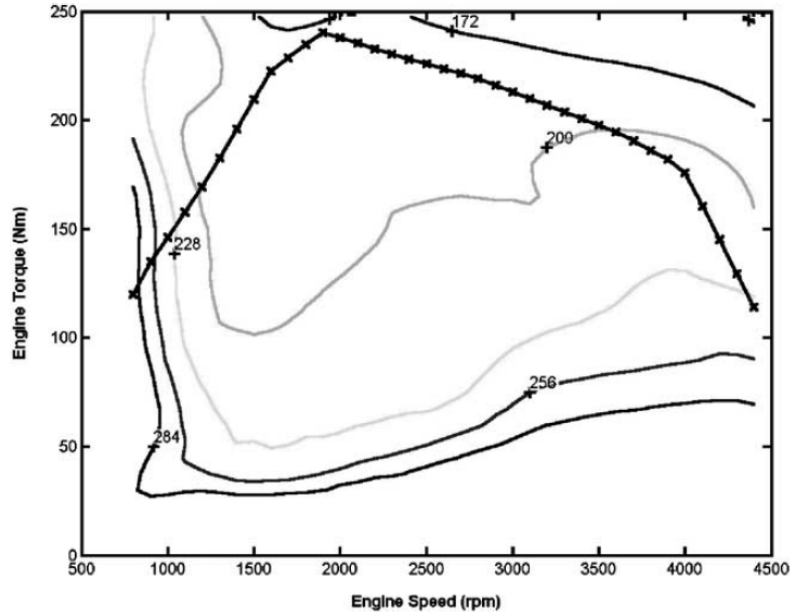


Figure 2-3. Typical engine fuel consumption data [15]

Soft ECM is a type of ECU that controls a series of actuators on engine to ensure optimum operation. This is done by reading values from a multitude of sensors within the engine bay, interpreting the data using performance maps and control algorithms. And then sends command to engine actuators so as to adjust the engine behavior. The main contributions of ECM include:

- Fuel System Request: fuel pump is enabled as the engine starts up, instantaneous fuel flow is estimated and commanded air/ fuel ratio is determined from this request of Soft ECM. The required fuel delivery is actuated by the fuel pump.
- Engine Torque Status: Soft ECM determines the actual output torque by comparing driver requested torque and engine limited torque as a function of speed, continually.
- Engine Run Active Status: this status is determined based on the engine speed, accelerator actual position, power train crank active status, brake pedal status, engine 12 Volt command, engine intake air boost pressure.

- Engine Chemical Power and Mechanical Power: the engine power consumption is calculated via the following equations:

$$P_{eng,mech} = \omega_{eng}\tau_{eng} \quad (2.1)$$

$$P_{eng,chem} = \dot{m}_{gas}LHV \quad (2.2)$$

2.2.2 ESS Model

Same with engine model, ESS model includes plant model and a soft Battery Control Module (BCM). The plant model is built on electrochemistry characteristics of ESS, accepting current as input where a positive value represents charging and a negative value represents discharging of the ESS. The output voltage and temperature are transmitted to soft BCM by the sensor.

The ESS voltage is calculated by the following equation. The values for open circuit voltage (VOC) and ESS internal resistance are determined via lookup table as a function of state of charge (SOC).

$$V_{ESS} = V_{ESS,OC} + I_{ESS}R_{ESS} \quad (2.3)$$

The soft BCM uses the data from the plant model to perform its calculations. The major functions of BCM are SOC calculation, buffers calculation and definition of maximum discharge or charge current by 2D look-up table.

- SOC Calculation: the coulomb counting method is adopted, calculating SOC by integrating the current in time. SOC is defined as the ratio of the transient capacity in the battery to its maximum charge capacity. It yields to the equation:

$$SOC = \frac{Q_{cap,init} - \int I_{ess}dt}{Q_{cap,max}} \times 100 \quad (2.4)$$

- Maximum Discharge and Charge Current: the maximum values for charge and discharge current are determined via 2D look-up map based on pack temperature and SOC.
- Buffer Calculation: The buffer is a way of current protection for the ESS. The peak current limit is reduced or increased by 100A/sec to the continuous operation value depends on charging or discharging when buffer reach 0 or 100. If ESS current exceeds the limit during operation, BCM will command to open contactor for self-protection, the vehicle will lose RWD function immediately. As Love Lor described in her thesis [16]:” 100A/sec is equivalent to approximately 100Nm/sec so if the vehicle is in the middle of accelerating at 360Nm, it will lose half of its torque in less than 2 seconds.”, in some real-world driving conditions this might be a hazard, thus the supervisory controller should manage current reduction at vehicle level so the ESS protection won't impact the vehicle torque directly when cruising [17].

The Buffer calculation when charge can be expressed as below, the ESS average current is defined in a 60 seconds rolling:

$$Buffer = (1 - \frac{I_{ess,avg\ chg}}{I_{ess,cont\ chg}}) \times 100 \quad (2.5)$$

The Buffer calculation when discharge:

$$Buffer = (1 - \frac{I_{ess,avg\ dis}}{I_{ess,cont\ dis}}) \times 100 \quad (2.6)$$

2.2.3 Electric Motor & MCU Model

The motor & MCU model could be divided to 2 parts as well, the electric motor plant model and soft MCU. The electric motor does dual jobs for the HEV. It provides positive torque to propel the vehicle when motoring and becomes a generator to recharge the ESS when

reversing. The plant model receives voltage and commanded motor torque and as inputs, it outputs current and actual torque. The performance data from plant model is sent to soft MCU for control and regulate purpose, the actual torque is determined by torque limit block using look-up table as a function of motor speed. The motor efficiency is defined by performance map base on motor speed and actual torque. The mechanical power of electric motor can be calculated as below:

$$P_{mot,mech} = \omega_{mot}\tau_{mot}\eta_{mot} \quad (2.7)$$

2.2.4 Vehicle Model

In addition to powertrain models, DC-DC converter model, transmission model, front and rear differential models, front and rear wheels model and chassis model are built to complete the PTTR vehicle model, shown in Figure 2-4.

The DC-DC converter model converts the high voltage from the battery and manages the power supply for the 12-volt accessory system. The accessory loads including the radiator fan, the electric coolant pumps, ignition, wipers, lights and so on. It first ensures the minimum current supplied is met for accessory load and then limit the output if maximum current is reached. Also the converter efficiency is taken into consideration.

The transmission model is the torque manager of engine. It calculates the torque loss due to the gear efficiencies then multiplies the rest of torque by gear ratio to get the available torque to differential. The embedded Internal Mode Switch (IMS) block interprets the shift lever position. To enable automatic gear shifting, the soft Transmission Control Module (TCM) first reads the accelerator pedal position and current gear position and then determine if gear shift is needed or not according to the current vehicle speed.

The purpose of the front and rear differential models is to transmit torque from transmission or electric motor to the wheels. For FWD, it takes in actual torque from transmission and output the front differential torque base on differential efficiency and ratio. The same rule applies to the RWD, only the input torque is from electric motor.

The front and rear wheels models compute the wheel force, wheel mass and shaft speed by accepting vehicle speed, wheel torque and inertia.

The chassis model is responsible for calculating road load related performance. EcoCAR2 design rules requires an attached trailer containing the equipment for emissions testing, so the road load for the trailer is taken into account too. The total road load is the sum of aerodynamic drag force, the rolling resistance force and force to overcome gradient for both vehicle and the trailer. The governing road load equation is as follow:

$$F_{total} = F_{veh,aero} + F_{veh,rolling} + F_{veh,grad} + F_{trailer,aero} + F_{trailer,rolling} + F_{trailer,grad} \quad (2.8)$$

The transient vehicle speed is calculated using equation (2.9):

$$v_{veh} = \frac{F_{fw} + F_{rw} - F_{total}}{m_{fw} + m_{rw} + m_{veh}} \times t + v_{veh,pre} \quad (2.9)$$

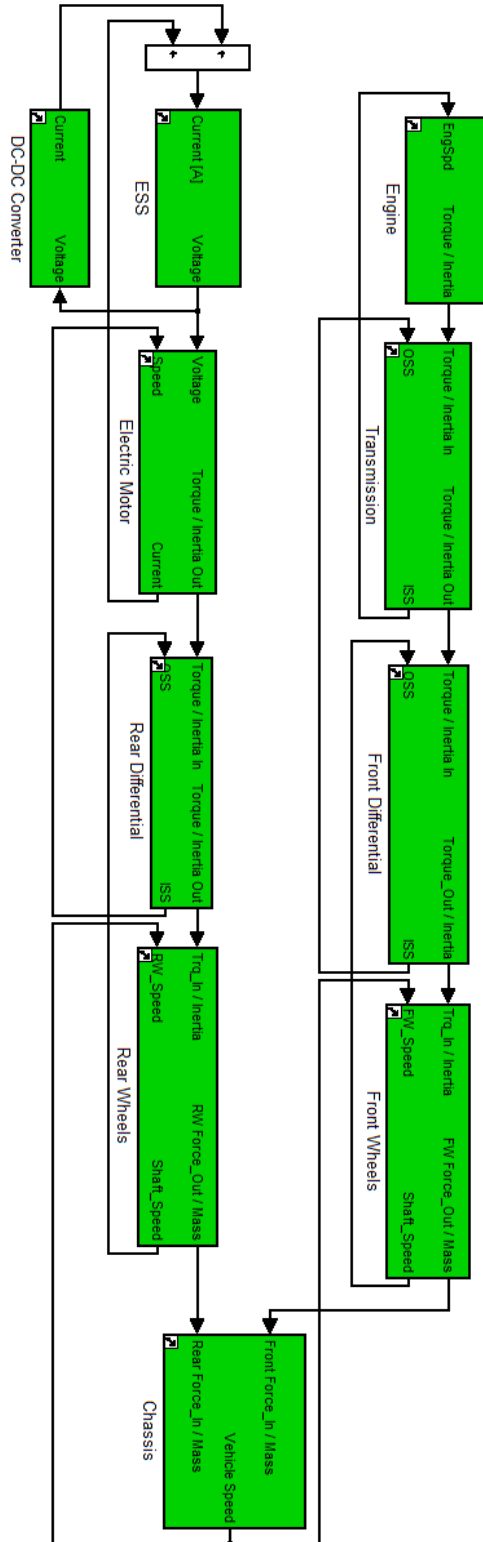


Figure 2-4. PTTR Hybrid Vehicle Plant Model

2.3 Vehicle Supervisor Controller

The supervisory controller and the control strategy are developed by team leader Love Lor [16]. The stock Malibu is a conventional ICE vehicle which doesn't have supervisory controller, the ECUs employed in the plant models work individually to operate the component itself rather than the vehicle as a whole. However, the hybridization of the stock vehicle requires a higher level controller to operate the interactions among various powertrain components due to the rise of complexity. The proposed supervisory controller determines the vehicle operation mode, interprets the driver demand and commands component controllers on vehicle level. In the meanwhile, the component controllers adopt commands from supervisory controller and provide feedback to supervisory controller for further analyses. The hierarchy of supervisory control level and component level is presented in Figure 2-5.

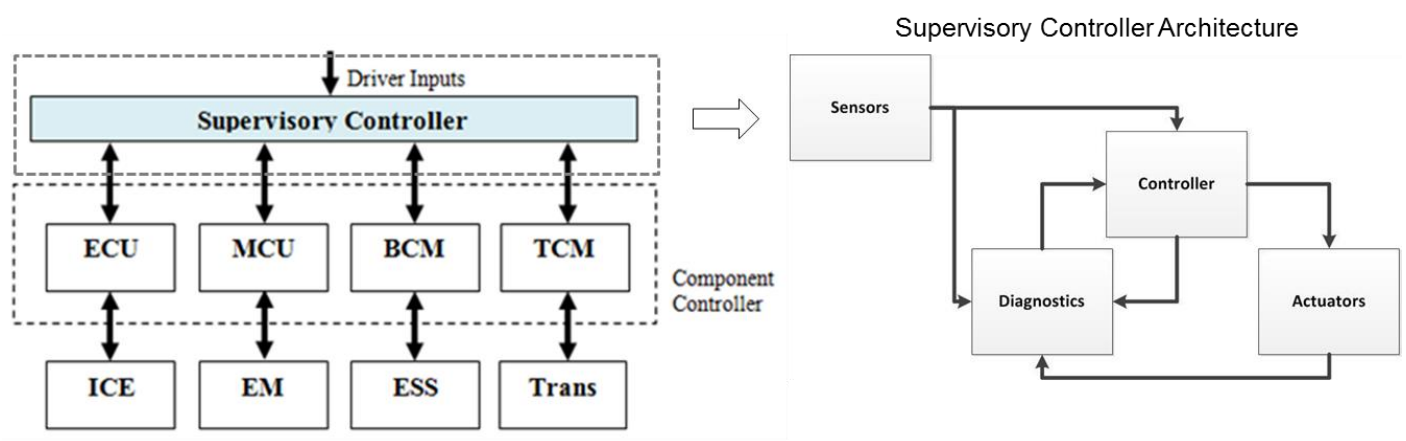


Figure 2-5. Hierarchical Control in HEV (ECU: Engine Controller Unit, MCU: Motor Controller Unit, BCM: Battery Control Module, TCM: Transmission Control Module; EM: Electric Motor)

Figure 2-5 also illustrates the architecture of supervisory controller, there are four main blocks: sensors, diagnostics, controller and actuators. The sensors read and send the data (CAN, analog, digital, etc.) to diagnostics block and controller block, thus bring in any available information from other controllers or physical sensors on the vehicle. The diagnostics block

detects failure mode and interprets it into fault code when malfunction, communicating issues to the user. The main block of the supervisory code is the controller, this decision maker consists of four subsystems: Drive Requests subsystem is responsible for analyzing driver's inputs, Vehicle Mode Selection as explained in following section, Powertrain Manager is made up of FWD, RWD, and ESS managers, and Safety Critical Policing Director (SCPD) who takes care of the fault codes provided by diagnostics block. Within subsystems there are blocks called "Managers". These managers are derived from different higher level requirements. They are the heart of the code, the algorithms. Finally the decisions and commands produced by the controller are outputted and executed by actuators.

The proposed thermal manager which contains control algorithms for thermal management will be integrated in the controller block.

2.3.1 Vehicle Operation Mode

One of the major responsibilities of supervisory controller is to decide the vehicle operation mode. For proposed HEV, the vehicle operation mode falls into 2 kinds, the Charge Depleting (CD) mode and Charge Sustaining (CS) mode. The former mode is all-electrical, the vehicle is dependent on energy from ESS and torque from electric motor, the engine is shut off in the duration of this operation mode. The CS mode will be activated when minimum SOC threshold is reached, then the engine will be the prime working powertrain while the motor helps restoring regenerative braking energy or boosting the engine as an assistant.

The control algorithm uses SOC to determine which vehicle mode will be applied, as summarized in Table 2-1. In all of the scenarios, the motor will only reverse to regenerate energy when accelerator pedal position is 0, meaning that accelerator pedal must be released.

The vehicle will be operated in CD mode until the SOC drops below the minimum threshold 20%. When enters CS mode, the engine becomes the main power source to propel the vehicle, but both powertrain will be used in alternation for the sake of vehicle performance and fuel economy. CS mode uses the engine for the majority of the drive cycle when operating at normal speed. The electric motor assists at high speed high torque demand. Since the motor is capable of higher torque at the wheels than the engine, it provides additional torque to the engine when necessary to maintain the same drivability characteristics. When the vehicle is below 10mph the engine reduces torque while the motor increases torque to a point where the motor is the sole torque supplier. This strategy is to avoid engine from operating at inefficient low loads and also limits idle fuel use. During CS period the RWD will be charging the HV battery through regenerative braking by using excess torque supplied by engine when it is not required to supply its full torque capability to the wheels, as seen in CS_Normal Speed mode. When the SOC drops below 19.5% threshold, the control strategy tends to recharge the battery as fast as possible to transit back to CD mode in the interest of better efficiency. The mechanical energy from the excessive engine load or regenerative braking will be converted to electrical energy to help ESS recharging. Also another control strategy is applied for faster recharge: the engine will keep idling even at zero vehicle speed to produce extra energy for ESS.

Table 2-1. Vehicle Operation Mode [16]

| Mode Number | Mode Name | Working Powertrain | SOC | Speed | APP=0 Regen | Charging Regen |
|-------------|-----------------|--------------------------|--------------|-------------------------------------|-------------|----------------|
| 1 | CD (RWD Only) | Motor | 100%- 20% | All | 100Nm | N/A |
| 2 | CS_Low Speed | Motor | 20%- 21% | <10mph | 100Nm | N/A |
| 3 | CS_Normal Speed | Engine (Motor for Regen) | 20-21% | >10mph | 100Nm | 50Nm |
| 4 | CS_High Speed | Engine & Motor | 20-21% | If engine alone cannot supply 80mph | 100Nm | N/A |
| 5 | Low Battery | Engine (Motor for Regen) | <19.5% | Keep engine at idle in 0mph | 100Nm | 100Nm |

2.3.2 Fault Detection and Mitigation Control Strategy

The Diagnostics subsystem in the controller block serves as the safety guard of the vehicle model by detecting the failure modes. It is responsible for "Fault Detection" by comparing the signals with their desired operating range and then generating the fault code if these signals do not fall within the limits of normal operation. If the fault has no effect on

passenger safety or vehicle performance, the fault can be analyzed after the operation. If the fault is defined as unintended or urgent, actions must be taken by decreasing vehicle performance such as degraded or limp home mode, if the fault is defined as safety critical, the vehicle will be required to shutdown. The priority level of fault and urgency of actions is shown in Table 2-2. The mitigation requirements are done in their respective managers while safety critical mitigation requirements belong to SCPD subsystem.

Powertrain component thermal runaway is a major concern of SCPD, especially HEV must account for the significant heat generation from the second power source and additional energized system. Therefore the proposed thermal model is of great importance for the over-all vehicle controls.

Table 2-2. Fault Levels and Required Action [16]

| Priority Level | Status | Action Required | Immediate Action Required | Indicator |
|----------------|---------------------------------------------------------------------------------|-------------------------------|--------------------------------------------------|------------------------------------------------------------------|
| 0 | Regular Operation, no warnings | N/A | N/A | N/A |
| 1 | Warning, unexpected behavior | Maintenance required | No performance de-rating required | Maintenance light ON |
| 2 | De-rate Fault, not SC but will lead to shut-down if not addressed immediately | Service required | De-rate performance - 30% of motor and/or engine | Maintenance & engine lights ON, maintenance requested on display |
| 3 | Limp Home Fault, not SC but will lead to shut down if not addressed immediately | Full stop as soon as possible | De-rate performance - 70% of motor and/or engine | Maintenance & engine lights ON, maintenance requested on display |
| 4 | Safety Critical Fault will lead to shutdown | Shutdown vehicle | Shutdown of motor and/or engine immediately | Shut down indication ON |

2.4 Component Model Library and Initial File

Once a model is completed it is categorized as a “library”, this applies to all the subsystem models like component plant models and managers within controller block. Library is the template for each model saving on a separate file from the main simulation model where it can be called back during execution.

Besides libraries, there is another separated file keeping provided data like component specification, physical property and performance map named “initial files”, it is categorized by component. For example, there is a designated ESS initial file, which loads all the specifications necessary for ESS simulation.

This tool can greatly help software management and version control. Once libraries and initial files are available for the components, each team member can be assigned to work on a library in parallel where they can make changes to the local copy of the model, and push these changes to the library file, where the uploaded file can be inserted seamlessly in the over-all vehicle model. This can avoid multiple people working on the same over-all model, leading to possible versioning mess and unwanted trouble-shooting time.

The initial files can keep the provided data in a separated place to protect the important specs from being modified during the process. On the other hand, when it is necessary to change the specs, it can be done easily by updating initial files without even open the model. This is very convenient when the specs are used in different places.

In compliance to the team rules, the thermal model will be compiled in designated library and a specific thermal initial file will be created to document the add-on specifications like heat exchanger dimensions and thermal properties.

2.5 GUI as Analysis Tool

It is important to develop an engineering tool which supports readability and understandability to minimize the learning curves for student engineers without prior knowledge about modeling and simulation in Mathworks Simulink environment. The user friendly Setup Graphical User Interface (GUI) and analysis GUI are created by team leader Idan Kovent [14] to execute simulation and support investigation. The tool is flexible and allows customization, which is very useful when facing various conditions and analyzing large amount of data.

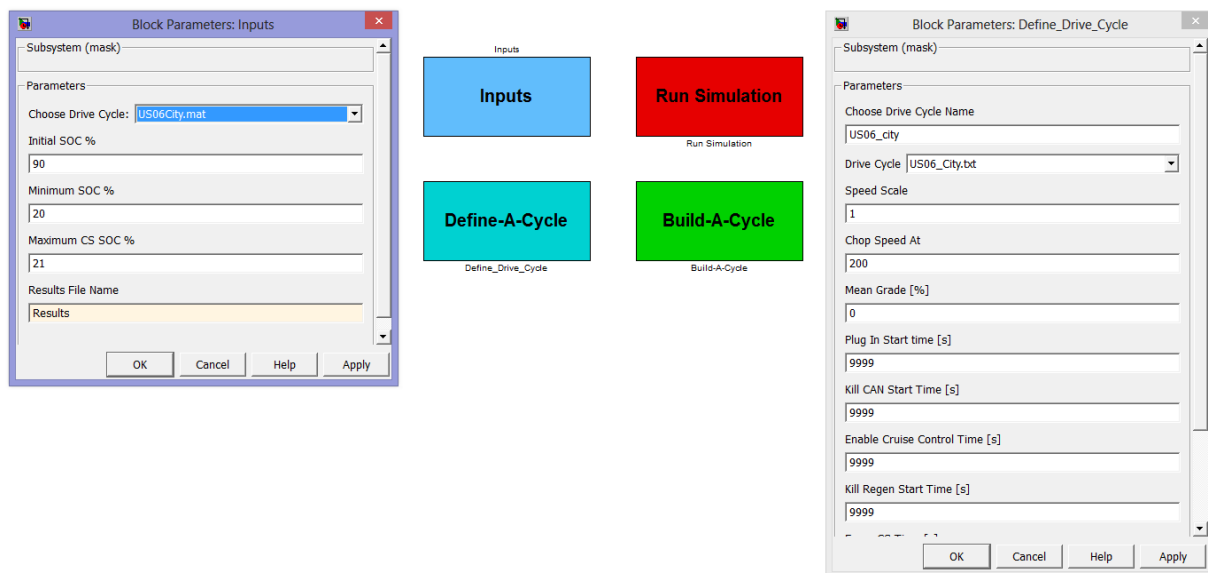


Figure 2-6. Analysis Tool-Setup GUI

Figure 2-6 shows the features of the Setup GUI. This GUI consists of 4 colored buttons. When selected Inputs button, the menu on the left will appear, allowing the user to choose drive cycle and SOC limitations. Then the simulation can be executed by double clicking the Run Simulation button.

A drive cycle is a series of data points in vehicle speed of versus time. It is used extensively to assess vehicle performance through simulations. Drive cycles can simulate various

speed characteristics that can closely reflect real world driving patterns. The creator understands the importance and variety of driving conditions, so Define-A-Cycle button is built to setup drive cycles based on several templates and create these effortlessly. When select this button, the menu on the right will pop up, the user definable parameters includes mean grade, speed scale, chop speed, etc. After defining the parameters, the customized drive cycle can be generated and saved automatically by clicking Build-A-Cycle button.

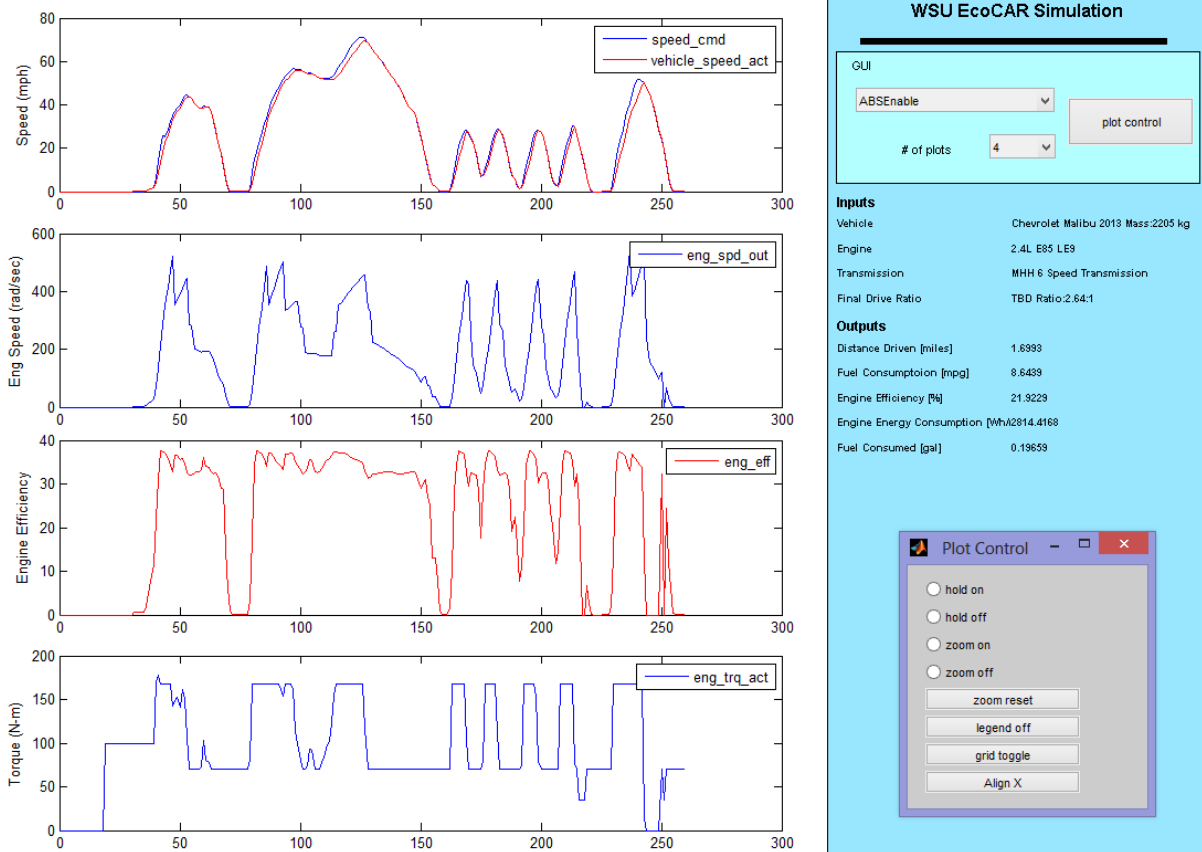


Figure 2-7. Analysis Tool-Analysis GUI

Figure 2-7 presents the Analysis GUI. After the simulation is done, the Analysis GUI will pop out automatically for the user's review. This window allows the user to investigate up to 32 variables at the same time by plotting up to 8 variables in each graph. The pull-down menu at the

right hand side of the window allows the user to select desired variables. The Plot Control button is a manipulation toolbox, it offers useful features like zoom in, zoom out, hold on (add another variable on the same graph), adding a grid and aligning all graphs to the same time window.

With the provided techniques the user is free to analyze the result as needed.

The usefulness of the analysis tools and the ability to customize them as needed is greatly appreciated during the development of thermal modeling, the validation and result analysis in later section can't be done without the help of these tools.

2.6 Thermal Model Organization

The thermal model is in compliance with hierarchy in HEV, as illustrate in Figure 2-8, the add-on thermal models are marked in dashed block. The engine, ESS, Motor/MCU thermal model is created within the each component plant model, which is responsible for predicting temperature based on physics. There are 2 levels of control actions – component control and supervisory control. The component ECUs are compiled as per component documentation. ECM already has its own thermal control algorithm compiled it reports its thermal request to thermal manager in supervisory controller. BCM and MCU provide their temperature signals to thermal manager. Body Controller Module (BodyCM) reports cabin temperature and user thermal request. Finally the thermal manager on top level makes final decision according to comprehensive analysis.

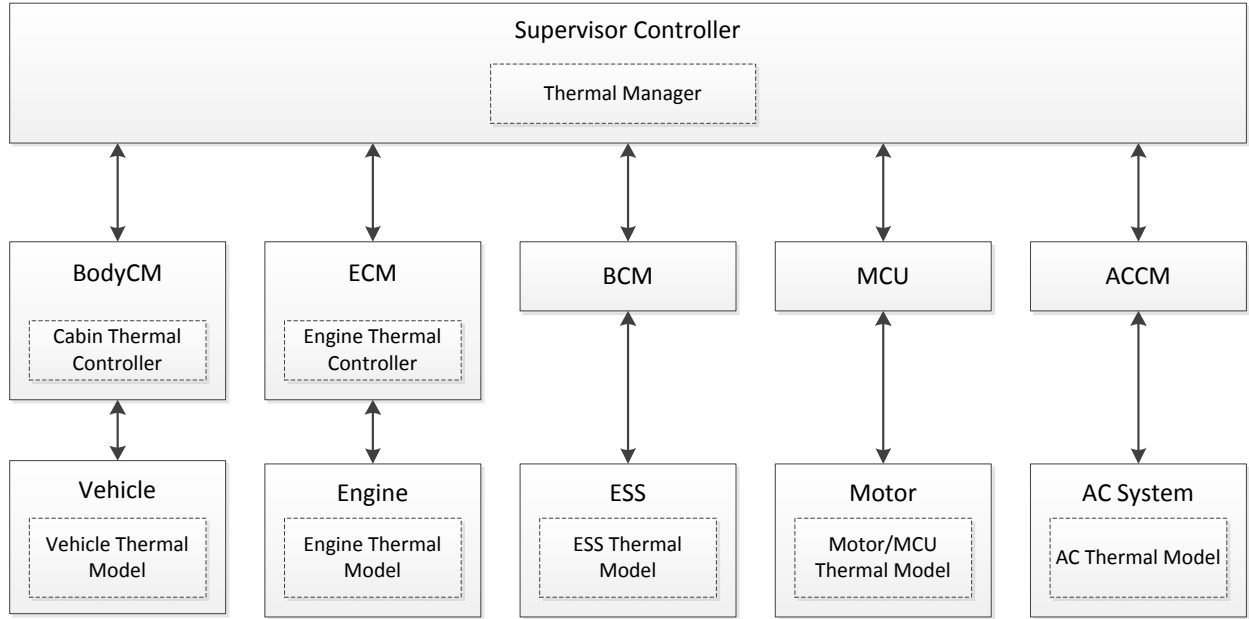


Figure 2-8. Thermal Model Organization

CHAPTER 3. PTTR HYBRID VEHICLE SYSTEM COOLING LOOPS

3.1 Cooling Loop Design

WSU PTTR vehicle is equipped with three fully independent cooling loops, as shown in Figure 3-1. The complete and detailed component list is given in Appendix A. Table 3-1 summarizes the control target temperature of each powertrain component. Additional radiators, pumps, valves and circuits are necessary to satisfy the various requirements. The guideline of cooling loop design is to reach maximum efficiency and space utilization.

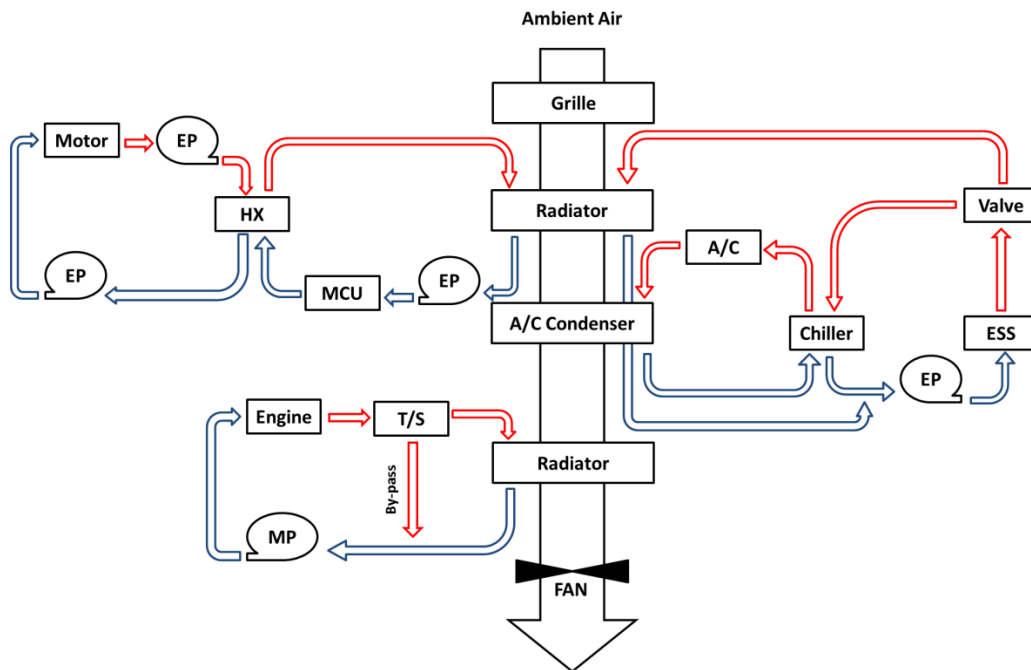


Figure 3-1. Vehicle Cooling System Architecture (EP: Electric Pump, MP: Mechanical Pump, T/S: Thermostat, HX: Heat Exchanger)

Table 3-1. Component Target Temperature

| Component | Control Target Temperature (°C) |
|-----------------------|----------------------------------------|
| Engine | 120 |
| ESS | 40 |
| Electric Motor | 90 |
| MCU | 70 |

The engine cooling loop is specific to cool the 2.4L E85 engine, this cooling loop basically carried over the stock engine cooling system with minor change in cooling line routing. The engine cooling system includes the heat source ICE, the stock belt-driven pump, the thermostat and the radiator. Since the pump is mechanically controlled by engine speed rather than ECU, the thermostat serves the purpose to regulate the operating temperature of the engine.

The ESS cooling loop is specific in cooling the high voltage battery. The heating of ESS is not in the scope of this design. The major components including heat source ESS, a 2-way chiller valve, a battery chiller, the stock AC system and the radiator. The ESS loop has its own 12-volt electric pump to circuit the coolant.

There are two circuits in ESS cooling loop, the chiller valve routes the coolant through the radiator or the battery chiller depends on the coolant temperature of ESS. The battery chiller acts as a heat exchanger transferring heat carried by coolant to AC system, which is a complete refrigeration cycle shared with cabin. As emphasis is placed on thermal modeling of HEV powertrain, the modeling of AC system and cabin is simplified. The cabin temperature is assumed to be the same with ambient temperature (25°). In this design, AC compressor shall respond to cooling request from cabin and ESS based on their temperature. The reason for

integrating ESS cooling loop with stock AC system is because of the ESS operation temperature is close to cabin temperature. Also due to the performance of battery is strongly temperature-dependent, when regular radiator cooling can't meet demand, the AC system can act as an effective cooling device to protect the ESS from thermal runaway.

The Motor/MCU cooling loop is dedicated to prevent the important power electronics from overheat during use. This loop has electric motor and MCU as dual heat sources, and a liquid-to-liquid heat exchanger to connect them. The waste heat is finally dissipated at radiator. A dry sump oiling/cooling system is adopted for electric motor for the safety concern, but the MCU required water cooling. To avoid fabricating another separated cooling loop, the liquid-to-liquid heat exchanger is adopted for 2 main reasons. First, the operation temperature of motor and MCU is relatively similar, making it possible for a connected thermal management. Second, the combined cooling design can reduce cost while save room.

3.2 Cooling Component Sizing

This section will mainly discuss the cooling components sizing for add-on ESS and Motor/MCU cooling loop. The engine cooling loop retains the stock components.

Cooling performance and packaging are the 2 major constrains in cooling component sizing. First, the cooling components must be capable of removing the heat generated by heat source component, and then the size has to be limited by the available packaging space of the vehicle. The cooling components should be carefully sized to satisfy both constraints.

Heat exchanger and pump sizes play the most important part in determining cooling performance. A thermal assessment method is applied for the estimation of heat exchanger and pump sizes. From thermal management standpoint, the optimal scenario will be the heat

generated at component peak power can be removed easily. However, that will lead to the risk of oversizing. In order to achieve a reasonable trade-off relationship between capacity and sizing, the thermal assessment is based on continuous performance of heat source component. Generally, the thermal assessment method can be divided into 4 steps:

- Determine heat generation rate
- Calculate radiator performance
- Design battery chill plate
- System pressure drop

3.2.1 Determine Heat Generation Rate

The EcoCAR2 competition has a designated 4-cycle drive schedule which blends 4 standard certification test cycles includes “505” portion of UDDS, HWFET, US06 City and US06 Highway. The baseline is to ensure the proposed heat sink components, under nominal operation condition, have enough capacity to remove the heat generated by the heat source components under competition required drive cycles.

The heat generation rates of ESS, motor and MCU under the 4 driving conditions, at ambient temperature 25°C, are compared to find the maximum heat load for the cooling system. Figure 3-2 represents the heat generation performance of RWD powertrain components under US06_city drive cycle. The average heat generation rates are summerzied in Table 3-2.

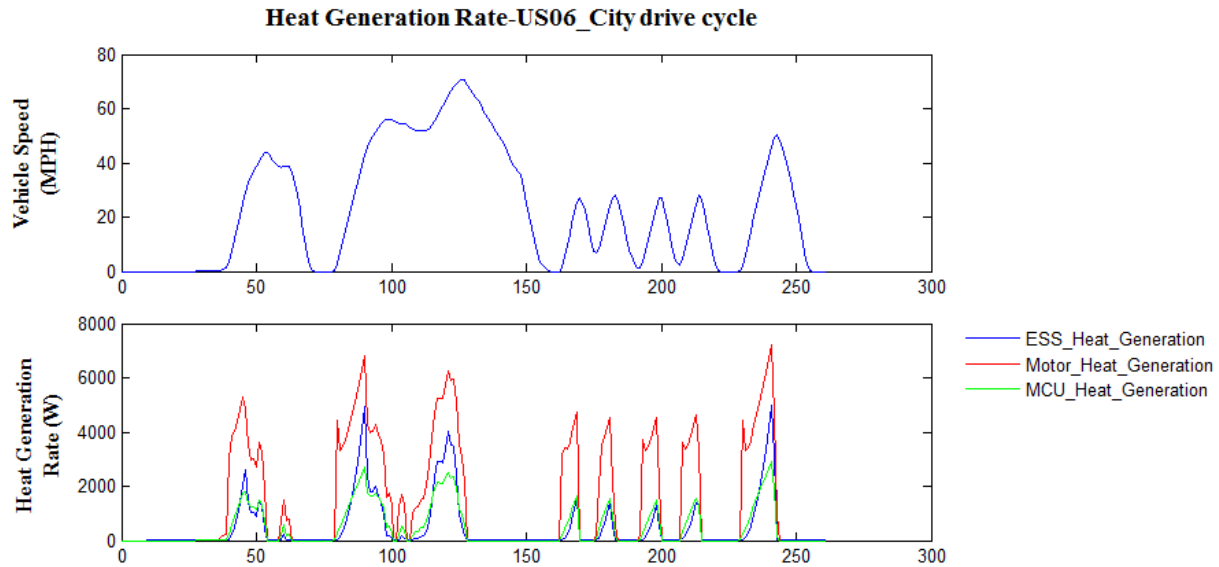


Figure 3-2. Heat Generation Rate under US06_City Drive Cycle

Table 3-2. The Average Heat Generation Rate for Each Drive Cycle

| Component | Average Heat Generation Rate (W) | | | | Maximum Heat Generation Rate (W) |
|-----------|----------------------------------|-------|-----------|--------------|----------------------------------|
| | 505 | HWFET | US06_City | US06_Highway | |
| ESS | 95 | 140 | 468 | 487 | 487 |
| Motor | 781 | 1319 | 1459 | 2214 | 2214 |
| MCU | 243 | 404 | 463 | 691 | 691 |

Maximum heat generation of each powertrain component is the guideline for the cooling component sizing. As seen above, the heat generation rate under designated drive cycle is estimated by vehicle simulation, of which the US06_Highway drive cycle is the most severe condition. The maximum heat generation rate above is used for heat exchangers sizing.

3.2.2 Calculate Radiator Performance

A dual-partition radiator is desired due to the very limited space behind the grill. It is preferred to adopt an off-shelf radiator rather than design a custom one. Fortunately, there is an option might meet the team's need—Chevy Volt radiator.

Chevy Volt radiator is analyzed to determine if the heat transfer rate can meet heat generation rate calculated above for prescribed flow rates and temperatures. The radiator model is created as a “calculator” to perform the analysis, it accepts air speed, coolant flow rate and coolant temperature as inputs and compute heat capacity. The engineering equations applied to perform the calculation will be addressed in detail in 4.2.1 Radiator section, and the proposed radiator model is given in Figure 4-7. The prescribed condition and calculated result is listed in Table 3-3. Note that for Motor/MCU cooling loop, the nominal coolant flow rate is the water coolant flow rate of MCU circuit. In theory it shall be able to manage both motor and MCU heat generation, so the total heat of Motor/MCU loop shall be 2905W.

The calculated heat capacity of radiator is greater than maximum heat generation rate for ESS, Motor/MCU loop, respectively. Both partitions of Chevy Volt radiator are capable of removing heat under the most severe driving condition. It can be an ideal choice for the team because it meets both packaging and capacity requirement.

Table 3-3. The Calculated Radiator Capacity

| | ESS cooling loop | Motor/MCU cooling loop |
|------------------------------------|------------------|------------------------|
| Ambient temperature (°C) | 25 | 25 |
| Intake air velocity (m/s) | 10 | 10 |
| Nominal coolant flow rate (LPM) | 15 | 12 |
| Operation coolant temperature (°C) | 30 | 60 |
| Calculated heat capacity (W) | 1152 | 3408 |

3.2.3 Design ESS Chill Plate

The team needs a custom chill plate designed to cool down the battery pack. The chill plate will be placed under the battery pack in the interest of easy packaging. The coolant can be circulated through to maintain low temperature gradients within the ESS. An aluminum chill plate with serpentine copper coolant pipes running a 50/50 mix of water and glycol is used to cool the battery.

A battery chill plate design calculator was created to predict the performance of the chill plate. Assumptions were made for the chill plate design input parameters such as plate dimensions, coolant flow rate, copper tube inner diameter and thickness, inlet temperature of the coolant, maximum allowable coolant outlet temperature, number of passes of tubes within the plate, etc. Figure 3-3 shows the calculator interface built for the required calculations.

| Inputs | | | | | | | | | | | | | | | | | |
|----------------------------------------------------------------------------------------------------------------------------------------------------------------------------------------------------------------------------------------------------------------------------------------------------------------------------------------------------------------------------------------------------------------------------------------------------------------------------------------------------------|----------|------------------------|--|---------------------------------|------|----------------------------------|-----|--------------------------------------|---------|-----------------------|----------|------------|---|----------------------------------|-----|-------------------------------|-------|
| <table border="1"> <thead> <tr> <th colspan="2">Heat Generation</th> </tr> </thead> <tbody> <tr> <td>Max Power drawn (KW)</td> <td>61.2</td> </tr> <tr> <td>Nominal Pack Voltage (V)</td> <td>340</td> </tr> <tr> <td>No of Modules in Pack</td> <td>7</td> </tr> <tr> <td>Module Specifications</td> <td>15 S 3 P</td> </tr> </tbody> </table> | | Heat Generation | | Max Power drawn (KW) | 61.2 | Nominal Pack Voltage (V) | 340 | No of Modules in Pack | 7 | Module Specifications | 15 S 3 P | | | | | | |
| Heat Generation | | | | | | | | | | | | | | | | | |
| Max Power drawn (KW) | 61.2 | | | | | | | | | | | | | | | | |
| Nominal Pack Voltage (V) | 340 | | | | | | | | | | | | | | | | |
| No of Modules in Pack | 7 | | | | | | | | | | | | | | | | |
| Module Specifications | 15 S 3 P | | | | | | | | | | | | | | | | |
| <table border="1"> <thead> <tr> <th colspan="2">Coolant Flow Condition</th> </tr> </thead> <tbody> <tr> <td>Flow Rate (L/min)</td> <td>15</td> </tr> <tr> <td>Inlet Temperature (degree C)</td> <td>20</td> </tr> <tr> <td>Max Allowable Outlet temperature (C)</td> <td>25</td> </tr> <tr> <td>Inlet pressure (bar)</td> <td>1.08</td> </tr> </tbody> </table> | | Coolant Flow Condition | | Flow Rate (L/min) | 15 | Inlet Temperature (degree C) | 20 | Max Allowable Outlet temperature (C) | 25 | Inlet pressure (bar) | 1.08 | | | | | | |
| Coolant Flow Condition | | | | | | | | | | | | | | | | | |
| Flow Rate (L/min) | 15 | | | | | | | | | | | | | | | | |
| Inlet Temperature (degree C) | 20 | | | | | | | | | | | | | | | | |
| Max Allowable Outlet temperature (C) | 25 | | | | | | | | | | | | | | | | |
| Inlet pressure (bar) | 1.08 | | | | | | | | | | | | | | | | |
| <table border="1"> <thead> <tr> <th colspan="2">Cold Plate Parameters</th> </tr> </thead> <tbody> <tr> <td>Length (mm)</td> <td>874</td> </tr> <tr> <td>Width (mm)</td> <td>612</td> </tr> <tr> <td>Copper tube ID (mm)</td> <td>10.2108</td> </tr> <tr> <td>Copper tube OD (mm)</td> <td>12.7</td> </tr> <tr> <td>No of Pass</td> <td>4</td> </tr> <tr> <td>Di-electric layer thickness (mm)</td> <td>0.5</td> </tr> <tr> <td>Aluminum plate thickness (mm)</td> <td>9.525</td> </tr> </tbody> </table> | | Cold Plate Parameters | | Length (mm) | 874 | Width (mm) | 612 | Copper tube ID (mm) | 10.2108 | Copper tube OD (mm) | 12.7 | No of Pass | 4 | Di-electric layer thickness (mm) | 0.5 | Aluminum plate thickness (mm) | 9.525 |
| Cold Plate Parameters | | | | | | | | | | | | | | | | | |
| Length (mm) | 874 | | | | | | | | | | | | | | | | |
| Width (mm) | 612 | | | | | | | | | | | | | | | | |
| Copper tube ID (mm) | 10.2108 | | | | | | | | | | | | | | | | |
| Copper tube OD (mm) | 12.7 | | | | | | | | | | | | | | | | |
| No of Pass | 4 | | | | | | | | | | | | | | | | |
| Di-electric layer thickness (mm) | 0.5 | | | | | | | | | | | | | | | | |
| Aluminum plate thickness (mm) | 9.525 | | | | | | | | | | | | | | | | |
| <table border="1"> <thead> <tr> <th colspan="2">Start-up Case</th> </tr> </thead> <tbody> <tr> <td>Initial Battery temperature (C)</td> <td>45</td> </tr> <tr> <td>Expected Battery Temperature (C)</td> <td>30</td> </tr> </tbody> </table> | | Start-up Case | | Initial Battery temperature (C) | 45 | Expected Battery Temperature (C) | 30 | | | | | | | | | | |
| Start-up Case | | | | | | | | | | | | | | | | | |
| Initial Battery temperature (C) | 45 | | | | | | | | | | | | | | | | |
| Expected Battery Temperature (C) | 30 | | | | | | | | | | | | | | | | |
| <div style="border: 2px solid cyan; padding: 5px; display: inline-block; background-color: cyan; color: black; font-weight: bold;">Calculate</div> | | | | | | | | | | | | | | | | | |
| Outputs | | | | | | | | | | | | | | | | | |
| Overall Heat Generation (W) | 2381.4 | | | | | | | | | | | | | | | | |
| Coolant Outlet temperature (C) | 22.7436 | | | | | | | | | | | | | | | | |
| Chill plate surface temperature (C) | 26.6461 | | | | | | | | | | | | | | | | |
| Pressure drop (mbar) | 686.979 | | | | | | | | | | | | | | | | |
| Outlet pressure (bar) | 0.393021 | | | | | | | | | | | | | | | | |
| Time required to cool down (min) | 21.581 | | | | | | | | | | | | | | | | |

Figure 3-3. Battery Chill Plate Design Calculator

Based on whether the flow is laminar or turbulent, the dimensionless temperature gradient, Nusselt Number was calculated to find the convection heat transfer coefficient.

$$\text{Laminar Flow: } Nu_D = \frac{hL}{k} = 4.36 \quad (Re < 2300) \quad (3.1)$$

$$\text{Turbulent Flow: } Nu_D = \frac{hL}{k} = \frac{(f/8)(Re - 1000)Pr}{1 + 12.7(f/8)^{\frac{1}{2}}(Pr^{\frac{2}{3}} - 1)} \quad (Re > 2300) \quad (3.2)$$

Also depends on fluid condition, friction factor can be computed as:

$$\text{Laminar Flow: } f = 64/Re \quad (Re < 2300) \quad (3.3)$$

$$\text{Turbulent Flow: } f = (0.790 \ln Re - 1.64)^{-2} \quad (Re > 2300) \quad (3.4)$$

An equivalent thermal series circuit was considered in one dimensional heat flow from chill plate top surface to the coolant flow through dielectric layer, aluminum plate and copper tube.

$$R_{total} = R_{die} + R_{Al} + R_{Cu} + R_{conv} \quad (3.5)$$

To calculate the battery surface temperature by using:

$$T_s = T_{cht,in} + \dot{E}_{ess,gen} * R_{total} \quad (3.6)$$

For a design of 4 return bends, the pressure drop was calculated to find the minimum required inlet pressure. Given loss coefficient k_L is 0.2 for minor loss at 180° return bend, the pressure drop is the sum of major pressure loss and minor pressure loss:

$$\Delta P = N_{bend} \times \frac{\rho \times k_L \times V^2}{2} + \rho \times \frac{L}{D} \times \frac{V^2}{2} \times f \quad (3.7)$$

At start-up case, when the battery was soaked at 45°C ambient temperature, the time required to cool down the battery pack to 30°C was calculated by using the first law of thermodynamics.

After design calculation and CFD analysis, finally a 874×612×19.05 mm aluminum chill plate with bended coolant pipe, of which inner diameter is 10.21mm, outer diameter is 12.7mm, was fabricated, shown in Figure 3-4.



Figure 3-4. Battery Chill Plate

3.2.3 Cooling System Pressure Drop

Controllable electric pumps are chosen for the proposed cooling design. To properly predict pump performance one must first approximate the total pressure drop through the cooling system. The system curve should be plotted against the pump characteristics curves at commanded speed, and the cross points are the actual duty points of the pump. System resistance concept is applied to calculate the pressure drop across various components in the cooling loops. First the pressure loss of each component is identified, from manufacturer rating or hand calculation, and then the system resistance could be determined as the sum of individual pressure loss. The pump performance will be addressed later in Fluid Delivery Component section in Chapter 4.

3.2.3.1 ESS Cooling Loop

The ESS loop contains 2 circuits, as shown in Figure 3-5, the total pressure loss is the sum of resistances depending on which circuit coolant flow through.

The pressure drop in the radiator circuit is calculated as:

$$\Delta P_{ess,rad} = \Delta P_{chill\ plate} + \Delta P_{chiller\ valve} + \Delta P_{rad} + \Delta P_{pipe} \quad (3.8)$$

The pressure drop in the by-pass circuit is calculated as:

$$\Delta P_{ess,chiller} = \Delta P_{chill\ plate} + \Delta P_{chiller\ valve} + \Delta P_{chiller} + \Delta P_{pipe} \quad (3.9)$$

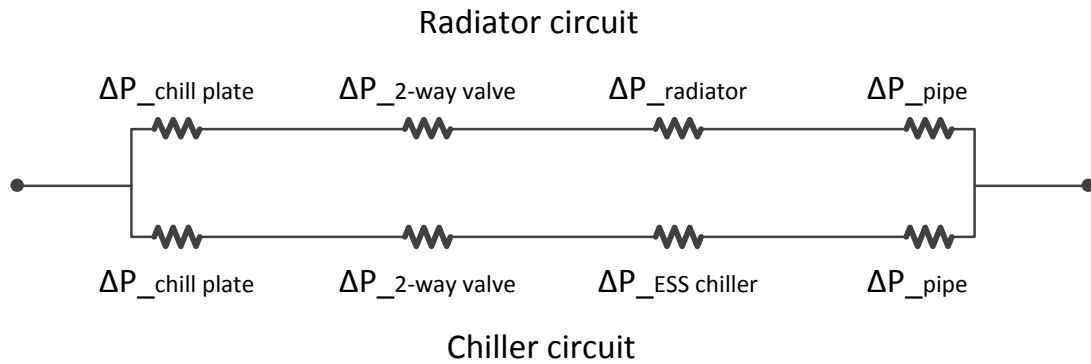


Figure 3-5. System Resistance of ESS Loop

The total pressure drops across different components of ESS cooling system is shown in Figure 3-6. Where the pressure drop of radiator is calculated from friction factor of smooth flat tubes, addressed in Figure 4-6. Currently the pressure drop of ESS chiller is approximated, analysis of internal geometry or experiment needs to be done in the future to obtain more accurate data. The pressure loss of chill plate is calculated with chill plate design calculator in Figure 3-3.

The chiller valve is considered as a tube with 90° elbow bend, given the loss coefficient k_L is 0.3.

$$\Delta P = N_{bend} \times \frac{\rho \times k_L \times V^2}{2} \quad (3.10)$$

The pressure loss of pipe is calculated using Equation 4.12. The standard plastic pipe specification is given in Table 4-4. The friction factor of pipe for laminar flow and turbulent flow can be calculated with Equation (3.3) and (3.4).

$$\Delta P = \rho \times \frac{L}{D} \times \frac{V^2}{2} \times f \quad (3.11)$$

The total pressure drop of ESS cooling system at various coolant flow rate is presented in Figure 3-6.

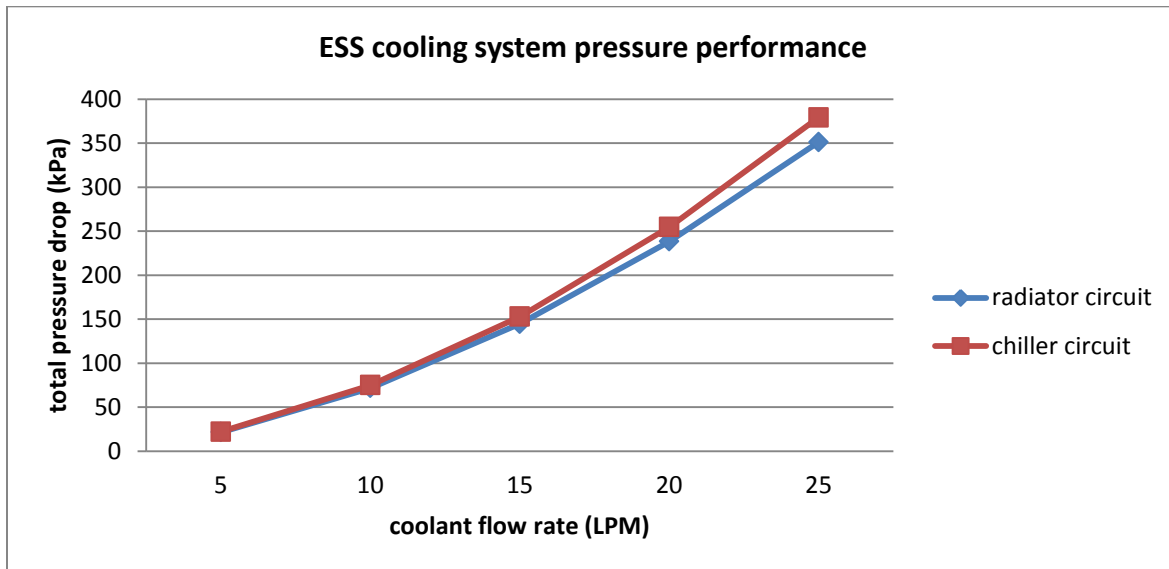


Figure 3-6. Total Pressure Drop of ESS Cooling Loop

3.2.3.2 Motor /MCU Cooling Loop

As shown in Figure 3-7, the Motor/MCU also contains 2 circuits, but each circuit has its own pump to circulate the coolant.

The pressure drop in motor circuit yields to:

$$\Delta P_{mot} = \Delta P_{hx} + \Delta P_{motor} + \Delta P_{pipe} \quad (3.12)$$

The pressure drop in MCU circuit yields to:

$$\Delta P_{mcu} = \Delta P_{mcu} + \Delta P_{hx} + \Delta P_{rad} + \Delta P_{pipe} \quad (3.13)$$

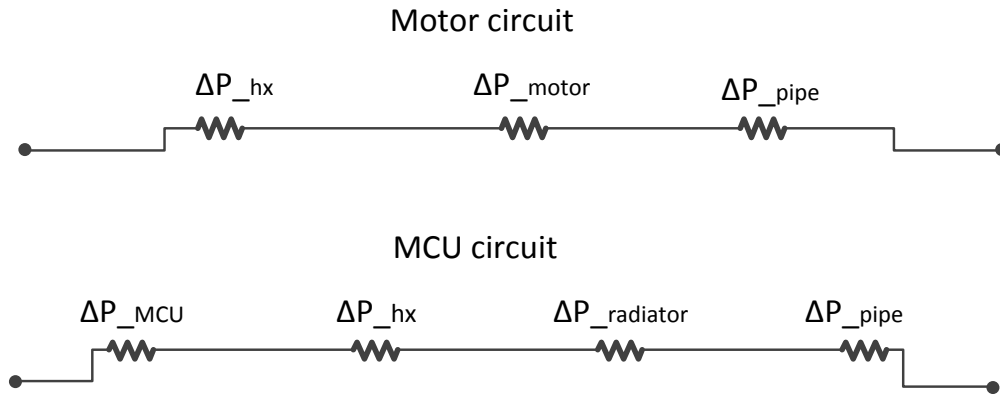
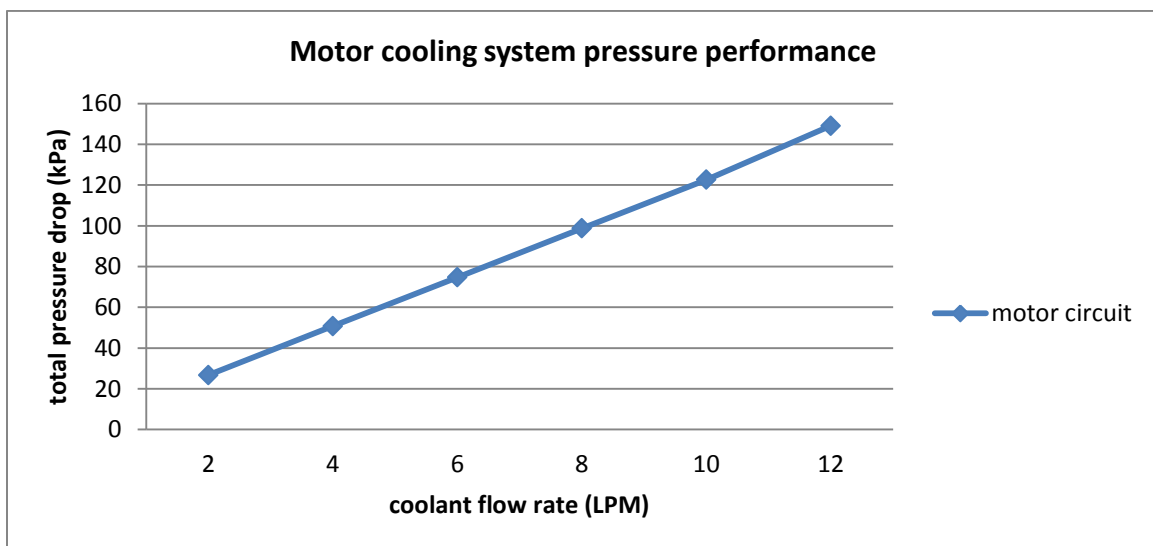


Figure 3-7. System Resistance of Motor/MCU Loop

The total pressure drops across Motor/MCU loop are summarized in Figure 3-8. The pressure losses across electric motor, MCU are provided by manufacture. Since Motor/MCU shares the same 2-partition radiator with ESS loop, the calculation method of pressure drop through radiator is the same with ESS. The pressure drop through the oil-to-water heat exchanger is obtained from performance map by manufacture.



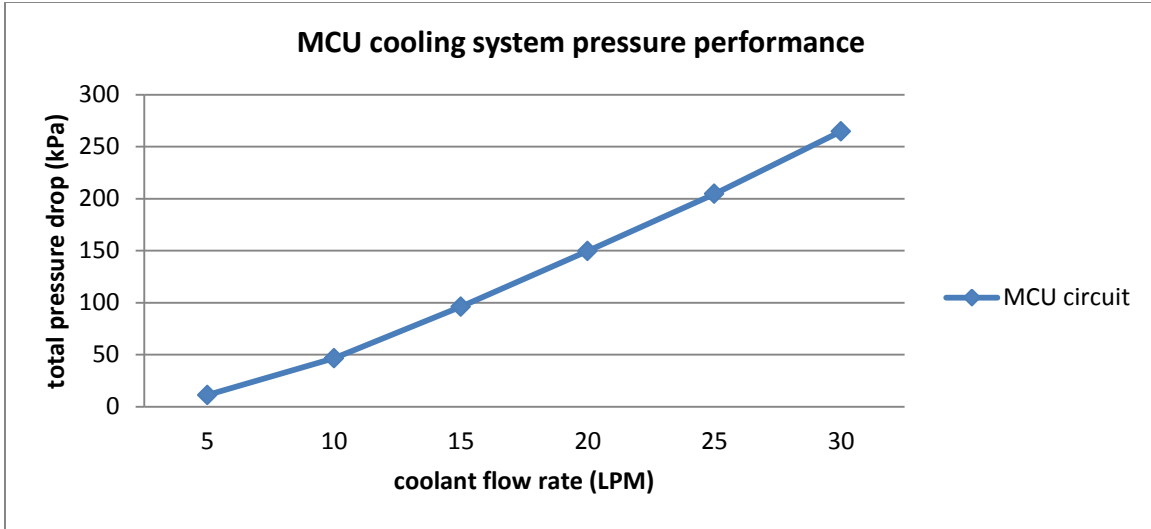


Figure 3-8. Total Pressure Drop of Motor/MCU Cooling Loop

3.2 Cooling Loop Configuration

The final ESS cooling loop configuration is presented in Figure 3-9. The team designed ESS cooling loop is analogous to Chevy Volt battery cooling system, except that Chevy Volt battery cooling system has another heater circuit to satisfy battery heating requirements [18]. The team had suggested introducing a heating element in cases of extremely low ESS temperatures, the team keeps this option for extreme weather cases but this is not necessary to meet current requirements.

The similarity between the 2 cooling design had offered the team great convenience to select off-shelf components from Chevy Volt and take advantage of their easy packaging. The original Malibu compressor is replaced with the Chevy Volt compressor for larger capacity. The dual-partition Volt radiator serves both ESS and Motor/MCU cooling loops, and the one-of-a-kind Volt reservoir has 2 independent containers to store water coolant for ESS and MCU. The ESS chiller is a coolant-to-refrigerant heat exchanger, so the AC system can be used to decrease the temperature of the ESS coolant to archive enhanced cooling effects. The available options for

ESS chiller is relatively small due to its limited application, the Volt chiller is chosen because its similarity in application and reliability. Another Thermal Expansion Valve (TXV) is needed to regulate the refrigerant flow to ESS chiller, one is supplied with the stock vehicle for cabin climate control and the team chose the same TXV for ESS chiller for the sake of easy flow management. The evaporator, accumulator and condenser are carried over from stock Malibu.

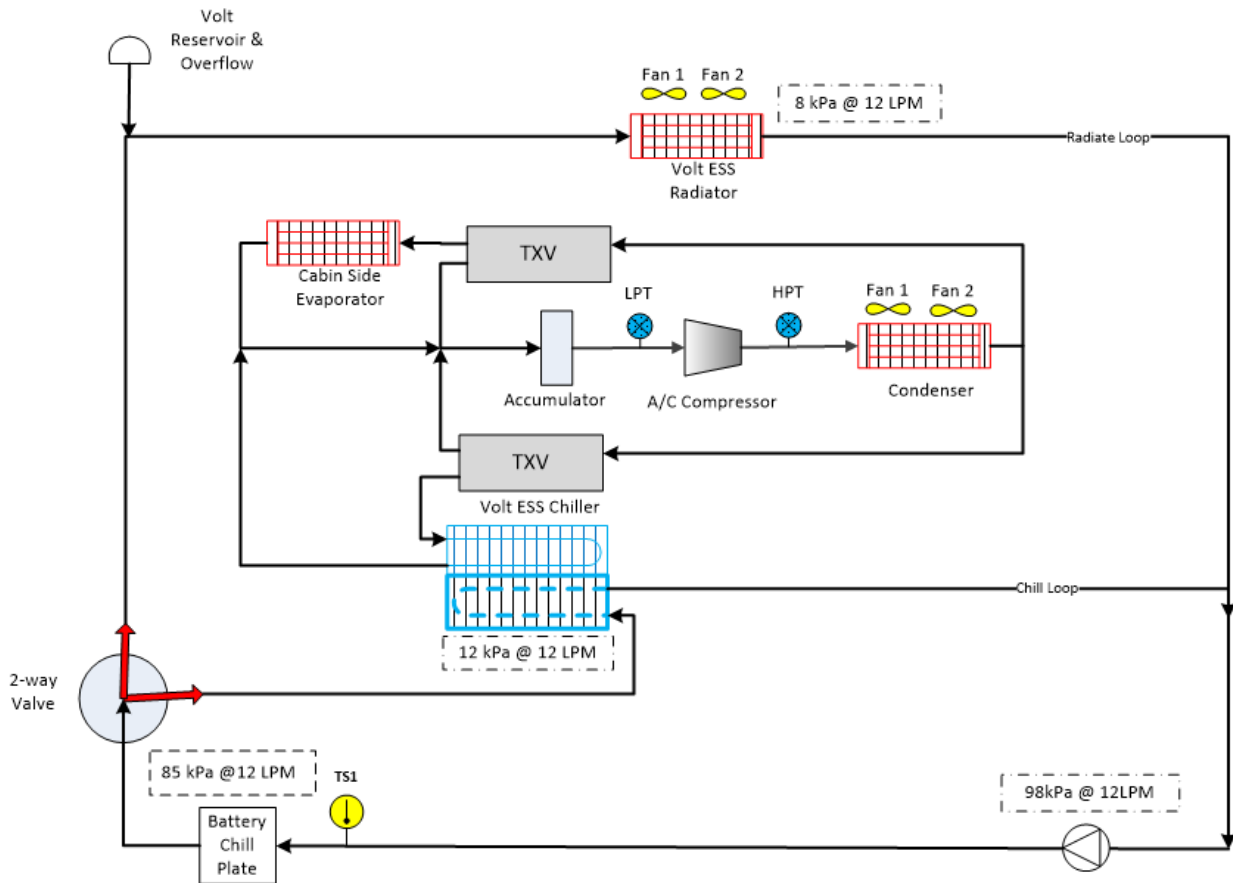


Figure 3-9. ESS Cooling Loop Configuration

Figure 3-10 shows the Motor/MCU cooling loop configuration. It shares the same Volt radiator and reservoir with ESS cooling loop.

A dry sump oiling/cooling system is adopted for electric motor for the safety concern. Sufficient scavenging during operation must be offered to ensure that oil does not collect in the air gap, oil accumulation in the air gap can result in large increases in frictional drag; heat rejection requirements increase many times due to the shearing of the fluid, and if these requirements are not met, motor damage can occur. In a dry sump design, extra oil is stored in a sump outside motor housing, the feed pump draws oil from the sump and sends it to lubricate and cool the motor, the evacuation pump pulls oil from motor and circuits it back to the sump. As motor manufacturer requires the cooling fluid to be filtered to 60 microns or less to ensure protection of internal bearings, windings and other internal components, a 45 micron filter is chosen. A one-way check valve is also added to prevent back-flow.

One major design changes made during Year 2 included the modification from 2-electric-motor design to single motor due to motor housing design difficulties that may affect component integration. It is suggested by manufacture to use the commercially available Laminova C43-180 (diameter 43mm, length 180mm) oil-to-water heat exchanger for the 2-motor architecture. The team downsizes the heat exchanger to C43-90 (diameter 43mm, length 90mm) in response to the design change.

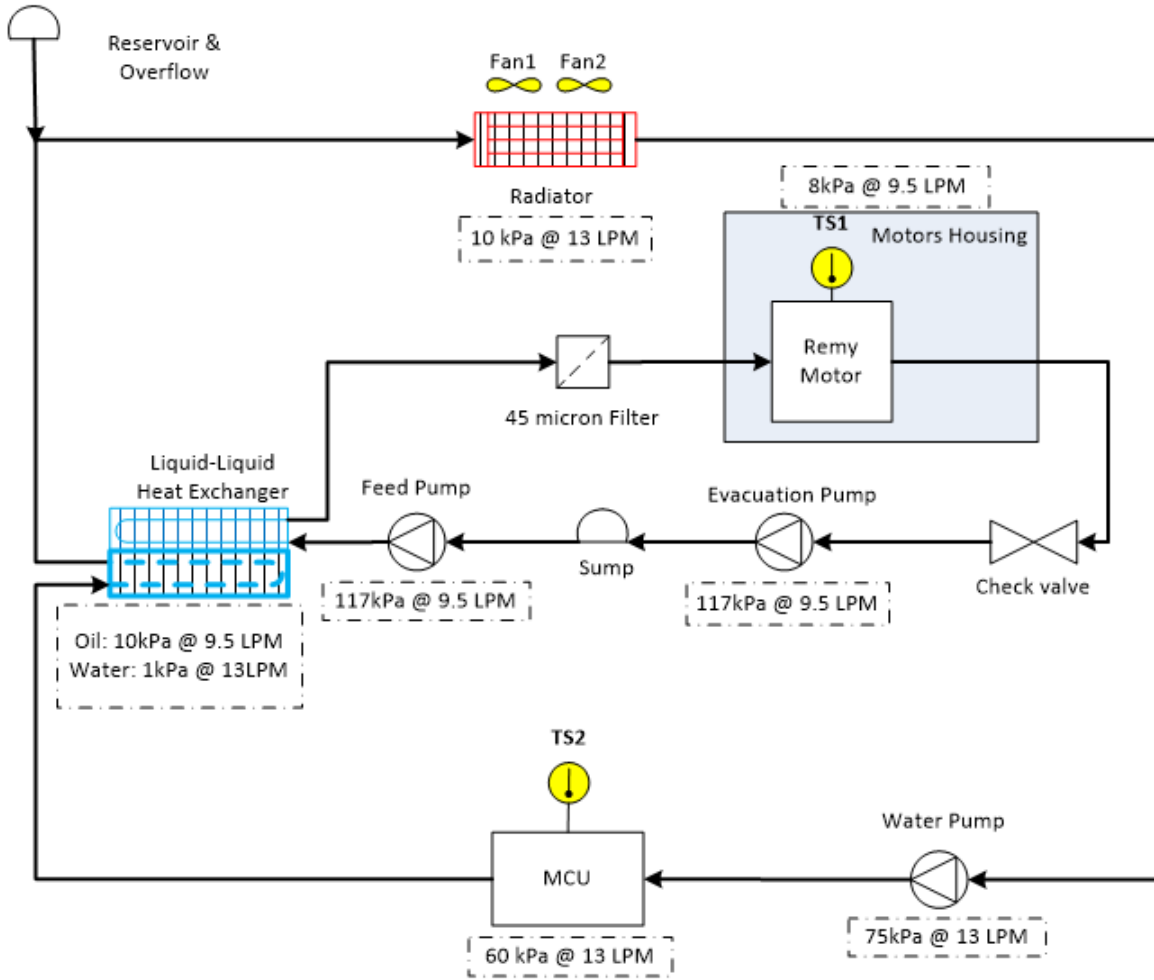


Figure 3-10. Motor/MCU Cooling Loop Configuration

CHAPTER 4. COMPONENT AND SUB-SYSTEM THERMAL PLANT MODEL DEVELOPMENT

The components mentioned in foregoing cooling system can be categorized by their function into heat source, heat sink and fluid delivery components.

The thermal model is based on a simple lumped thermal mass approach, which treats the entire component with all the subcomponents inside of it as a single homogenous material with averaged properties, with an assumed uniform temperature. From a modeling standpoint, it means that the component temperature is assumed to be represented by a system-level average temperature [5].

Figure 4-1 explains the heat flow in a general cooling loop, which consists of heat source component, heat sink component, and the pipes connected between the two.

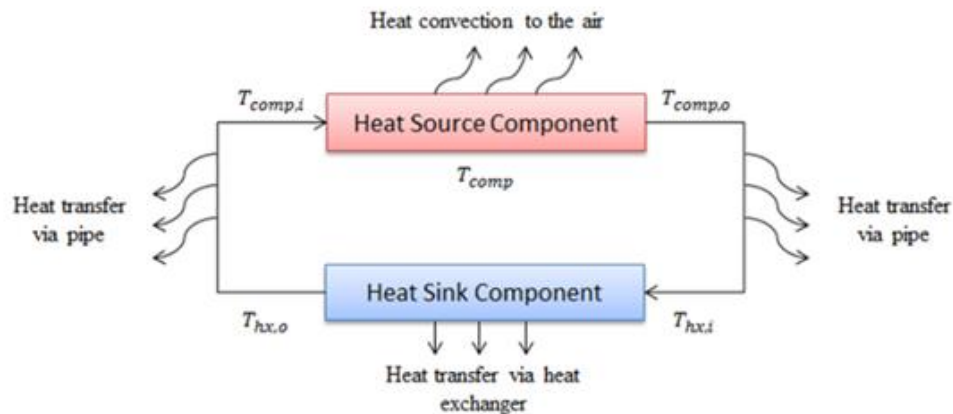


Figure 4-1. The Heat Flow Diagram

Consider the entire heat source component as the control volume, where the control surface will be the geometry surface of the component, the entire component block is treated as a single isothermal object. Equation (4.1) is derived from applying the law of conservation of energy to a heat source component. The temperature of component will increase or decrease

depends on whether heat generated inside the component and inflow heat is more or less than the outflow heat.

$$m_{comp}C_{p,comp}\frac{dT_{comp}}{dt} = q_{comp} + \dot{m}_cC_{p,clt}(T_{comp,i} - T_{comp,o}) \quad (4.1)$$

Initially, $T_{comp,i}(0)$ is assigned as ambient temperature. In this equation at each time step t , $T_{comp,i}(t - \Delta t)$ can be obtained from previous time step, $T_{comp,o}(t)$ needs to be solved. It is assumed that $T_{comp}(t) = T_{comp,o}(t)$. Therefore both can be calculated from Equation (1). This assumption is necessary because only one unknown can be solved from one single equation.

On the heat sink component side, the NTU method is used to calculate the rate of heat transfer in heat exchanger, which will be discussed in detail in Heat Sink Component section.

$$\dot{m}_{clt}C_{p,clt}(T_{hx,o} - T_{hx,i}) = \varepsilon C_{min}(T_{hx,i} - T_{air}) \quad (4.2)$$

On the right hand side of Figure 4, the coolant temperature at the exit of component is different from the coolant temperature at the entrance of heat exchanger, due to heat loss through the pipe. Equation (4.3) represents the solution for a plain pipe with combined internal-external flow.

$$\frac{T_{\infty} - T_{hx,i}}{T_{\infty} - T_{comp,o}} = \exp\left(-\frac{UA}{\dot{m}_{clt}C_{p,clt}}\right) \quad (4.3)$$

4.1 Heat Source Component

In this proposed study there are four major heat source components: flexible-fuel engine, ESS, electric motor and MCU.

There are previous work show detail and extensive numerical modeling about powertrain components. However, few have focused on system-level component temperature modeling for

the use within the existing over-all vehicle model. The heat generation of each component is constructed using available information within the plant model.

The heat of the engine targeted for removal is calculated as the fuel chemical power minus mechanical power, heat loss to the exhaust and forced convection to the air. In that, map-based performance model is employed to obtain fuel chemical power; mechanical power is a function of engine speed and torque, which already exist in the PTTR vehicle model. Exhaust heat is assumed to be a constant fraction of chemical power.

$$q_{eng} = \dot{E}_{fuel} - \dot{E}_{mech} - \dot{E}_{exh} - q_{eng,conv} \quad (4.4)$$

Since the ESS is placed in the trunk basically separated from external airflow, the convection from ESS to ambient air is regarded as negligible. The heat of ESS targeted for removal is mainly because of the heat generation in the core of the battery due to resistive heating:

$$q_{ess} = I^2 R \quad (4.5)$$

The heat target to remove by the electric motor and MCU is calculated by the power they delivered and the efficiency minus the forced convection heat transfer.

When motor is propelling:

$$q_{mot} = \omega_{mot} \times \tau_{mot} \times \left(\frac{1 - \eta_{mot}}{\eta_{mot}} \right) - q_{mot,conv} \quad (4.6)$$

$$q_{mcu} = \left(\frac{\omega_{mot} \times \tau_{mot}}{\eta_{mot}} \right) \times \left(\frac{1 - \eta_{mcu}}{\eta_{mcu}} \right) - q_{mcu,conv} \quad (4.7)$$

When motor is generating:

$$q_{mot} = |\omega_{mot} \times \tau_{mot}| \times (1 - \eta_{mot}) - q_{mot,conv} \quad (4.8)$$

$$q_{mcu} = |\omega_{mot} \times \tau_{mot} \times \eta_{mot}| \times (1 - \eta_{mcu}) - q_{mcu,conv} \quad (4.9)$$

4.1.1 Convection Heat Transfer Model

Boglietti and Cavagnino [19] had brought together useful heat transfer formulations that can be successfully applied to thermal analysis of powertrain components. Empirical heat transfer for the basic geometric shapes in terms of dimensionless numbers is used to predict the heat transfer coefficient.

Laminlar flow:

$$Nu = 0.664R^{1/2}Pr^{1/3} \quad (Re < 5 \times 10^5) \quad (4.10)$$

Turbulent flow:

$$Nu = (0.037Re^{4/5} - 871)Pr^{1/3} \quad (Re > 5 \times 10^5) \quad (4.11)$$

For the engine, in the usual case of a vehicle moving at variable velocity, forced convection due to the underhood air flow and nature convection caused by the temperature gradient between the heat source component and surroundings must be taken into account. For the ESS, as it is placed inside the trunk, it is fair to consider that natural convection is the primary contributor.

The engine block is simplified to a 3-D rectangular solid, with 4 vertical flat surfaces for the sides and 1 horizontal surface for the top. Since the bottom surface of engine is covered by splash shield, the convection from bottom surfaces is accounted as negligible. The electric motor is considered as a horizontal finite-length cylinder. The MCU is a well-defined 3-D rectangle, with the mounting surface assumed adiabatic. It is noted that this is a rather crude approximated approach, knowing that ICE, motor and MCU all have a front and a back surface that are perpendicular to the flow direction.

The air velocity has to be estimated to compute the formula, in their work of underhood flow analysis proposed by Ng and Watkins [20], the experimental result of average air velocity

across grille, airdam and fans and shroud at different vehicle speed is presented in Figure 4-2.

Even though motor and MCU are placed in rear compartment, it is assumed that they experience the similar air flow due to lack of specific experimental study.

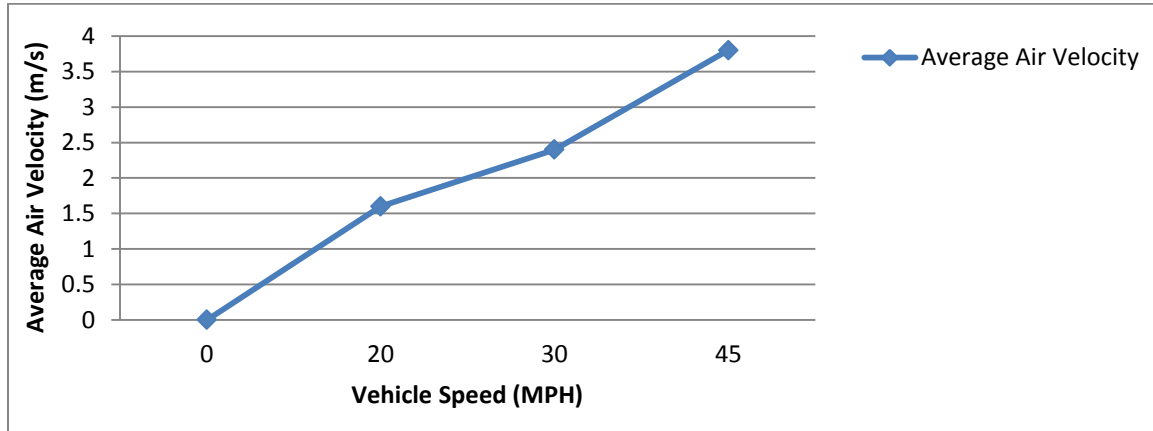


Figure 4-2. Underhood Air Velocity

Finally the convection from the component surface can be modeled as:

$$q_{conv} = hA(T_{comp} - T_{air}) \quad (4.12)$$

4.2 Heat Sink Component

4.2.1 Radiator

The radiator is a heat exchanger with the function of dissipating heat from cooling loop to environment. The cross-flow compact heat exchanger with louvered fins is employed in the proposed cooling design shown in Figure 4-3, the model can solve the overall heat transfer coefficient by given air flow and coolant flow, thus predict the heat rejection capacity of the radiator.

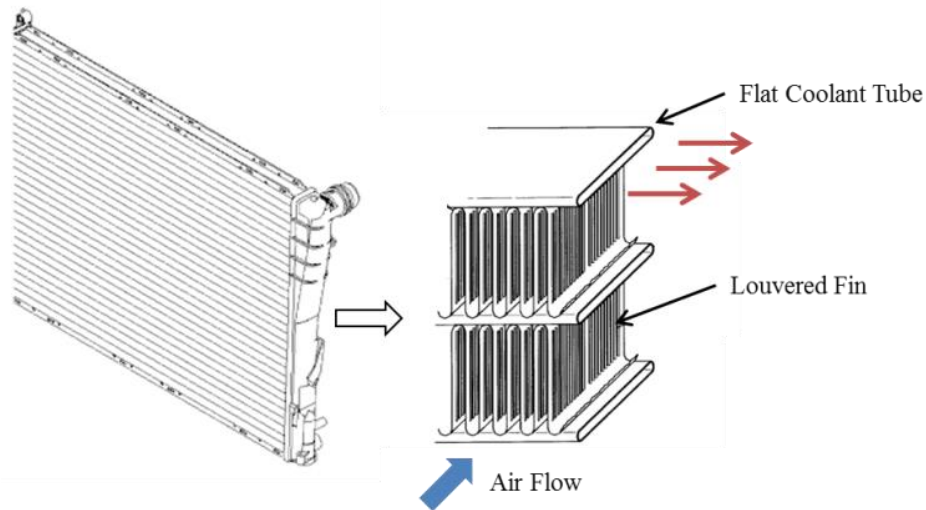


Figure 4-3. Schematic of Radiator

There are 3 major thermal resistances in the process of heat rejection from coolant to air. The first is convection from coolant to internal surfaces of tube, next conduction through the tube wall, then convection from external surface of tube plus conduction and convection from extended fin surfaces to air. Typical engineering approach to the problem of convection from a system level is to determine the convection coefficients for coolant side and air side, separately. After the individual resistances are modeled, the overall heat transfer coefficient and heat transfer rate can be calculated.

The air side convection heat transfer coefficient is calculated by using direct test data for finned flat tubes application proposed by Kays and London [21]. As shown in Figure 4-3, the actual fins are extremely narrow sinusoidal waves. However, they can be assumed be straight, rectangular fins, as shown in Figure 4-4, in order to take advantage of data available from Kays and London's study. A correction factor of 2 is applied in this model, as through measurement the louvered fins can be "flattened" to approximately twice the convective surface area.

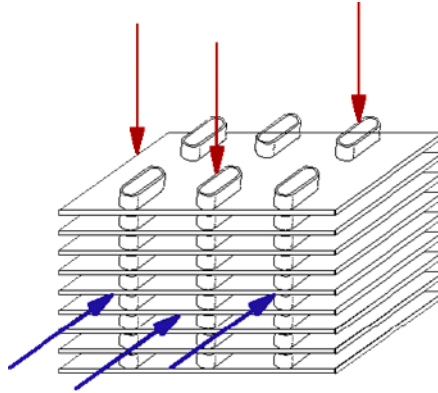


Figure 4-4. Finned Flat Tube Geometry

The heat transfer characteristic is correlated in terms of the Colburn j factor and the Reynolds number.

The heat transfer results are correlated in terms of the Colburn j factor and the Reynolds number, shown in Figure 4-5. Thanks to the similarity, the fin specification data for this geometry is also used to calculate the fin related parameters, as given in Table 4-1.

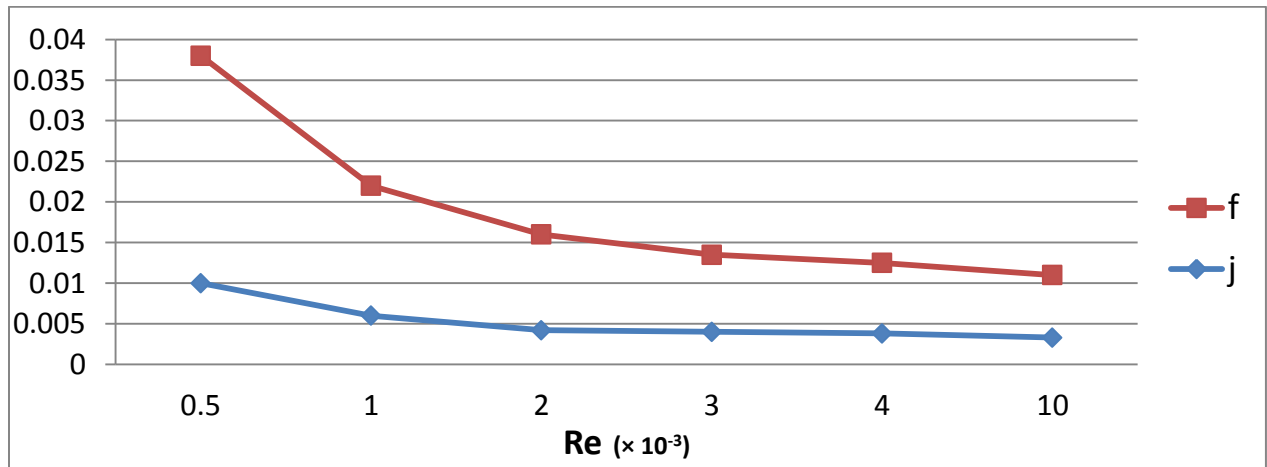


Figure 4-5. Heat Transfer Characteristic and Friction Factor for Finned Flat Tubes

Table 4-1. Specification for Finned Flat Tubes Heat Exchanger Core

| Specification for finned flat tubes | Value |
|---------------------------------------|---------------------------------------|
| Fin pitch | 381 per m |
| Free flow area/frontal area | $\sigma = 0.697$ |
| Total heat transfer area/total volume | $\alpha = 751 \text{ m}^2/\text{m}^3$ |
| Fin area/total area | 0.795 |

In that, the dimensionless Reynolds for the external flow can be obtained by:

$$Re_D = \frac{GD_h}{\mu_{air}} \quad (4.13)$$

$$G = \frac{\rho_{air}V_{air}A_{fr}}{A_{ff}} \quad (4.14)$$

Note that free flow area and frontal area ratio in Equation 4.14 is presented in Table 4-1.

The conversion between volumetric flow rate and air velocity is given by:

$$Q_{air} = V_{air}A_{fr} \quad (4.15)$$

The calculation of mass flow rate for air yields

$$\dot{m}_{air} = V_{air}\rho_{air}A_{fr} \quad (4.16)$$

The j_H factor correlation with heat transfer coefficient is defined as follow:

$$j_H = \frac{h_{air}}{GC_{p,air}} Pr^{2/3} \quad (4.17)$$

Given that the internal tube surface of the radiator is not finned, the fin efficiency calculation will only be for the air side. The overall fin efficiency can be defined as:

$$\eta_o = 1 - \frac{A_f}{A_{total}} (1 - \eta_f) \quad (4.18)$$

In that, the total heat transfer area can be obtain from α ratio in Table 4-1 when total volume is measured from stock radiator. And the fin area can be known using fin area/total area ratio provide in Table 4-1 as well.

Both Park [3] and Jung and Assanis [22] had applied the following fin efficiency formula in their study. It is assumed that the fin is insulated at the center, meaning that temperature differences between the tubes that share the fins are negligible. The fin efficiency can be computed for the case with an adiabatic tip:

$$\eta_f = \frac{\tanh(m(L_f/2))}{mL_f/2} \quad (4.19)$$

Also as in compact heat exchanger application, the width of the fin is much larger than its thickness, m may be approximated as:

$$m = \sqrt{\frac{2h_{air}}{k_f t_f}} \quad (4.20)$$

The convection heat transfer coefficient for coolant side can be obtained from thermal performance of the same geometry. In their paper Olsson and Sunden [23] had conducted an experimental investigation of the heat transfer characteristics of 10 real radiator tubes for cars, including the type of flat smooth tube, applicable to this study. The heat transfer data for smooth tube is also presented as the Colburn j factor and the Reynolds number correlation in Figure 4-6.

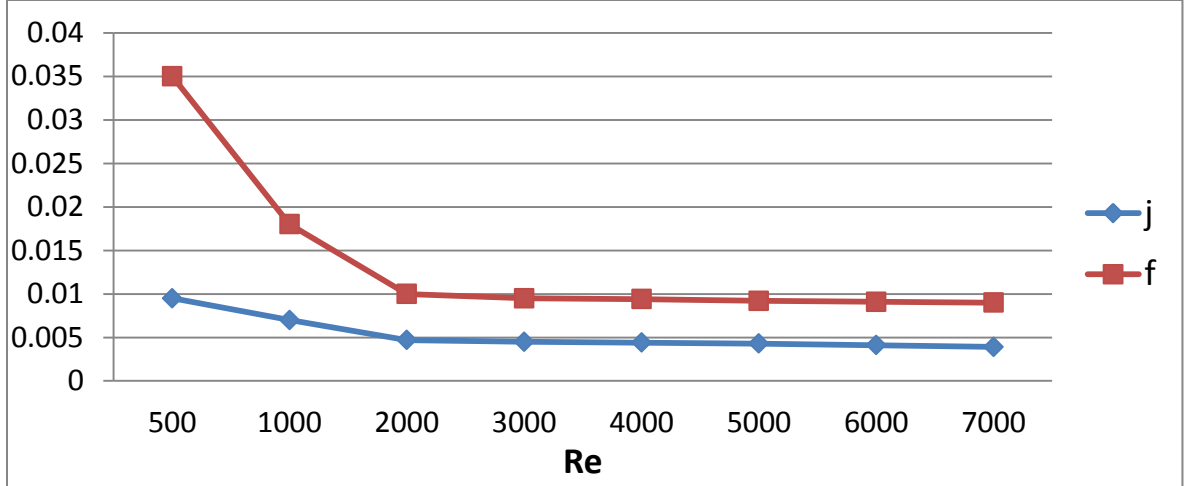


Figure 4-6. Heat Transfer Characteristic and Friction Factor for Coolant

The j factor correlation follows:

$$j_H = \frac{h_{clt}}{\rho_{clt} v_{clt} C_{p,air}} Pr^{2/3} \quad (4.21)$$

When the tube has noncircular cross-section, the hydraulic diameter should be calculated

as:

$$D_h = \frac{4A_{cr,tube}}{L_{p,tube}} \quad (4.22)$$

The dimensionless Reynolds number based on hydraulic diameter is expressed as:

$$Re_D = \frac{\rho_{clt} V_{clt} D_h}{\mu_{clt}} \quad (4.23)$$

In the modeling, the conversion between volumetric flow rate and coolant velocity is given by:

$$Q_{clt} = V_{clt} A_{cr,tube} N_{tube} \quad (4.24)$$

To compute mass flow rate of coolant:

$$\dot{m}_{clt} = V_{clt} \rho_{clt} A_{cr,tube} N_{tube} \quad (4.25)$$

After convection heat transfer coefficients for coolant side and air side are solved, the overall heat transfer coefficient of the proposed heat exchanger model can be computed using the following equation:

$$\frac{1}{UA} = \frac{1}{h_{clt}A_{tube}} + \frac{t_{tube}}{k_{tube}} + \frac{1}{\eta_o h_{air}A_{tota}} \quad (4.26)$$

Note that the calculation of UA product doesn't require the determination whether it is based on air side or coolant side, however, the calculation of overall heat transfer coefficient U does because surface area for air side or coolant side is different, thus the corresponding U is different.

Finally the heat transfer rate of the radiator can be calculated as below:

$$q_{rad} = \varepsilon C_{min}(T_{hx,i} - T_{air}) \quad (4.27)$$

Where effectiveness can be computed with the number of transfer units, NTU:

$$NTU \equiv \frac{UA}{C_{min}} \quad (4.28)$$

$$\varepsilon = 1 - \exp\left[\left(\frac{1}{C_r}\right)(NTU)^{0.22}\{exp[-C_r(NTU)^{0.78}] - 1\}\right] \quad (4.29)$$

In that, the smaller one of coolant or air heat capacity rate is defined as C_{min} while the larger one is defined as C_{max} . And C_r is the capacity ratio:

$$C_r = \frac{C_{min}}{C_{max}} \quad (4.30)$$

4.2.1.1 Radiator Model Performance

The radiator model was built according to the foregoing engineering method, shown in Figure 4-7. It was tested under baseline working conditions prior to integration, as listed in Table 4-2. The heat transfer performance of the radiator is strongly dependent on both thermal fluids.

This study shows the behavior of the radiator over a wide flow range, while maintaining the geometry and the temperature levels at the baseline condition. The thermal properties at the designated temperature could be found in Thermal Properties section

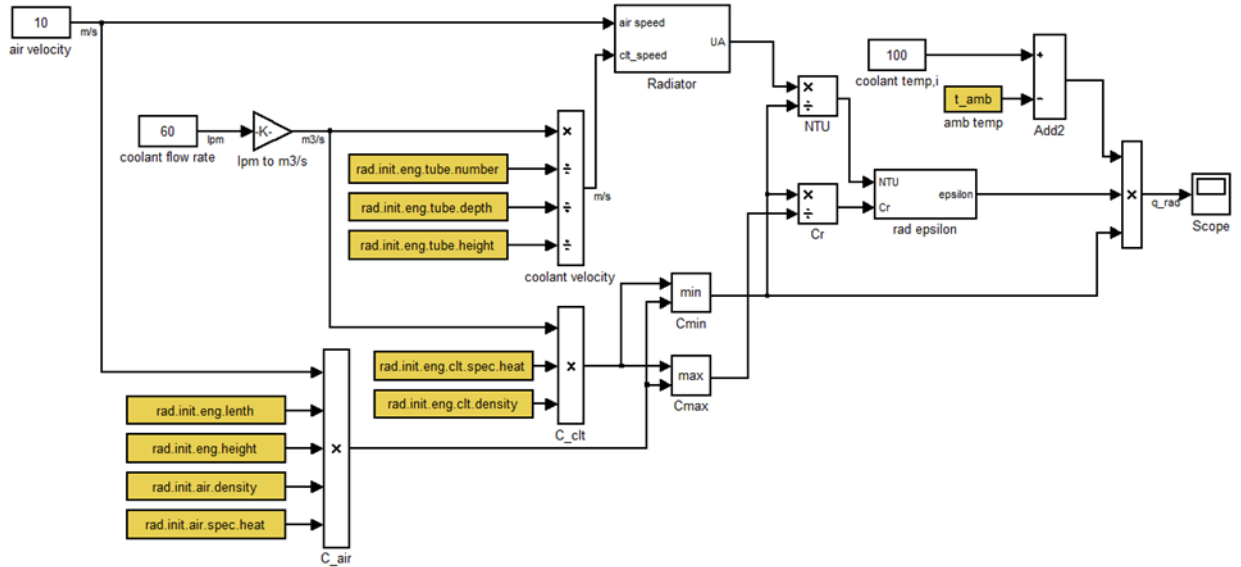


Figure 4-7. The Radiator Model

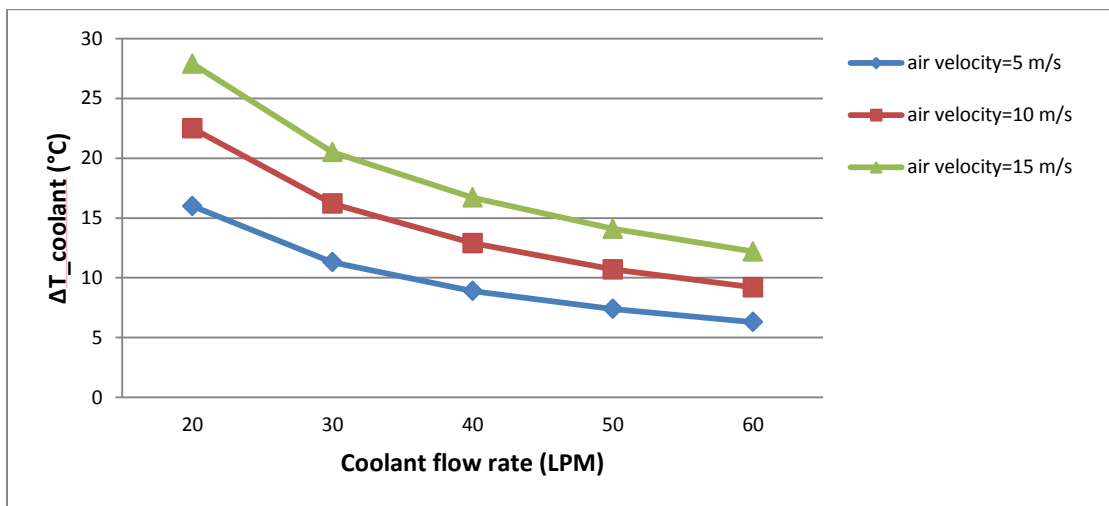
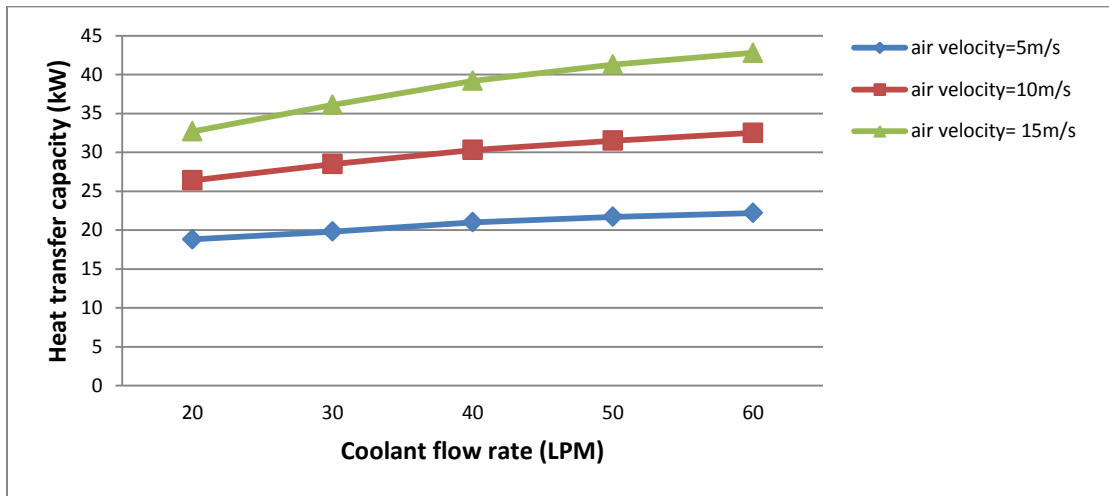
Table 4-2. The Radiator Working Conditions under Study

| | | | | | |
|--------------------------------------|--------------------------------------|-----------|-----------|-----------|-----------|
| Air inlet temperature (°C) | 25 | | | | |
| Air velocity (m/s) | 5 | 10 | 15 | | |
| Coolant fluid | Water/ethylene glycol (50/50) | | | | |
| Coolant inlet temperature(°C) | 100 | | | | |
| Coolant flow rate (LPM) | 20 | 30 | 40 | 50 | 60 |

Figure 4-8 shows the heat transfer capacity of the radiator increase with both air and coolant flow. The curve shows typically a stronger dependency on air velocity because air

usually has the highest thermal resistance. This overall trend and magnitude agrees with the results reported by parametric study of Oliet and Oliva [24].

The temperature difference is a derivative of heat transfer capacity, it decreases monotonically with the increase of coolant flow rate as expected.



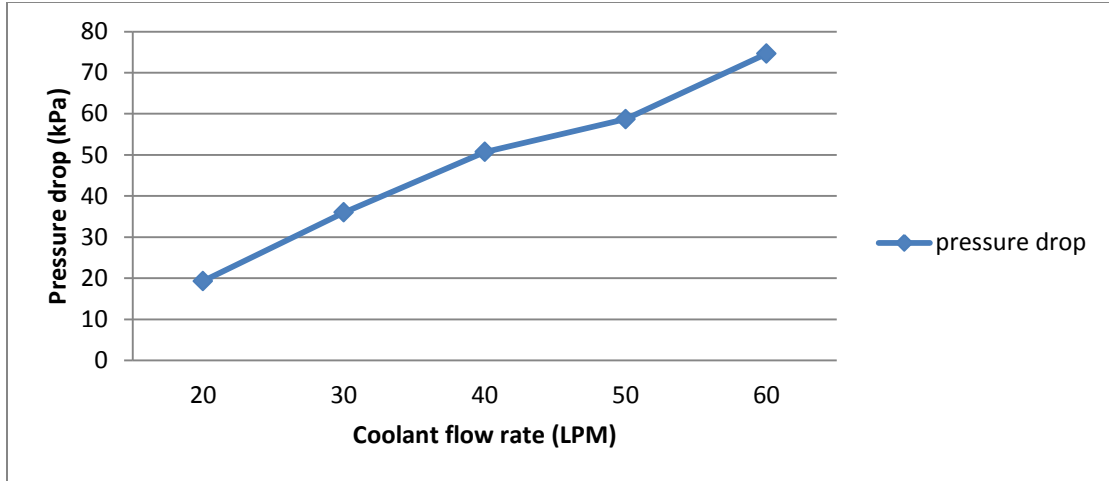


Figure 4-8. The Radiator Model Performance

4.2.2 Oil-to-water Heat Exchanger

In addition to the radiator, an oil-to-water heat exchanger is employed in the motor/MCU cooling system to combine the two cool circuits. As shown in Figure 6, water coolant run through the inner coolant channel while oil flow cross the outer fined area. A map-based performance model as a function of oil and water coolant flow rate and temperature is created based on the heat transfer and pressure drop characteristics provided by manufacturer. The test condition is summarized in Table 4-3. Figure 4-10 presents the performance results.

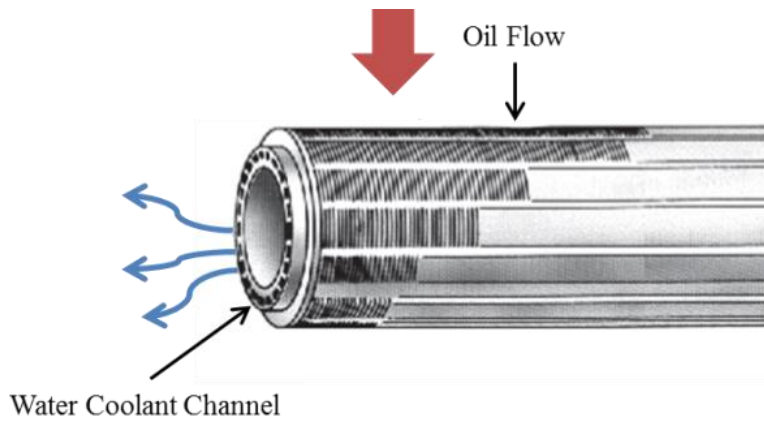


Figure 4-9. Schematic of Oil-to-Water Heat Exchanger

Table 4-3. The Oil-to-water Heat Exchanger Working Conditions under Study

| | | | | | |
|--------------------------------|--------------------------------------|----------|-----------|-----------|-----------|
| Oil coolant fluid | Automatic transmission fluid | | | | |
| Oil temperature (°C) | 80 | | | | |
| Oil flow rate (LPM) | 4 | 8 | 12 | | |
| Water coolant fluid | Water/ethylene glycol (50/50) | | | | |
| Water temperature(°C) | 60 | | | | |
| Coolant flow rate (LPM) | 4 | 8 | 12 | 16 | 20 |

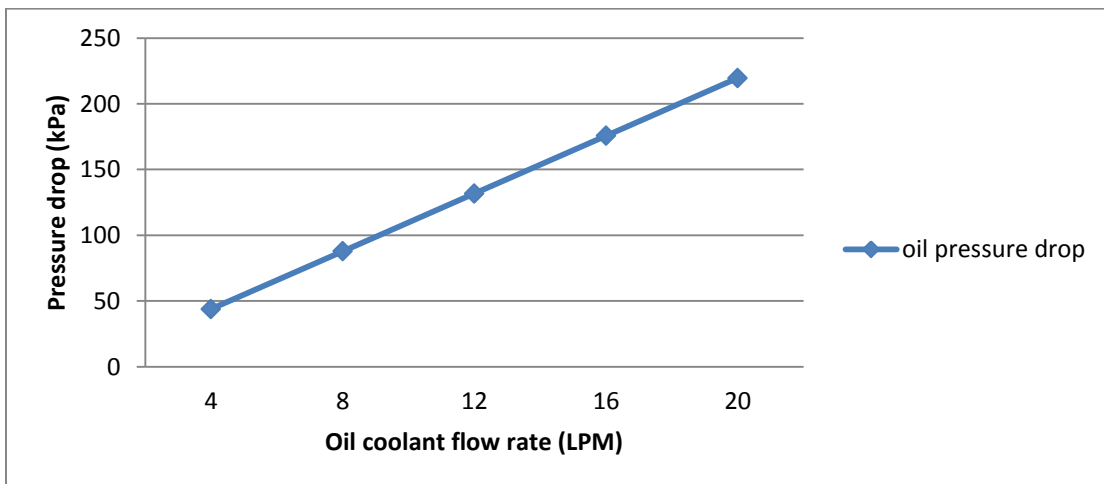
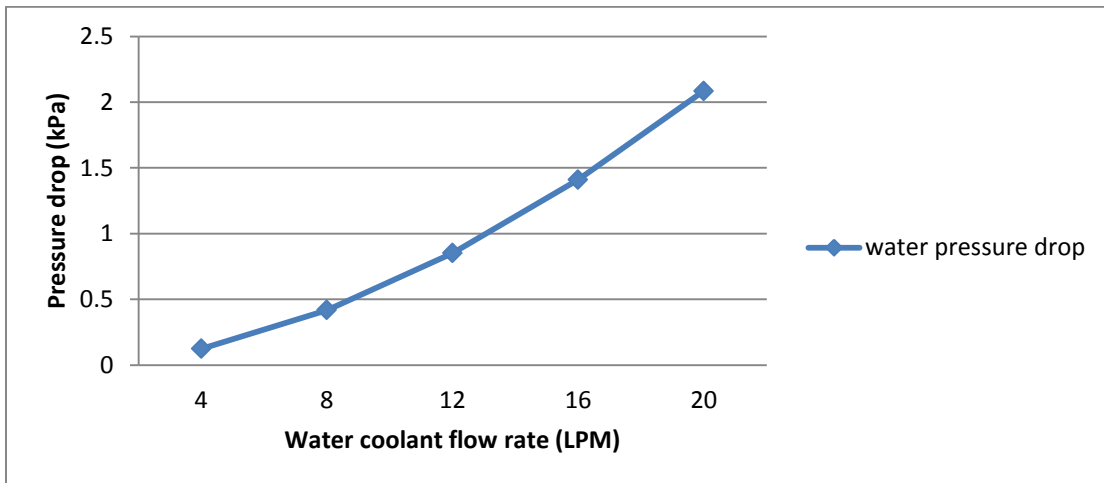
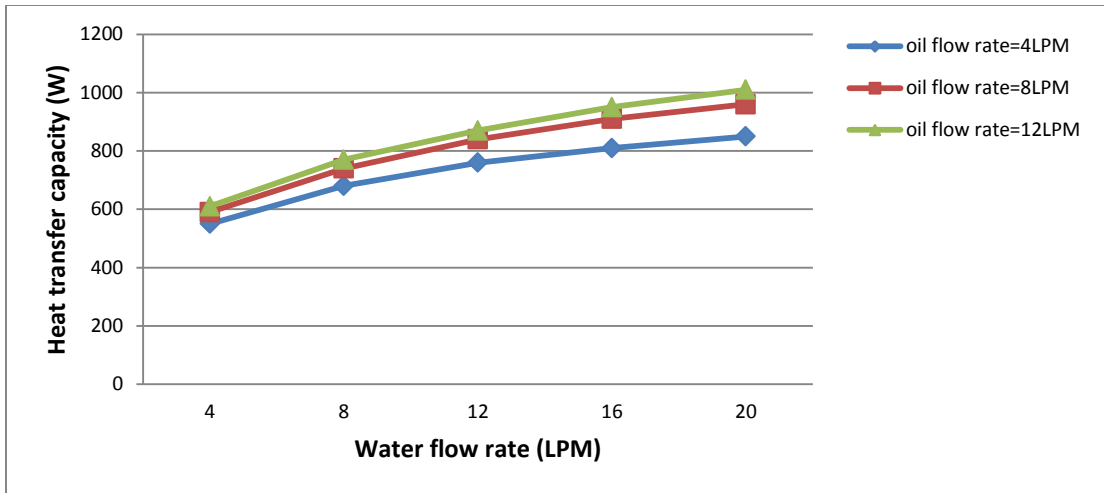


Figure 4-10. The Oil-to-water Heat Exchanger Model Performance

4.3 Fluid Delivery Component

4.3.1 Coolant Pipe

The cooling system shall account for the heat loss through coolant pipes. Consider standard plastic ½” ID pipes are applied in the cooling system. The specification of the pipes is given in Table 4-4. The length of the pipe can be estimated based on the location of heat source component. The thermal resistance method is also applied in the modeling of coolant pipes. The goal is to determine the heat transfer coefficient for both sides.

Table 4-4. Standard Plastic Pipes Specification

| Specification | Value |
|-----------------------------|-------------------------------------------------------|
| Pipe ID | 16mm |
| Pipe OD | 21mm |
| Wall thickness | 2.5mm |
| Thermal conductivity (25°C) | 0.2W/m·K |
| Pipe length (one way) | Engine loop: 1m ESS loop: 2m MCU/Motor loop: 2m |

The overall heat transfer coefficient of the pipe shall be determined by the following equation:

$$\frac{1}{UA} = \frac{1}{h_{air}A_{pipe,o}} + \frac{\ln(D_o/D_i)}{2\pi k_{pipe}L_{pipe}} + \frac{1}{h_{clt}A_{pipe,i}} \quad (4.31)$$

The coolant pipe application belongs to the cylinder in the cross flow condition, where the correlation for outer air flow yields to:

$$Nu_D = 0.3 + \frac{0.62Re_D^{1/2}Pr^{1/3}}{[1 + (0.4/Pr)^{2/3}]^{1/4}} \left[1 + \left(\frac{Re_D}{282000}\right)^{5/8}\right]^{4/5} \quad (4.32)$$

The convection heat transfer coefficient for coolant side yields to the correlation presented by Ginelinski [25]. The correlation below is modified from the Petukhov model, by Gnielinski using experimental data has extended the correlation to include both the transitional range ($2300 < Re_D < 10^4$) and fully developed turbulent range ($Re_D > 10^4$).

$$Nu_D = \frac{(f/2)(Re_D - 1000)Pr}{1 + 12.7(f/2)^{1/2}(Pr^{2/3} - 1)} \quad (Re_D > 2300) \quad (4.33)$$

Where friction factor f is given by:

$$f = (1.58 \ln Re_D - 3.28)^{-2} \quad (4.34)$$

The most commonly used relationship for laminar flow is the correlation proposed by Sieder and Tate [26]:

$$Nu_D = 1.86(Re_D Pr \frac{D_h}{L_{tube}})^{1/3} \left(\frac{\mu_{clt}}{\mu_s}\right)^{0.14} \\ (Re_D < 2300) \quad (4.35)$$

4.3.2 Thermostat

The thermostat is used in engine cooling loop to regulate the coolant flow. The thermostat remains closed under minimum temperature threshold to let the engine warm up quickly, then the valve opens gradually until it is fully opened to allow the coolant to circulate through the radiator. The engine coolant flow rate is dependent on the valve position which can be simplified to a linear relationship of coolant temperature [13]:

$$\eta_{thermo} = \begin{cases} 0; & \text{if } T_{eng,o} < T_{min} \\ \frac{T_{eng,o} - T_{min}}{T_{max} - T_{min}}; & \text{if } T_{min} < T_{eng,o} < T_{max} \\ 1; & \text{if } T_{eng,o} > T_{max} \end{cases} \quad (4.36)$$

4.3.3 Cooling Pump

The cooling pumps produce certain coolant flow to carry away the heat and maintain the heat source component under its control target temperature. The various-speed electric pump will be controlled at 3 steps: the minimum speed, half speed and full speed. The pumps performance characteristics can be obtained from the manufacturer. The pumps performance characteristics are given in Appendix 2. The operation point of pump is determined by the cross point of pump pressure curve and system pressure curve. With the given efficiency performance, the pump power consumption can be calculated as:

$$P_{pump} = \Delta P \times Q / \eta_{pump} \quad (4.37)$$

The calculated pump power consumptions at designated pump speeds are summarized in Table 4-5.

Table 4-5. Pump Power Consumption

| | Pump power consumption (W) | | | |
|---------------|----------------------------|----------|-----------------|-----------------------|
| | ESS pump | MCU pump | Motor feed pump | Motor evacuation pump |
| Minimum speed | 1.3 | 1.9 | 3.9 | 4.6 |
| Half speed | 14.8 | 16.5 | 26.3 | 31.6 |
| Full speed | 67.6 | 56.9 | 82.9 | 99.5 |

4.3.4 Cooling Fan

The stock fan system consists of 2 electrical cooling fans and 3 fan relays. The relays are arranged in a series/parallel configuration that allows controller to operate fans both together at low speed, single fan at high speed or both fans at high speed, as given in Table 4-6. The fan performance characteristics shall be provided by manufacturer.

Table 4-6. Fan System Status

| Fan status | Fan 1 | Fan 2 | Fan operation |
|------------|-------|-------|------------------------------|
| 1 | 0 | 0 | Both off |
| 2 | 1 | 0 | Both at low speed |
| 3 | 0 | 1 | Fan1 at high speed, Fan2 off |
| 4 | 1 | 1 | Both at high speed |

4.3.5 Thermal Properties

In order to compute the foregoing engineering equations, all the necessary parameters need to be determined. The lumped thermal capacitances of component are summarized in Table 4-7. The goal is to identify the active mass of the component and lumped specific heat capacity. The active mass is approximated by the product of the total mass and a certain proportion. For engine, motor and MCU, the lumped specific heat capacity is substituted by the metal it mainly made of due to lack of experimental data. The specific heat capacity for ESS is calculated by Equation 4.38 with given performance data provide by manufacture.

Table 4-7. Lumped Component Thermal Properties

| Parameter | Value | Description |
|-------------|-------------|------------------------------------------------------------|
| m_{eng} | 100kg | Assuming 80% of the engine mass is active material |
| $C_{p,eng}$ | 910 J/kg·K | Specific heat capacity of Aluminum at ambient temperature |
| m_{mot} | 50kg | Assuming 80% of the motor mass is active material |
| $C_{p,mot}$ | 910 J/kg·K | Specific heat capacity of Aluminum at ambient temperature |
| m_{MCU} | 12kg | Assuming 80% of the MCU mass is active material |
| $C_{p,MCU}$ | 910 J/kg·K | Specific heat capacity of Aluminum at ambient temperature |
| m_{ESS} | 150kg | The total mass of battery cell |
| $C_{p,ESS}$ | 1038 J/kg·K | $m_{ess} * C_{p,ess} * \frac{dT}{dt} = I^2 R \quad (4.38)$ |

The air properties at ambient temperature 25°C are given in Table 4-8 [21].

Table 4-8. Ambient Air Thermal Properties

| Parameter | Value (25°C) |
|-----------|-------------------------------|
| ρ_a | 1.18 kg/m ³ |
| μ_a | 1.85×10 ⁻⁵ kg/m·s |
| Cp_a | 1005 J/kg·K |
| k_a | 2.64×10 ⁻² W/(m·K) |
| Pr_a | 0.71 |

There are 2 kinds of coolant applied in the cooling system including oil-based ATF used in motor cooling circuit and water ethylene glycol 50/50 mixture applied in the other cooling circuits required water coolant. The oil coolant thermal properties at average operation

temperature 50°C are listed in Table 4-9 [27]. The water coolant properties are listed in Table 4-10 [28], under average operation temperature for ESS, MCU and engine, respectively.

Table 4-9. Oil Coolant Thermal Properties

| Parameter | Value (50°C) |
|-----------|------------------------------|
| ρ_o | 850 kg/m ³ |
| μ_o | 2.20×10 ⁻⁶ kg/m·s |
| Cp_o | 2040 J/kg·K |
| k_o | 0.16 W/(m·K) |
| Pr_o | 285.13 |

Table 4-10. Water Coolant Thermal Properties

| Parameter | Value (25°C) | Value (40°C) | Value (100°C) |
|-----------|------------------------------|------------------------------|------------------------------|
| ρ_c | 1053 kg/m ³ | 1045 kg/m ³ | 1013 kg/m ³ |
| μ_c | 3.37×10 ⁻³ kg/m·s | 2.24×10 ⁻³ kg/m·s | 6.04×10 ⁻⁴ kg/m·s |
| Cp_c | 3298 J/kg·K | 3329 J/kg·K | 3474 J/kg·K |
| k_c | 0.43 W/(m·K) | 0.44 W/(m·K) | 0.47 W/(m·K) |
| Pr_c | 25.82 | 16.91 | 4.43 |

CHAPTER 5. THERMAL CONTROL STRATEGY DEVELOPMENT

5.1 Thermal Manager Development

The thermal plant models and thermal controller will be integrated in the over-all PTTR vehicle model. The interactions between the vehicle model and the supervisory controller model follow the same communication architecture, shown in Figure 5-1, as implemented in the actual vehicle [1].

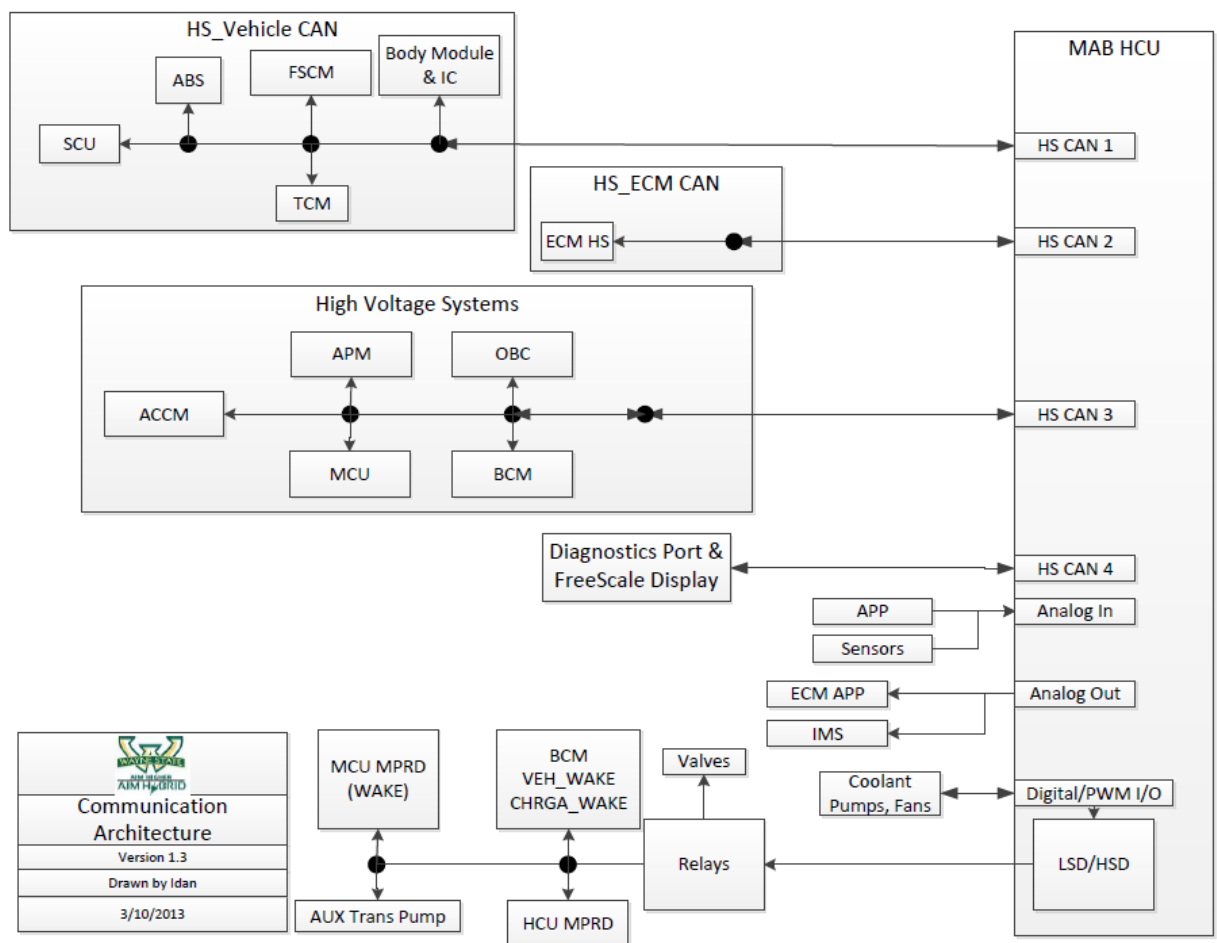


Figure 5-1. Communication Architecture

The thermal manager is in charge of coordinating the interactions between cooling system and powertrain components. The ultimate goal of thermal manager is to keep components in their optimal operation range while achieving best possible overall energy efficiency. As

shown in Figure 5-2 the thermal manager monitors temperature and outputs desired fan status, pump speed and AC compressor speed. The communications between ECUs and supervisor controller are done by CAN or digital bus as designated.

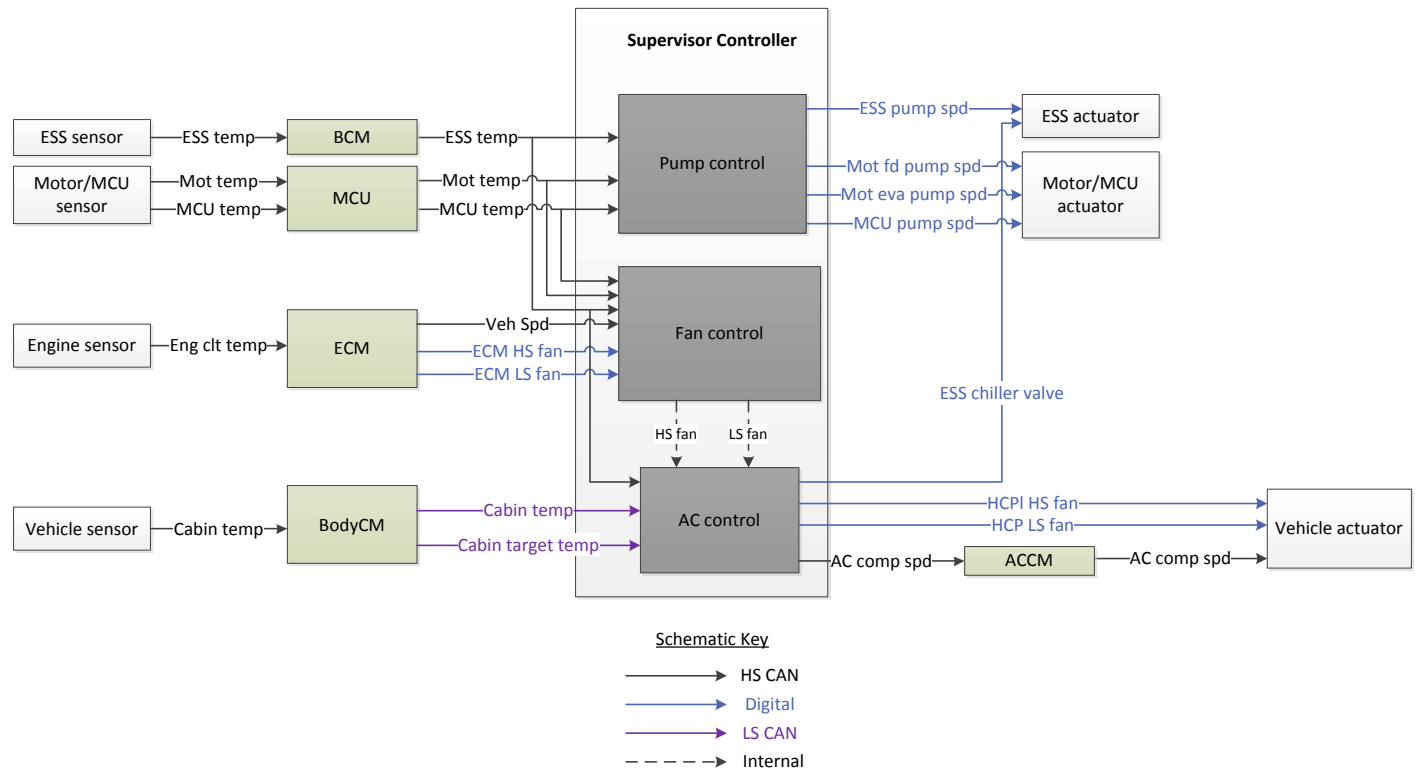


Figure 5-2. The Functional Diagram of Thermal Manager

The communications between thermal plant models and thermal manager are in compliance with the overall communication architecture, the used signals including CAN and digital are summarized in Table 5-1.

Table 5-1. The Used Signals of Thermal Model

| CAN signals | | | | |
|----------------------------|-------------|------------------------------|------------|--------|
| Signal Description | Signal Name | Message Name | Routing | Type |
| Engine coolant temperature | EngCltTmp | PPEI_Engine_General_Status_4 | ECM to HCP | HS CAN |

| | | | | |
|-----------------------------|-------------------------------------|--------------------------------|---------------|-------------|
| Cabin temperature | EstimatedBulkInteriorAirTemperature | Alarm_2_Request_LS | BodyCM to HCP | LS CAN |
| Cabin target temperature | ClmtCtrlTrgtTemp | Climate_Control_General_Status | BodyCM to HCP | LS CAN |
| ESS temperature | bcm_cell_tmax | BCM_Data1 | BCM to HCP | HS CAN |
| Motor temperature | D3_Motor_Temperature | M162_Temperature_Set_3 | MCU to HCP | HS CAN |
| MCU temperature | D1_Control_Board_Temperature | M161_Temperature_Set_2 | MCU to HCP | HS CAN |
| AC compressor speed | ThrmlRefCompSpd | Thrml_Ref_Compressor_Status_HS | HCP to ACCM | HS CAN |
| Digital Signals | | | | |
| Signal Description | | Routing | | Type |
| HCP fan status | | HCP to BodyCM | | Digital |
| ESS pump speed | | HCP to BCM | | Digital |
| Motor feed pump speed | | HCP to MCU | | Digital |
| Motor evacuation pump speed | | HCP to MCU | | Digital |
| MCU pump speed | | HCP to MCU | | Digital |
| Battery chiller valve | | HCP to BCM | | Digital |

Note that stock 2-electrical fan system is retained, however, it needs to serve not only the existing engine radiator and AC condenser, but also the additional dual-partition radiator for ESS and Motor/MCU loop, thus the fan status command is a comprehensive decision based on the performance of heat source components during certain vehicle speed range, because vehicle speed directly relates to volume of ram air, when at higher vehicle speed fan can take advantage of ram air so as to save power consumption of cooling system. Depending upon the speed of the

vehicle, ram air effect is provided by the vehicle's movement down the road, exposing the radiator to additional external air flow, indicating that when vehicle is at certain speed, fan system can be down-regulated.

The rating of an general automotive radiator fan system is 3000 CFM, given the frontal area of radiator, the required air velocity to provide equivalent volumetric flow rate is around 10 MPH. Considering the losses due to angle and resistance, it is fair to assume 20 MPH vehicle speed is the threshold for fan controls setup.

Originally the AC system only responds to cabin climate management, now another circuit designated to cool down battery is added to AC system. AC system shall react to requests from cabin and ESS accordingly to satisfy their cooling needs while maintain proper balance. As a result, thermal manager shall provide a final AC compressor speed according to cabin and ESS temperature.

Each cooling circuit has its own electric pump to circulate coolant except engine, which uses a mechanical pump. The speed of electric pump depends on the temperature of served heat source component. In modeling, the pump speed output is configured to be a proportion of maximum rated speed.

Note that in this study, ECM already has thermal control logic compiled. Thus the fan request for engine and AC request for cabin is read by ECM and then sent to thermal manager. Finally the thermal manager determines if higher fan status or higher AC compressor speed is desired accordingly. Since control strategy for engine is constrained by the existing ECM, the vehicle speed as another indicator of fan controls can only be executed in thermal manager. The I/O diagram of thermal manager is summarized in Figure 5-1.

The threshold temperatures as control set points are listed in Table 5-2. When component temperature reaches the threshold, the thermal manager shall command higher air flow or coolant flow according to the following control algorithm. The control flow chart for each cooling loop is listed below.

Table 5-2. The Temperature Threshold Set Points

| | Lower temp threshold (°C) | Medium temp threshold (°C) | Higher temp threshold (°C) |
|--------|------------------------------|-------------------------------|-------------------------------|
| ESS | 30 | 33 | 35 |
| Motor | 80 | – | 85 |
| MCU | 60 | – | 65 |
| Engine | 100 | 105 | 110 |

5.1.1 Control Work Flow for Engine Loop

The ECM determines engine fan request in terms of engine coolant temperature from plant model. The default fan status will be both off. There are 3 additional levels of temperature threshold corresponding to different fan status. The control flow chart for engine loop is given in Figure 5-3.

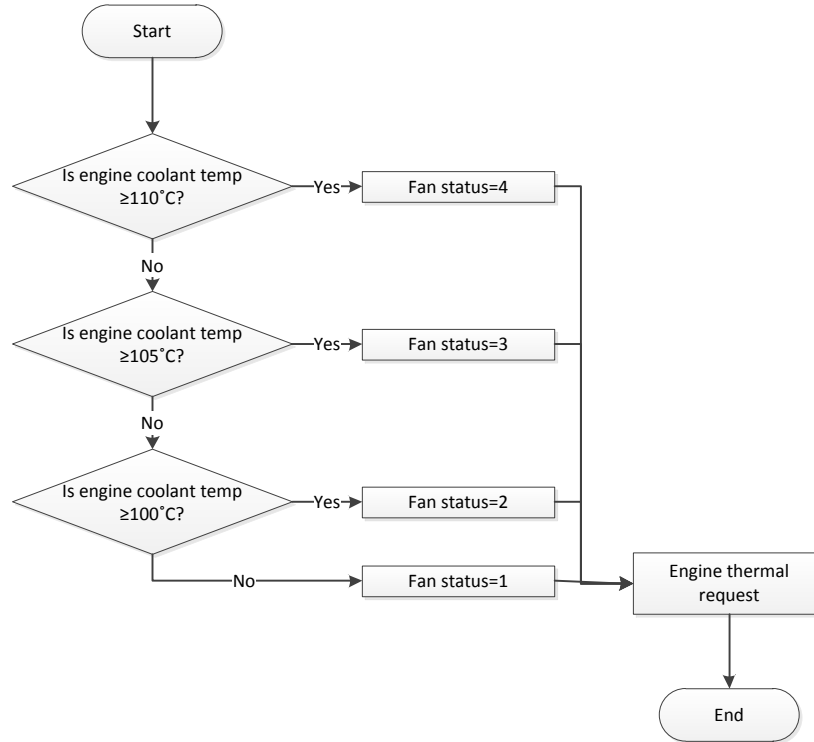


Figure 5-3. Control Work Flow of Engine in ECM

5.1.2 Control Work Flow for ESS Loop

The thermal manager is responsible for making 4 decisions for ESS loop. The fan status and pump speed go up along with increasing ESS temperature. As mentioned above, ESS loop has 2 circuits, controlled by 2-way chiller valve, the valve open to radiator circuit in default, however, when ESS temperature exceed 35°C , the valve will direct coolant to AC circuit. The control flow chart for ESS loop is shown in Figure 5-4.

1. ESS fan status as function of ESS temperature and vehicle speed.
2. ESS pump speed is set proportional to function of ESS temperature.
3. Chiller valve position, the default value is 0, for which valve opens to radiator circuit; when ESS temperature $\geq 35^{\circ}\text{C}$, the value is 1 and the valve opens to AC circuit.

4. ESS AC request, the default value is 0, with no AC request from ESS; when ESS temperature $\geq 35^{\circ}\text{C}$, the value is 1 and ESS AC request is activated.

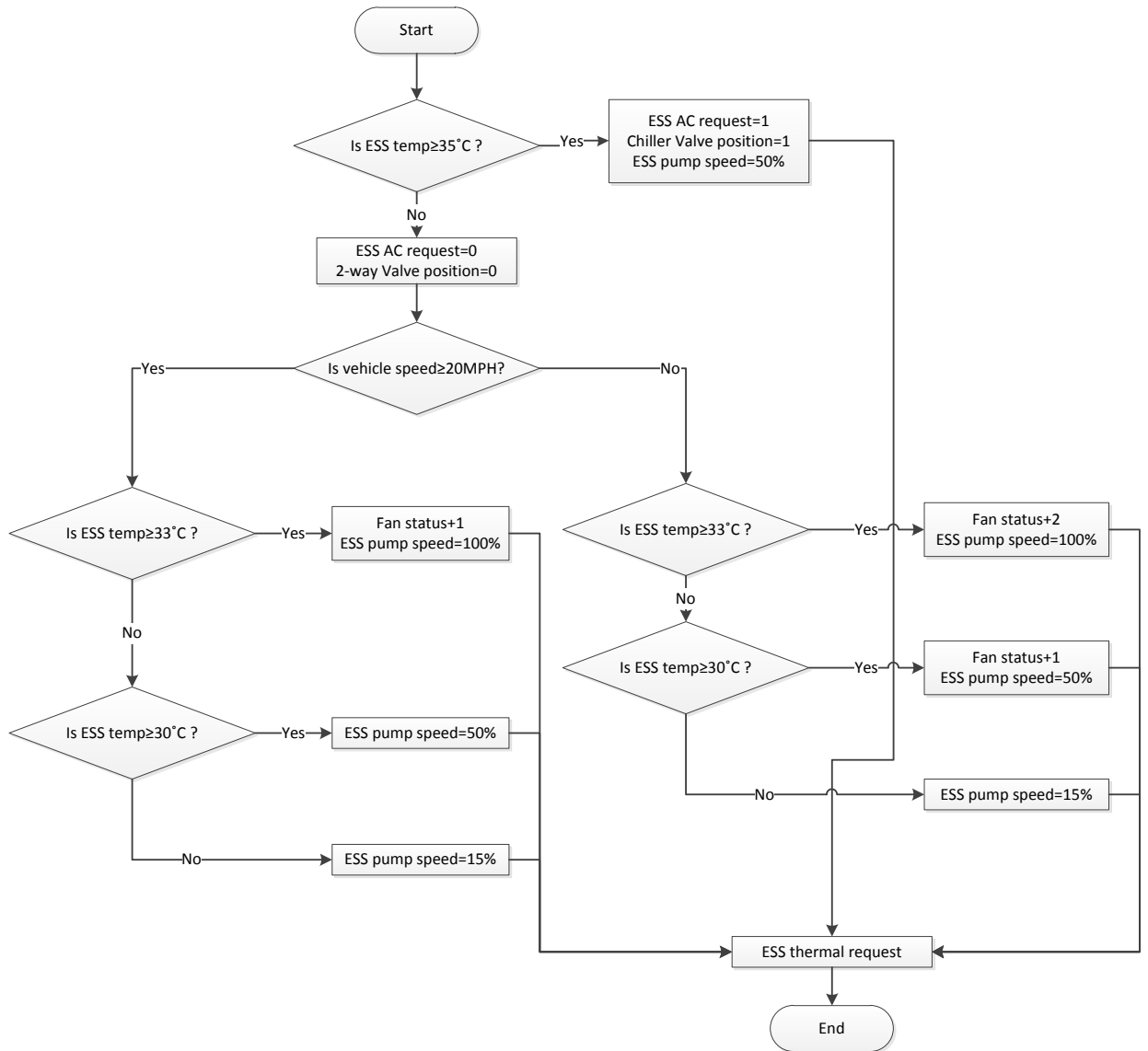


Figure 5-4. Control Work Flow of ESS in Thermal Manager

5.1.2 Control Work Flow for Motor/MCU Loop

The thermal manager takes charge of making 5 decisions for Motor/MCU loop. The control flow chart for motor and MCU is presented in Figure 5-5 and 5-6, respectively.

1. Motor fan status as function of motor temperature and vehicle speed.
2. Motor feed pump speed is set proportional to function of motor temperature.
3. Motor evacuation pump speed is set proportional to function of motor temperature.
4. MCU fan status as function of MCU temperature and vehicle speed.
5. MCU pump speed is set proportional to function of MCU temperature and motor temperature.

For the purpose of saving pump power consumption, when the component operates below the lowest temperature threshold, the pump only runs in minimum speed. In addition to providing coolant flow for MCU cooling, the MCU pump should also increase speed in response to motor temperature. When motor temperature exceeds the threshold, coolant flow rate on both sides need to rise simultaneously in order to maintain the efficiency of liquid-to-liquid heat exchanger, this control logic is independent to MCU performance.

In motor cooling circuit, an evacuation pump with higher capacity than feed pump is applied to prevent accumulation of oil inside the motor. The feed pump and evacuation pump are maintained at same speed ratio to achieve balanced flow rates in the cooling loop.

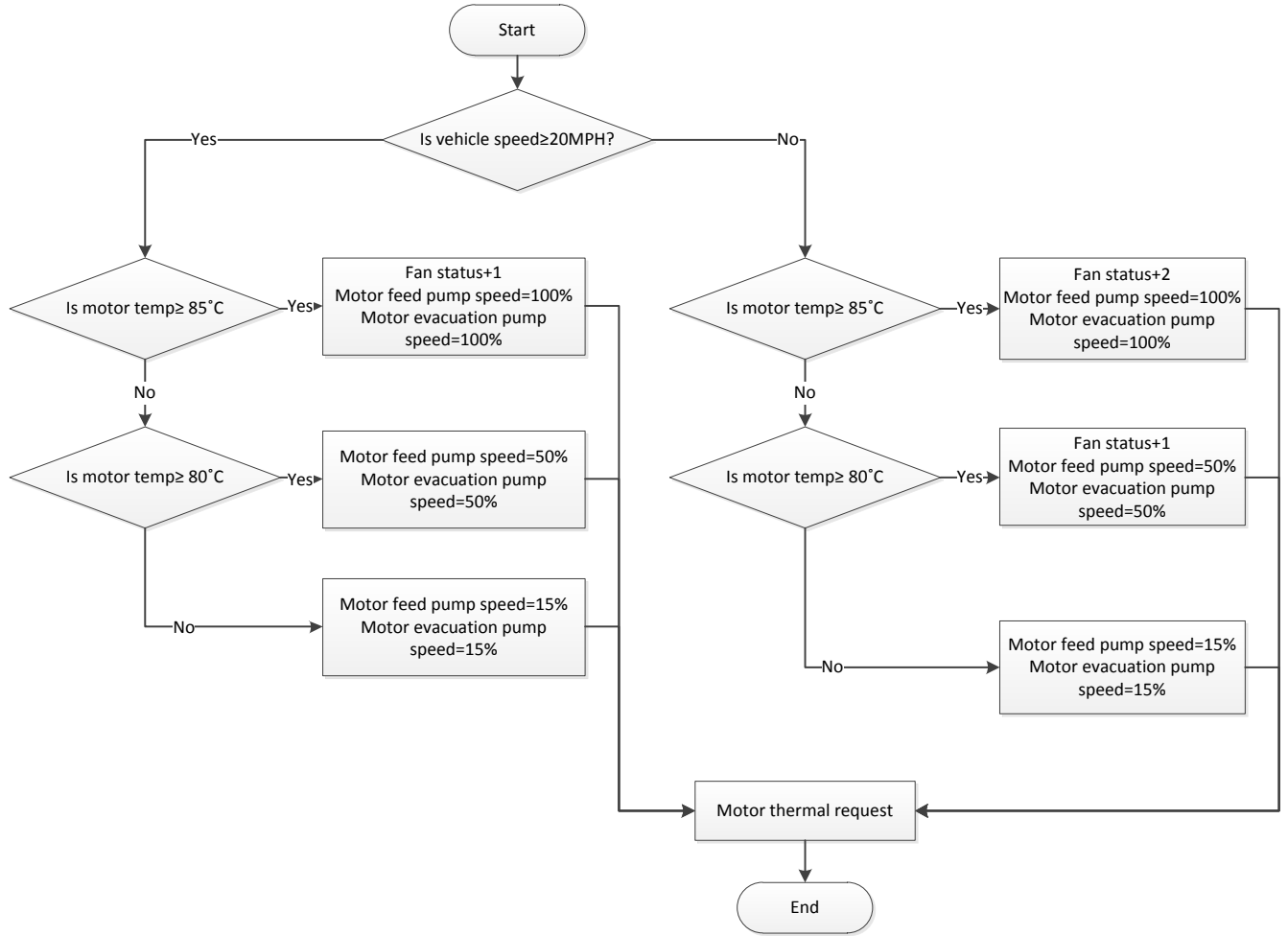


Figure 5-5. Control Work Flow of Motor in Thermal Manager

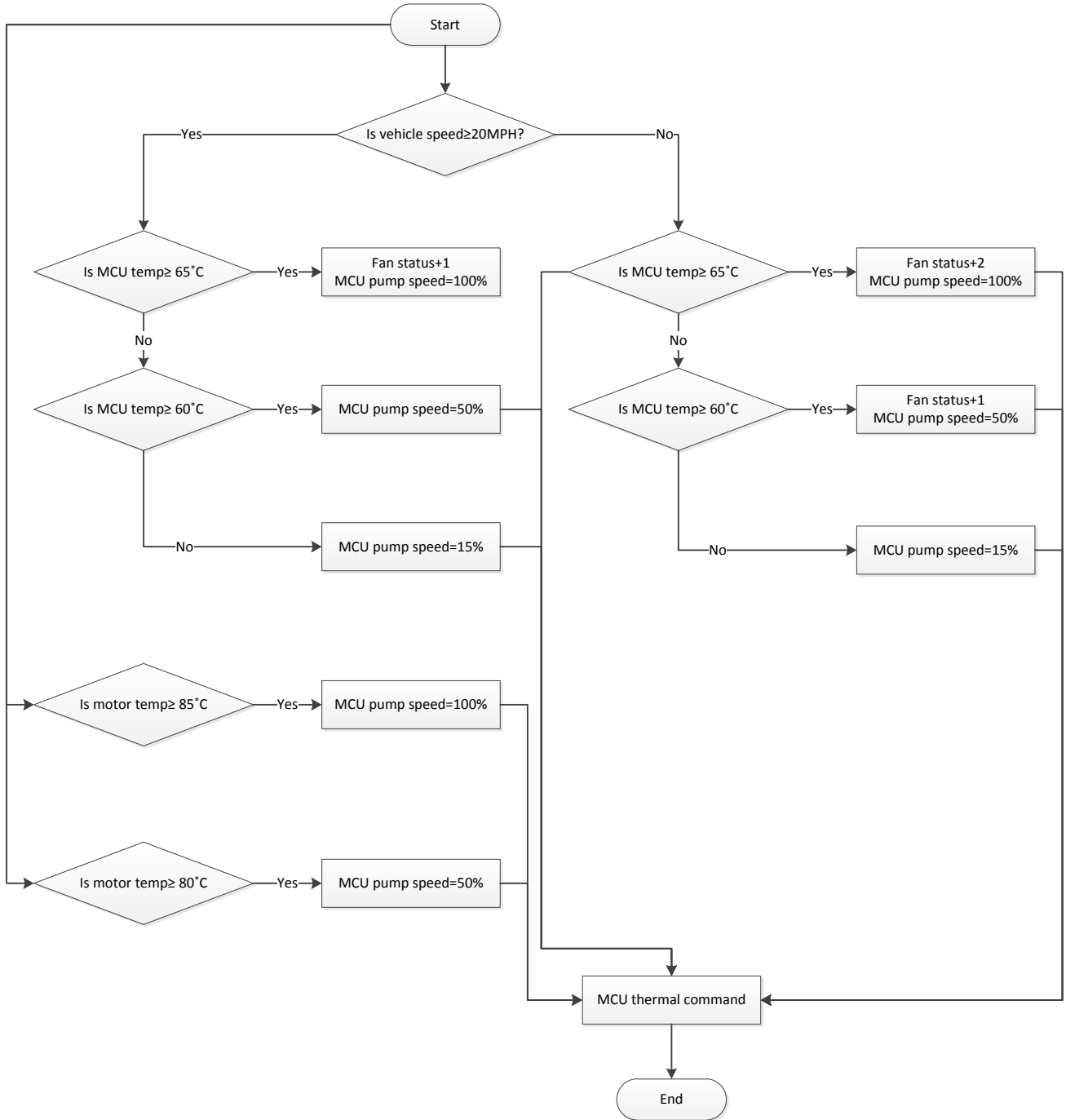


Figure 5-6. Control Work Flow of MCU in Thermal Manager

5.1.3 Control Work Flow for AC system

Thermal manager makes final decision for operation of AC compressor, which involves 3 scenarios as below. First thermal manager decides whether cabin AC request is true or not depends on measured cabin temperature and calibratable target cabin temperature. In this study the cabin temperature is assumed as ambient temperature (25°C) and target temperature is set at 28 °C. ESS AC request is activated when ESS temperature is greater than 35 °C. The control flow chart is given in Figure 5-7.

1. When cabin AC request is true, with no AC request from ESS, AC compressor will be set at half speed. The fan status will upgrade 1 level.
2. When ESS AC request is true, with no AC request from cabin, AC compressor will be set at half speed as well. The fan status will upgrade 1 level.
3. When both cabin AC request and ESS AC request are true, AC compressor will operate at full speed, with the cooling load divided equally between the cabin loop and the ESS loop. The fan status will go up 2 levels to support the AC system under full load.

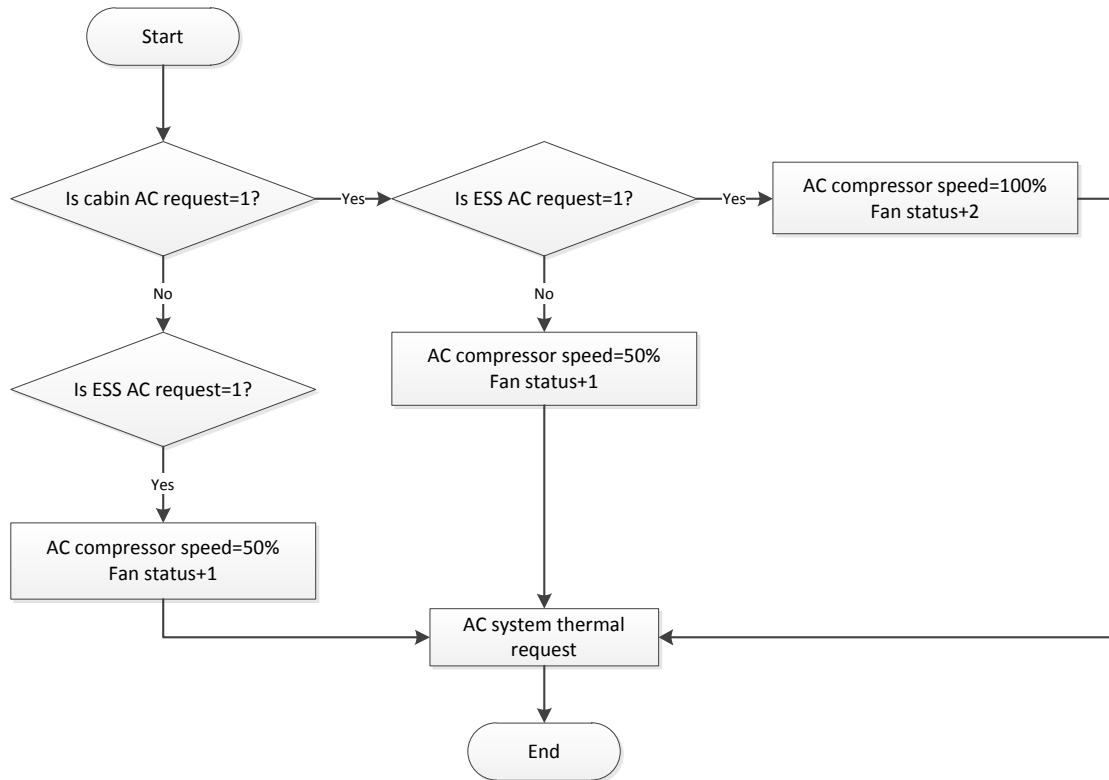


Figure 5-7. Control Work Flow of AC system in Thermal Manager

5.1.4 Over-all Fan Control Logic

Fan system works for engine radiator, ESS/motor/MCU radiator, and AC condenser, the final fan status is a comprehensive decision, as summarized in Figure 8, the fan request for each heat exchanger is defined step by step: at the starting point the cooling demand for engine radiator is decided by ECM; then thermal manager judges fan request to support the second radiator by analyzing ESS, motor and MCU temperature in parallel, the concept is among ESS, motor and MCU, fan system responds to the worst case of the three. At last it takes fan request for AC condenser into account and determined the final fan command.

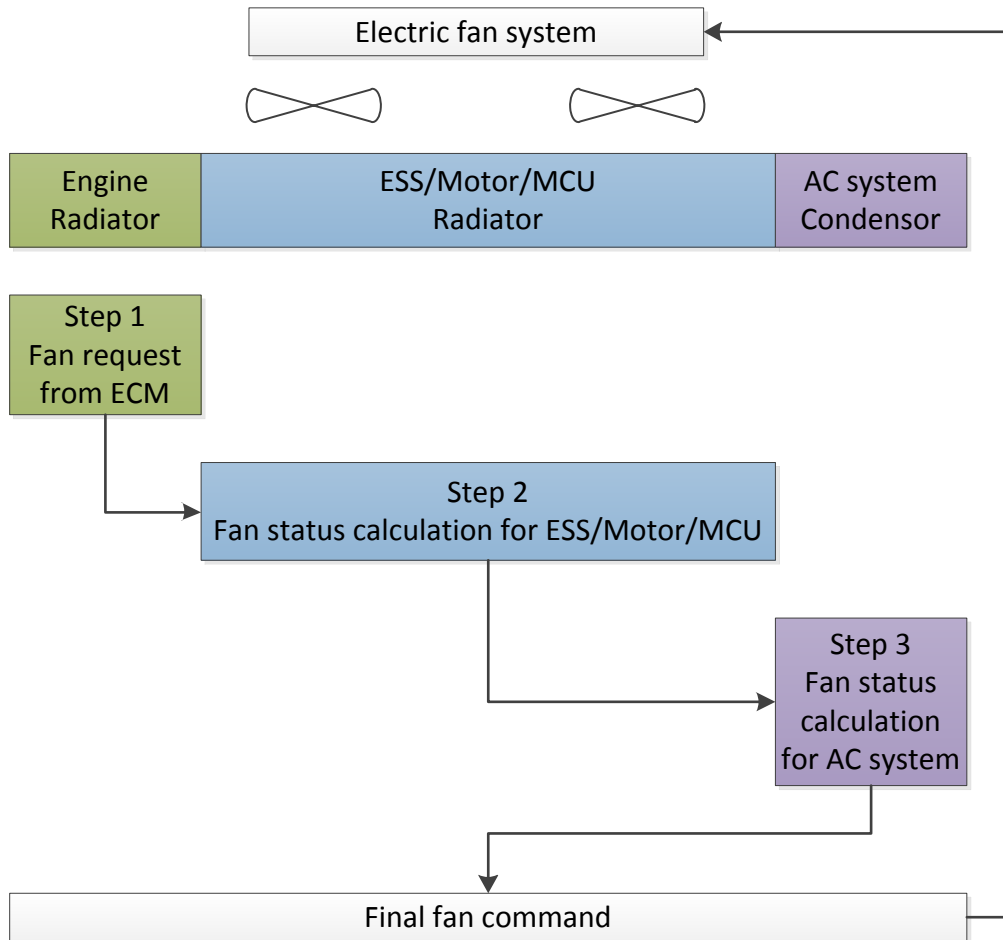


Figure 5-8. Over-all Fan Control

At step 2 in Figure 5-8, when vehicle speed ≤ 20 MPH, if any of the monitored temperature reaches the lower threshold, then the fan status will go up by 1, For example, if ESS is 32°C , both motor and MCU temperature are under the lower threshold, fan status goes up by 1, even later when motor temperature increase to 80°C or MCU temperature increases to 60°C but still under higher threshold, fan status remains.

If any of the monitored temperature exceeds the second threshold, fan status will go up by 2. For example, if ESS is 34°C , both motor and MCU temperature are under the lower threshold, fan status goes up by 2 due to ESS temperature being greater than the second threshold.

The final fan status is the sum of engine fan request and addend from thermal manager.

The maximum fan status is 4, as explained in Table 4-6.

5.2 Thermal Manager Bench Testing

Bench testing has to be done before integrating thermal manager into over-all vehicle model so as to clear away math or coding error in subsystem in advance. Several set conditions are initiated to verify if the expected responses are met.

The thermal manager is developed and coded per “Thermal Control Strategy Development” section, as shown in Figure 5-9, it is divided into 3 subsystems based on functionality: fan control block, pump control block and AC control block. The engine fan controller is placed in ECM as discussed above. It takes care of engine coolant temperature and output engine fan request for further analysis.

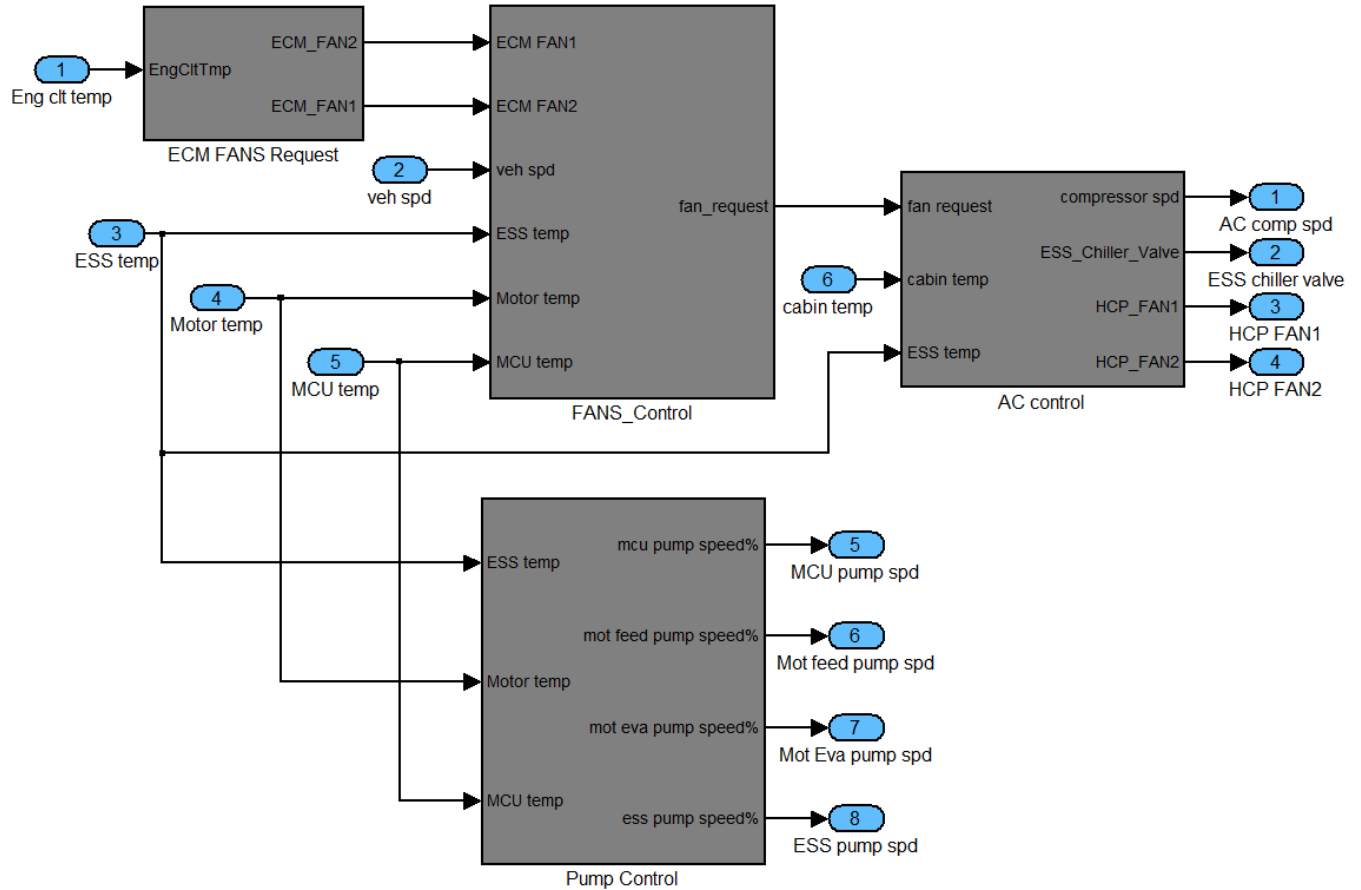


Figure 5-9. Thermal Manager Block

The test conditions are set to simulate the variation of component temperature. The inputs are created via Signal Builder embedded in Mathworks Simulink. The expected responses and simulation results should be in full compliance. The test conditions are shown in Figure 5-10 and 5-12, followed by the expected responses and simulation results and for comparison.

First, consider the vehicle is running on highway with electrified RWD only. Vehicle speed is 70MPH and Engine is off during the period. Assuming ESS initial temperature is above higher threshold. Thermal manager should open battery chiller valve and command AC system to cool down the battery. And the temperature of motor change from below lower threshold to above higher threshold. Thermal manager should increase both motor pump speed and MCU pump speed as they are sharing the same cooling loop.

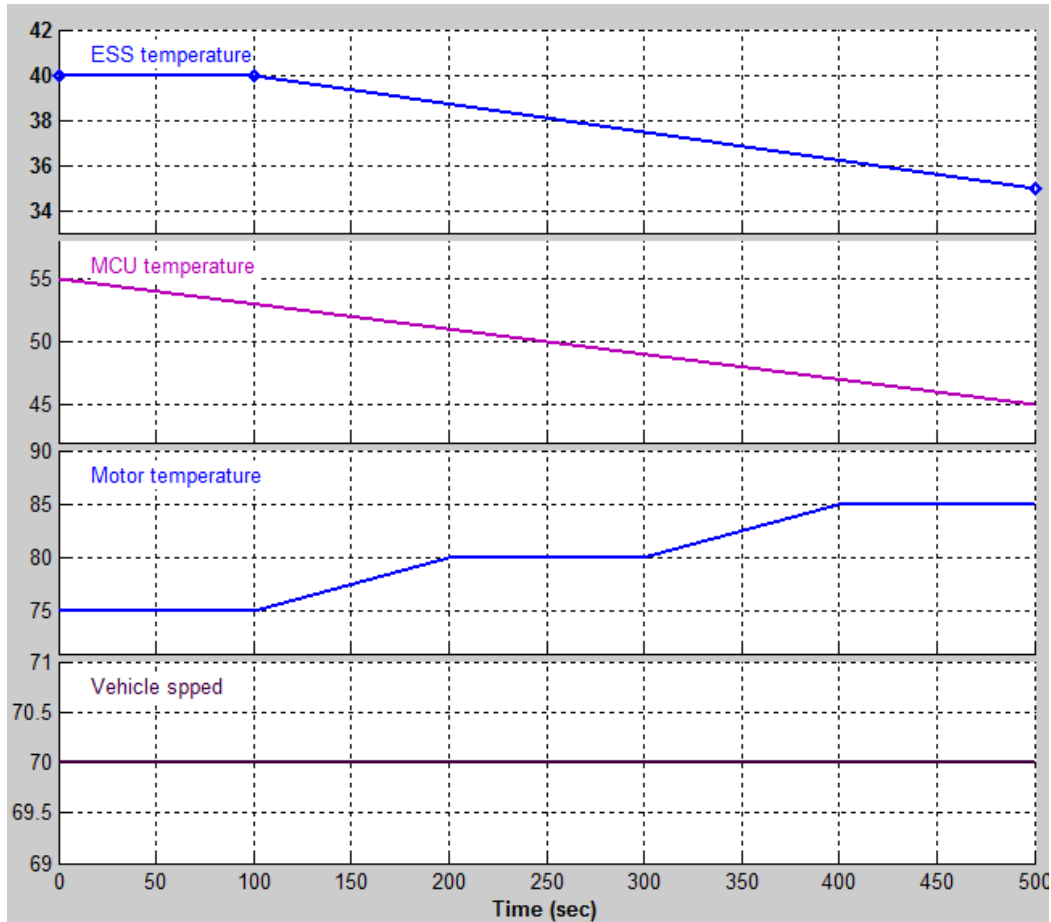


Figure 5-10. Simulated Component Temperature Performance under Highway Condition

As shown in Figure 5-11, the chiller valve is open and AC compressor speed is set at 50% to support AC cooling for battery system during the operation because ESS temperature is above higher threshold. ESS pump is set at 50% when transferring heat with AC system. As motor feed pump and evacuation pump are operated at the same speed, in the following table they are represented by single motor pump speed. Note the even though in this case MCU temperature is below lower threshold, MCU pump shall be synchronized with motor pump for effective cooling. The fan status determination can be computed through the 3-step method explained in Figure 5-8. In the duration engine temperature is assumed to be ambient temperature 25°C. Thus fan request from engine is always at status 1. In step2, there is “fan status+1” from motor as temperature

exceeds 85°C during 400~500s. AC system also request “fan status+1” during the period. The final fan status shall be 2 during 0~400s and rise to 3 during 400~500s. The final fan status is translated into HCP FAN1 and FAN2 command before sending out, as shown in Table 4-5.

| Outputs | Duration (s) | Expected results |
|-------------------|-----------------------|------------------|
| AC comp speed | $t \leq 500$ | 50% |
| ESS chiller valve | $t \leq 500$ | 1 |
| ESS pump speed | $t \leq 500$ | 50% |
| Motor pump speed | $t < 200$ | 15% |
| | $200 \leq t < 400$ | 50% |
| | $400 \leq t \leq 500$ | 100% |
| MCU pump speed | $t < 200$ | 15% |
| | $200 \leq t < 400$ | 50% |
| | $400 \leq t \leq 500$ | 100% |
| HCP FAN1 | $t < 200$ | 1 |
| | $200 \leq t < 400$ | 1 |
| | $400 \leq t \leq 500$ | 0 |
| HCP FAN2 | $t < 200$ | 0 |
| | $200 \leq t < 400$ | 0 |
| | $400 \leq t \leq 500$ | 1 |

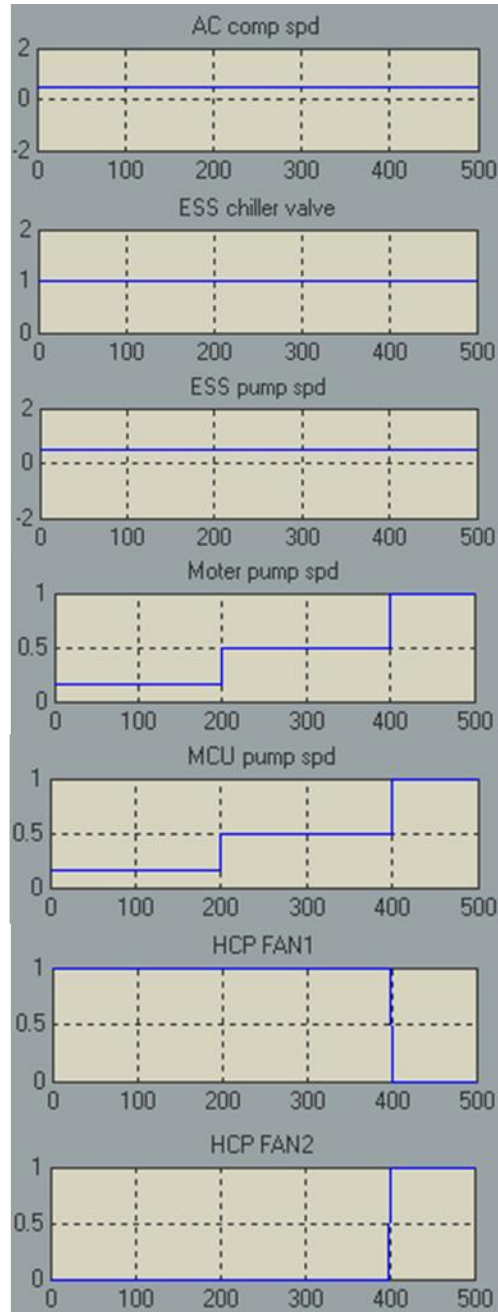


Figure 5-11. Results Comparison under Highway Condition

The second condition is when vehicle is operating at low speed 10MPH. The vehicle switches from CD to CS mode at 100s. Engine starts at 100s and increase to lower threshold. MCU and motor operate at lower threshold initially and keep decreasing as RWD is off in CS mode.

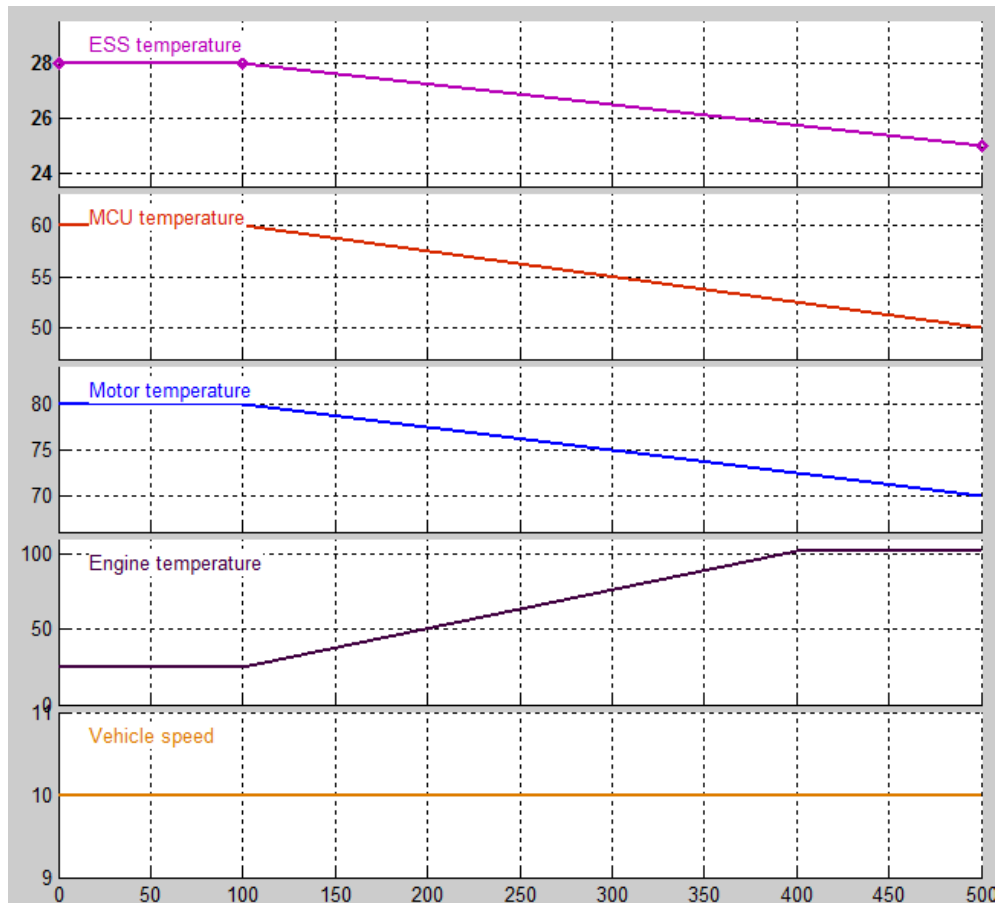


Figure 5-12. Simulated Component Temperature Performance under Mode Switch Condition

As shown in Figure 5-13, AC system is off during the period. ESS pump speed is at its minimum because ESS temperature is below lower threshold. Motor and MCU pump speed operate at 50% during 0~100s when temperatures are at lower threshold, respectively. The fan request from engine increases to 2 at 400s as engine temperature rises to 102°C. Note that in this

case, vehicle speed is below 20MPH. Thus During 0~100s, MCU and motor shall request “fan status+1”. The final fan status shall be 2 during 0~100s due to MCU and motor. Then fans are both off during 100~400s. Finally fans shall be turned on again in response to engine temperature rise.

| Outputs | Duration (s) | Expected results |
|-------------------|-----------------------|------------------|
| AC comp speed | $t \leq 500$ | 0 |
| ESS chiller valve | $t \leq 500$ | 0 |
| ESS pump speed | $t \leq 500$ | 15% |
| Motor pump speed | $t \leq 100$ | 50% |
| | $100 < t \leq 500$ | 15% |
| MCU pump speed | $t \leq 100$ | 50% |
| | $100 < t \leq 500$ | 15% |
| HCP FAN1 | $t \leq 100$ | 1 |
| | $100 < t < 400$ | 0 |
| | $400 \leq t \leq 500$ | 1 |
| HCP FAN2 | $t \leq 100$ | 0 |
| | $100 < t < 400$ | 0 |
| | $400 \leq t \leq 500$ | 0 |

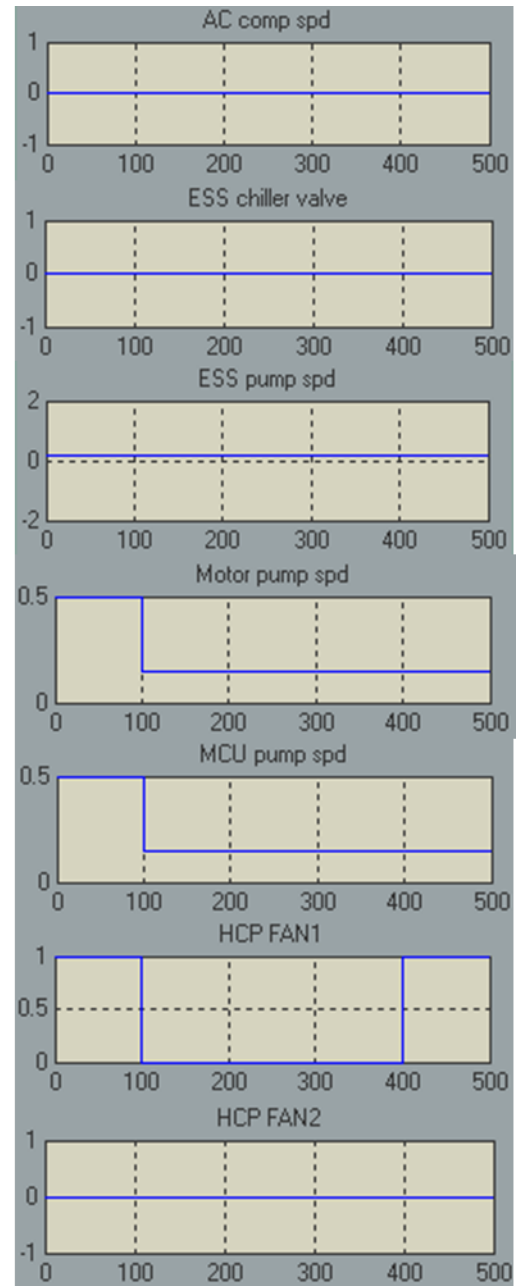


Figure 5-13. Results Comparison under Mode Switch Condition

As shown above, the simulation results are completely in conformity with control strategy, the proposed thermal manager is ready for integration.

CHAPTER 6. RESULTS AND DISCUSSIONS

6.1 Thermal Model Integration

The foregoing thermal manager and plant model were integrated into overall PTTR model for simulation. As shown in Figure 6-1, thermal manager was coded within supervisory controller. The inputs/outputs are in compliance with Figure 5-2. The control algorithm is categorized into fan control, pump control and AC control as described.

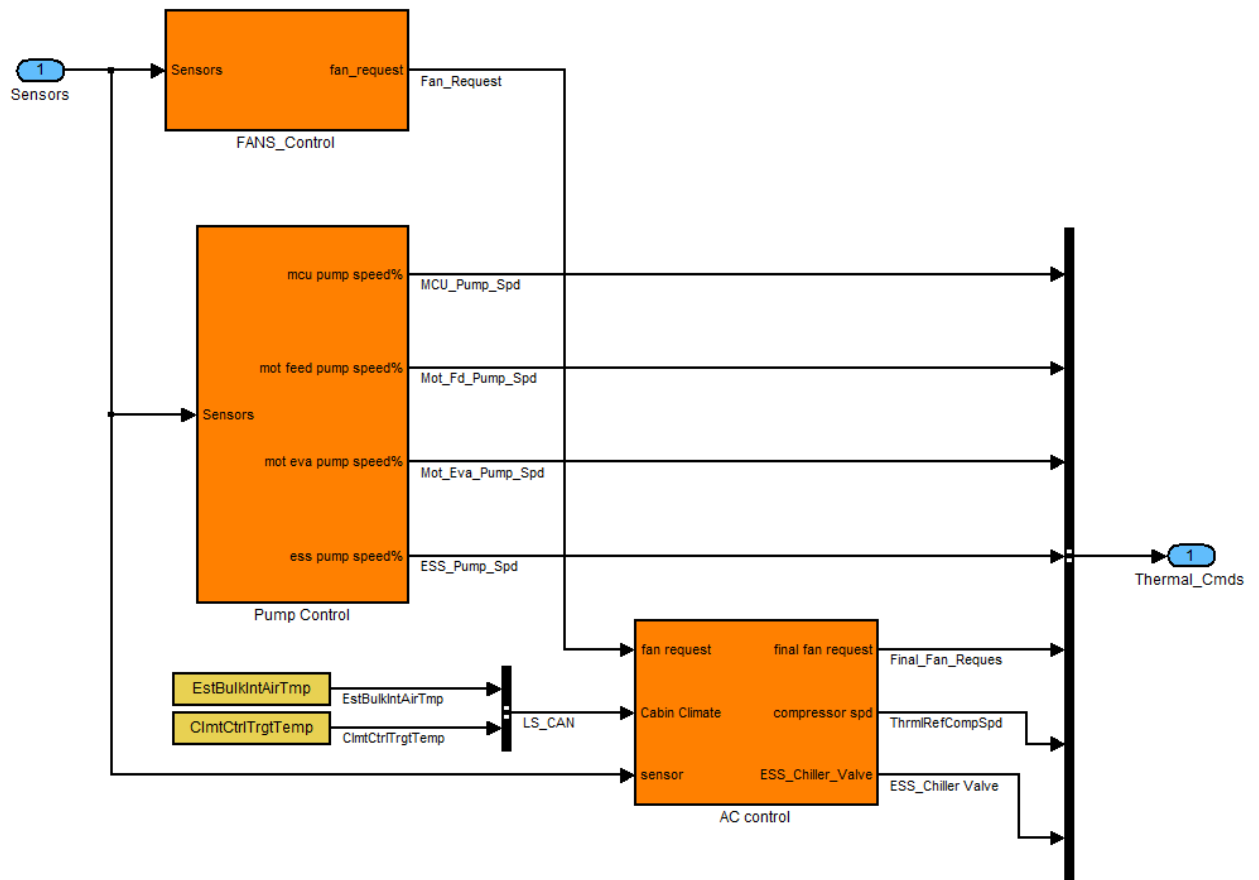


Figure 6-1. Thermal Manager Model

The powertrain component model contains corresponding thermal plant models use actuators to ensure optimum operation that resembles its hardware counterparts. This is done by reading temperature values from sensors, conducting thermal command and adjusting the

actuators. For example, as shown in Figure 6-2, BCM monitors ESS temperature by reading ESS sensor, and then reports it to thermal manager for future analysis. Thermal manager makes decision according to comprehensive control strategy. Finally ESS pump speed and chiller valve command is sent back to actuators for execution.

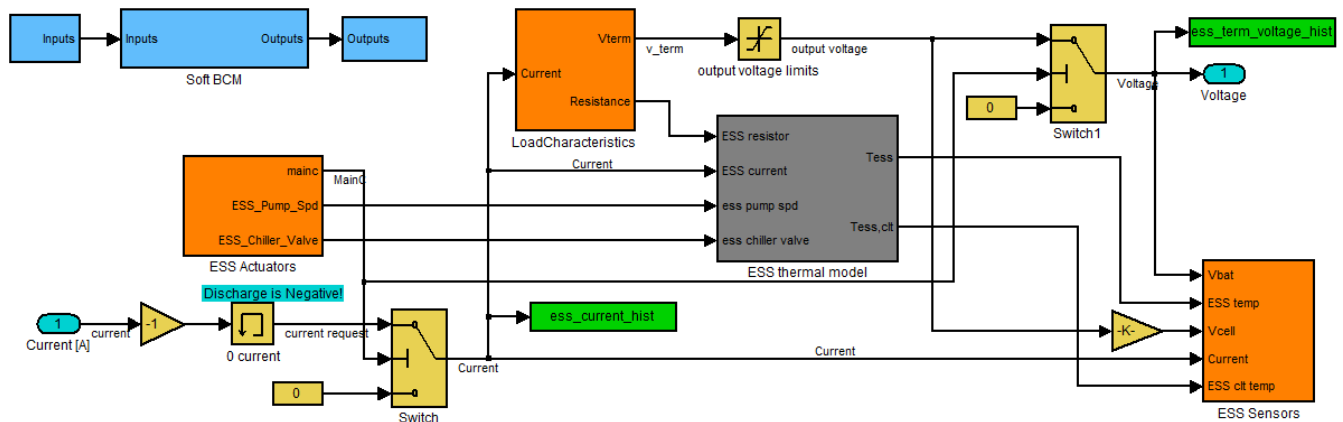


Figure 6-2. ESS Plant Model

6.2 Simulation Results

The thermal are tested through realistic driving conditions to demonstrate their reliability after integration. Some simulations are under extreme conditions for cooling system validation purposes.

First of all, the proposed model must demonstrate its compliance with competition requirement. The designated EcoCAR2 4-cycle drive schedule is repeated twice, as shown in Figure 6-3, to test the durability of the thermal model in extended time.

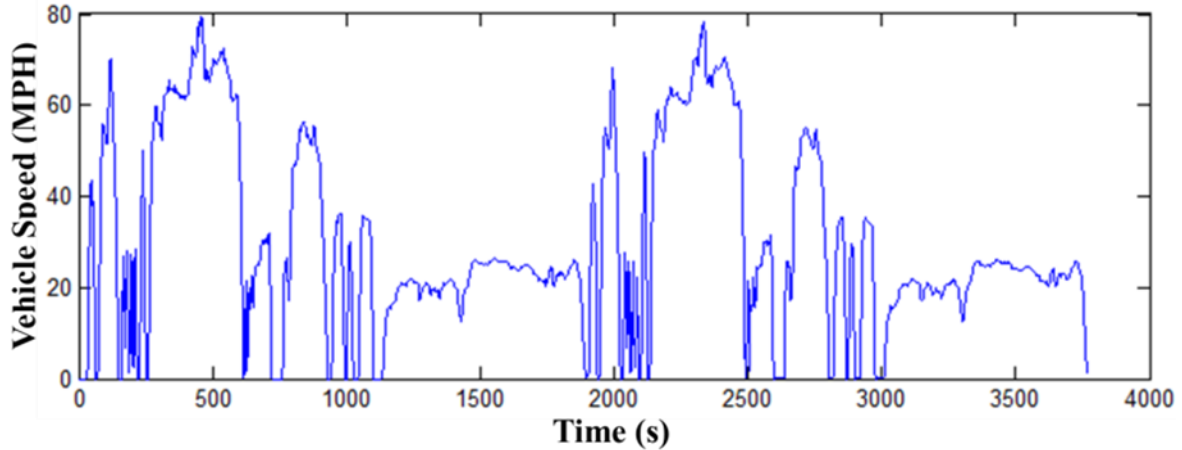


Figure 6-3. EcoCAR2 4-cycle Drive Schedule (2 times)

Park's research suggests that the heat generation under grade load condition is much larger than maximum speed or off-road condition [3], thus a grade load drive cycle is created to serve as the worst-scenario validation.

In both test cases the initial SOC are set so that the vehicle will switch from CD (charge-depletion) mode to CS (charge-sustaining) mode during simulation, the behavior of powertrain component under mode switching condition can be observed. The foregoing driving conditions for testing are summarized in Table 6-1.

Table 6-1. Driving Condition

| Condition | EcoCAR2 4-cycle schedule | Grade load |
|---------------|--------------------------|------------|
| Vehicle speed | As shown in Figure 11 | 27 MPH |
| Gradeability | 0% | 12% |
| Ambient temp. | 25 °C | 25 °C |
| Initial SOC | 50% | 100% |
| Minimum SOC | 20% | 20% |

| | | |
|----------------|----------------------|----------------------|
| Vehicle mode | CD switch to CS mode | CD switch to CS mode |
| Cycle duration | 3769s | 3600s |

Figure 6-4 shows the operating condition of powertrain components under EcoCAR2 4-cycle schedule. As can be seen, SOC drops below minimum setup 20% and engine starts to crank at 1734 s, the vehicle switches from CD mode to CS mode. The heat rates of each powertrain component are also shown, where engine starts to generate a large amount of heat after the start of operation. The RWD powertrain components experience much smaller heat rate because in CS mode they only assist to boost the engine or capture regenerative energy.

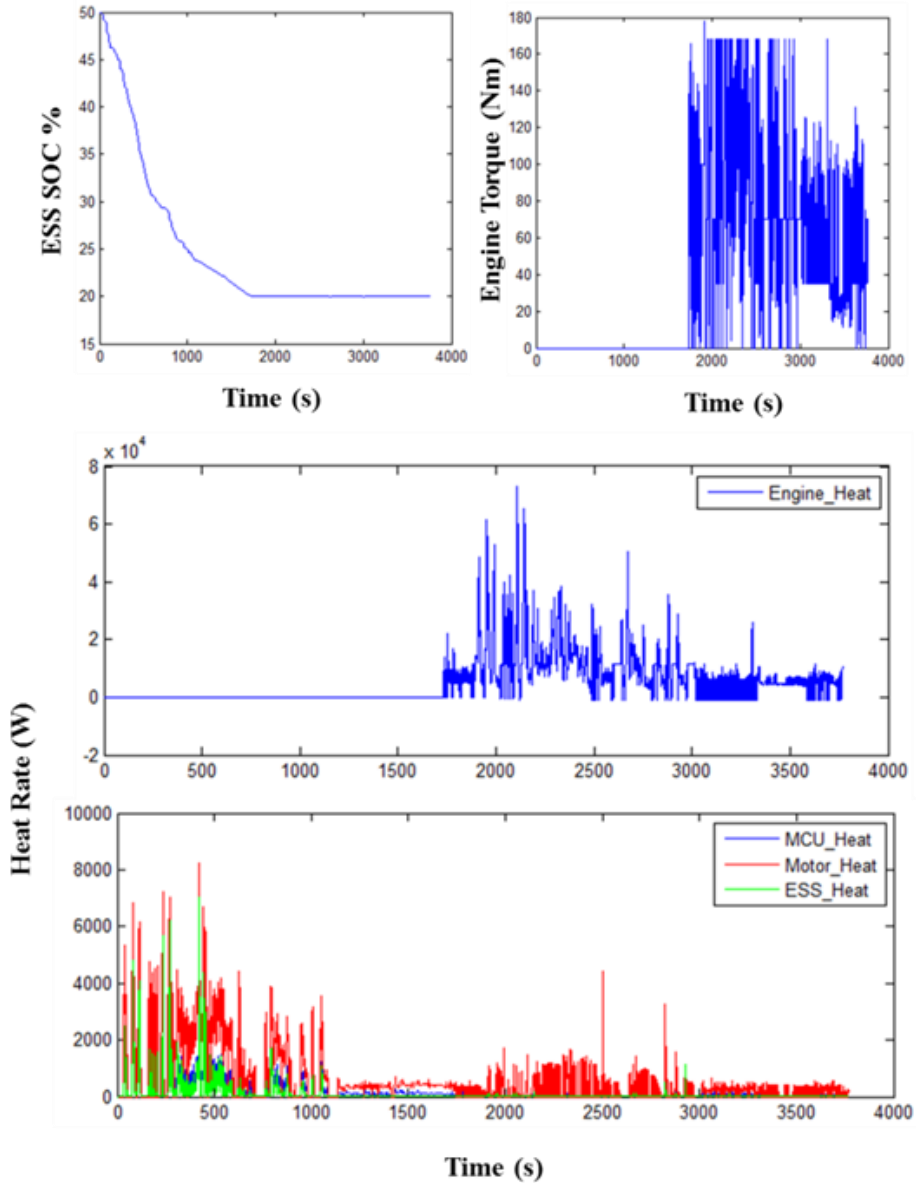


Figure 6-4. Powertrain Operation Condition under EcoCAR2 4-cycle Schedule

Figure 6-5 demonstrates the temperature traces of powertrain components and their corresponding coolant temperature. The temperature of the coolant entering the powertrain component is marked as “Clt_In_Temp”. During engine warm-up period, thermostat is closed to radiator circuit, thus no heat dissipation from coolant. Engine coolant inlet temperature drops when thermostat opens, and the temperature difference varies along with engine speed because

coolant flow rate of mechanical pump is directly controlled by it. During their operation in CD mode, the temperature of ESS, motor and MCU starts to decrease after the most aggressive part of drive cycle and continue to drop in CS mode. During this operation, ESS, motor and MCU stay below their lower temperature thresholds thus coolant flow rate remain at minimum. However, the coolant temperature varies with the vehicle speed as a result of changing air flow velocity over the radiator, which explains the rises in coolant temperature curve.

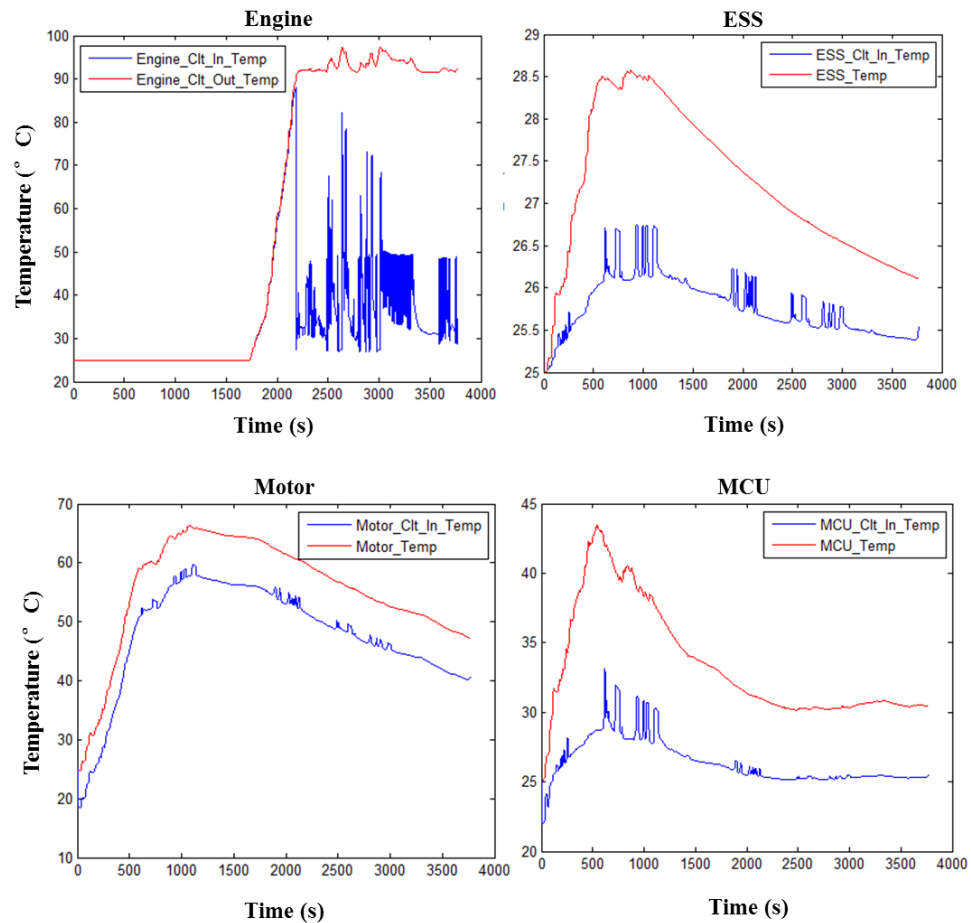


Figure 6-5. Thermal Performance under EcoCAR2 4-cycle Schedule

Figure 6-6 shows the temperature trace of powertrain components under the grade load condition. The vehicle switches from CD mode to CS mode at 1442 s. The ESS, engine and MCU temperatures are controlled well under their target temperature over the entire cycle.

However, the simulated peak temperature of motor during the severest condition is 131°C, which is greater than the target temperature 90°C but still below the demagnetization temperature 150°C. Noted that as defined in control algorithm of thermal manager, when motor temperature reach threshold, the coolant flow rate of MCU loop increases in response to motor temperature, independent of MCU temperature change. This explains the temperature decrease of MCU when motor temperature rises to 80°C.

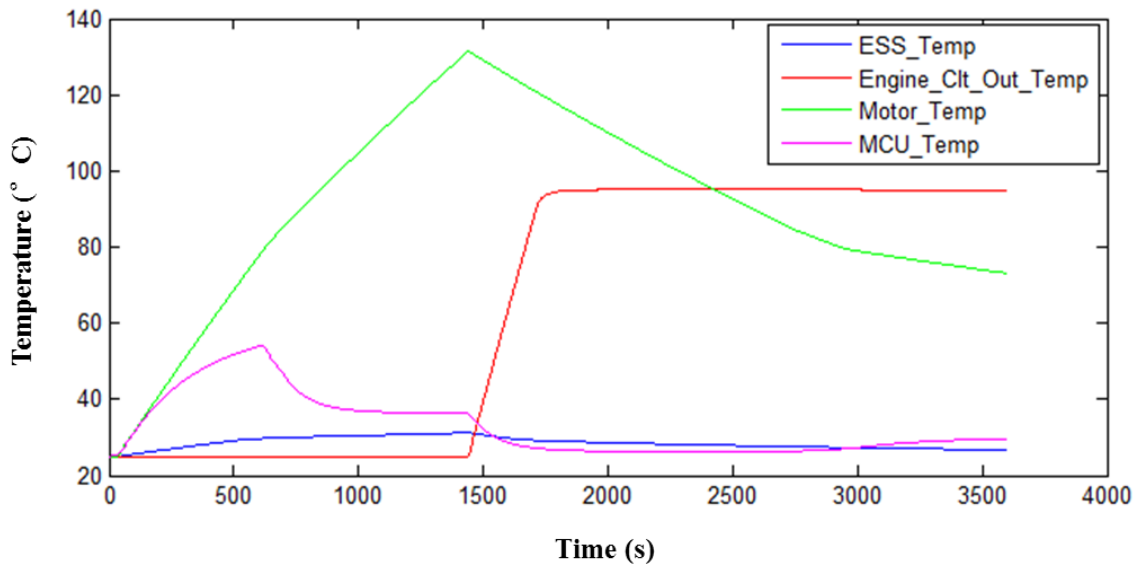


Figure 6-6. Thermal Performance under grade load condition

6.3 Conclusion

The vehicle thermal management system model including component thermal plant model and thermal manager has been developed for WSU parallel HEV. The model was verified through 2 selected test drive cycles to demonstrate the robustness of the designed cooling system under severe condition. The comparison between simulated peak temperature and target temperature is listed in Table 6-2. ESS, engine and MCU temperatures are maintained under target temperature as expected. Even through the temperature of electric motor is out of the

optimal range during the severest grade load condition, it is still within safety range. This could be mitigated if switch to higher capacity oil-to-water heat exchanger.

Table 6-2. Peak Temperature under Grade Load Condition

| Component | Control Target Temperature (°C) | Peak Temperature under Grade Load Condition (°C) |
|-----------------------|----------------------------------------|---------------------------------------------------------|
| Engine | 120 | 95 |
| ESS | 40 | 31 |
| Electric Motor | 90 | 131 |
| MCU | 70 | 54 |

However, it is observed that the temperature of MCU reaches a lower temperature than expected. Because MCU and motor share the same cooling loop, and motor has larger heat capacity than MCU, causing the MCU to cool down together with the motor unnecessarily. This result suggests the combined motor/MCU cooling loop is good for reducing cost, but perhaps at the cost of energy efficiency.

The proposed model is capable of providing fairly accurate results and fast simulation speed, making it ideal for system-level simulation and real-time vehicle controls. The model can be easily adjusted for more comprehensive studies, by varying component specifications, as well as temperature threshold and pump speed settings. The project team plans to compare and find tune the simulation results against experimental measurements to be conducted in a few months. The model can be a useful tool for design and assessment of thermal management systems for HEV.

6.4 Future Work

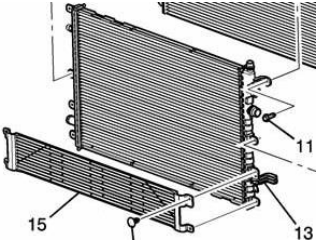
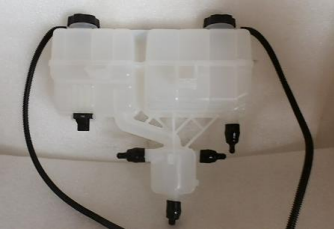


Although the results presented here have demonstrated the usefulness of the framework of HEV thermal modeling and controls, it could be further developed in a number of ways:




The plant model of AC system is not addressed in this study. The heat transfer rate of phase-change refrigerant flowing in evaporator, chiller and condenser can be obtained through engineering approach or performance map. The modeling of cabin climate also needs to be developed based on the heat transferred from the ambient to the cabin, considering radiation, convection and conduction. The AC system model and cabin climate model are needed for a more efficient design of thermal controls.




There have been many attempts to model the oil-to-water heat exchanger with heat transfer equations, regarding it as annular-finned tube heat exchanger. There are 2 major challenges due to the unique geometry. For the external oil flow, since the correlations of annular-finned tube are mainly developed for air fluid, the correlation is not in its best accuracy because Reynolds number is out of range. The oil flow requires smaller Re_D range for its low velocity and high viscosity. For the internal water flow, because the channel is in annulus, even though a correction factor is approximated to calculate heat transfer coefficient, the more accurate way would be to treat the partitions between 2 adjacent channels as fins. Finally the map-based model is used in this study due to the difficulties to apply desired correlations for both external and internal flow. However, it is encouraged to continue the model development based on the previous work if time allows.

Lastly, the thermal model only had been tested through visual environment. Real-world data from VIL testing can be used to further optimize the variables and improve algorithms that were implemented.

APPENDIX A. A COMPLETE COOLING COMPONENTS LIST

| | |
|--------------------------------------------------------------------------------------|--------------------------------|
| Chevy Volt Dual-partition Radiator | |
|  | |
| Dimension | 690mm×16mm×418mm |
| Part Number | 20925997 |
| Chevy Volt Dual-partition Coolant Fluid Reservoir | |
|  | |
| Part Number | 22940436 |
| ESS Chill Plate | |
|  | |
| Dimension | 874×612×19.05 mm |
| Material | Aluminum plate and copper pipe |
| Copper tube ID | 10.2 mm |
| Copper tube OD | 12.7 mm |
| Di-electric layer thickness | 0.5 mm |
| ESS Water Pump | |
|  | |

| | |
|-------------------------------------------------------------------------------------|-------------------------------------------------------------------------------------|
| Part Name | Pierburg CWA 100 |
| Flow Rate Range | 0-40LPM |
| Operating point | 30LPM @ 0.85 bar |
| Voltage | 12.5V |
| Temperature Range | -40 °C -140°C |
| ESS Electric 2-way Coolant Valve | |
|  | |
| Voltage | 12V |
| Motor Feed Pump | |
|  | |
| Part Name | Mocal Micro Oil Scavenge/Circulation Pump 17-530M |
| Rating | Flow 1-2 GPM / 30 psi |
| Temperature | Maximum 350°F |
| Dimensions | 6.5" x 3.75" x 2.75" |
| Weight | 4.5 lbs. |
| Voltage | 12 V |
| URL | http://97.74.32.155/files/pump.pdf |
| Motor Evacuation Pump | |
|  | |
| Part Name | Mocal Heavy Duty Oil Scavenge/Circulation Pump 17-530SL |
| Rating | 1-3 GPM / 50 psi |
| Temperature | Maximum 350°F |
| Dimensions | 6.2" x 4.1" x 4.0" |
| Weight | 6.2 lbs. |

| | |
|------------------------------------------------------------------------------------------------------------------|---------------------------------------------------------------------------------------------------------------------------------------------------------------------|
| Voltage | 12 V |
| URL | http://97.74.32.155/files/pump.pdf |
| <p>Motor Oil Filter</p>  | |
| Part Name | Monster Mesh 8300 Series |
| Housing Length | 4.03'' |
| Housing Diameter | 2.460'' |
| Mesh | 45 micron |
| Weight | 10.88 Ounces |
| Port | 12AN male flare |
| URL | http://www.kinsler.com/handbook163.html |
| <p>Motor 1-way Check Valve</p>  | |
| Part Name | Flapper check valves |
| Cracking Pressure | 0.5 psi |
| Port | 12 AN male inlet/outlet |
| URL | http://www.kinsler.com/handbook189.html |
| <p>Motor oil sump</p>  | |
| Part Name | OBX Oil Dry Sump Tank |
| Dimension | 11"x5" |
| Capacity | 2.5 QUARTS |
| Material | Aluminum |
| URL | http://www.racingpartdepot.com/servlet/the-794/OBX-ALUMINUM-OIL-DRY/Detail |
| <p>Oil-to-water Heat Exchanger</p> | |



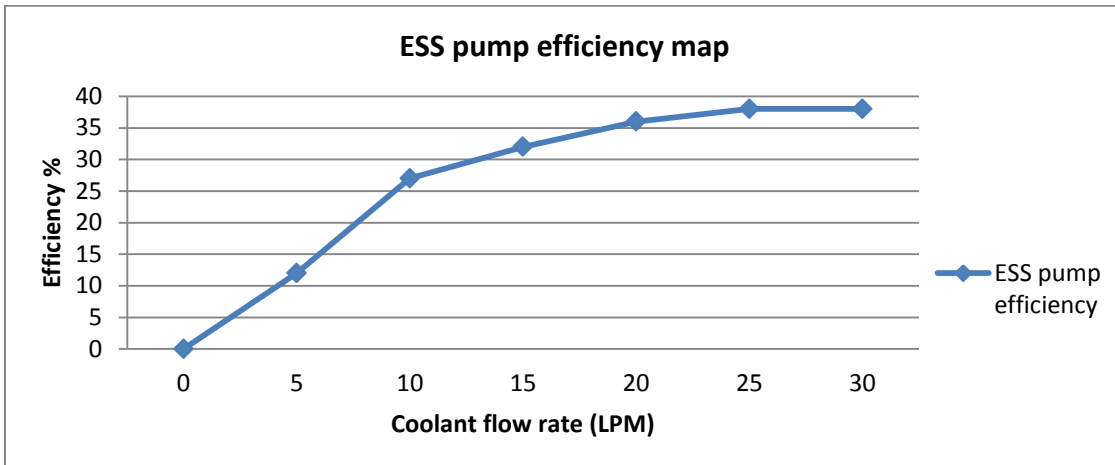
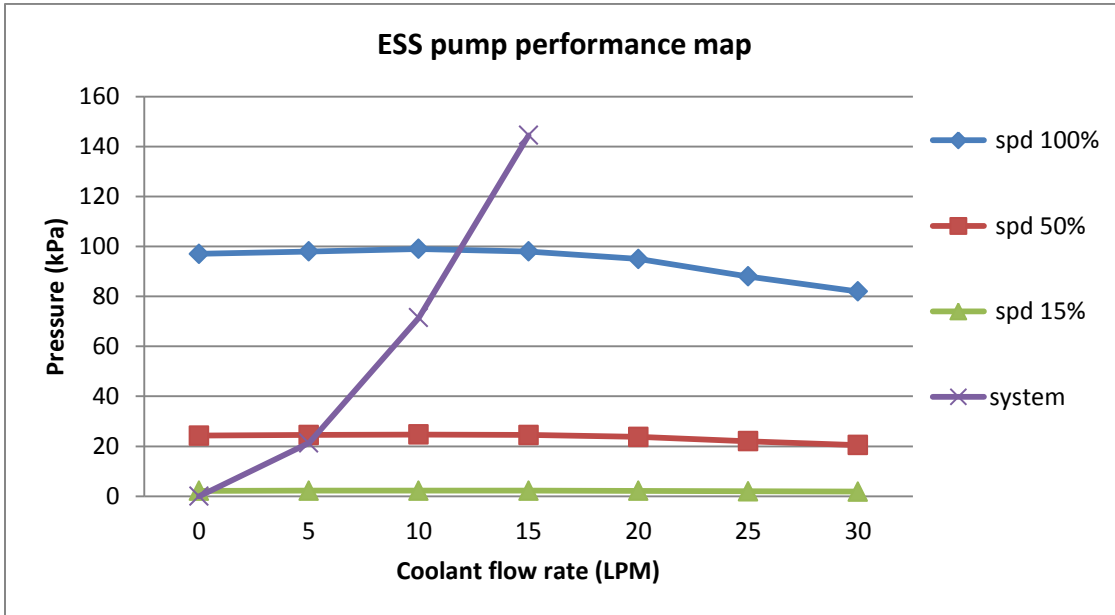
| | |
|-----------------|-------------------------------------------------------------------------------------------------|
| Part Name | Laminova A43-90A cooler with thread-on water connections |
| Diameter | 43mm |
| Length | 90mm |
| Oil port size | 12AN |
| Water port size | 16AN |
| URL | http://www.batinc.net/files/laminova.pdf |

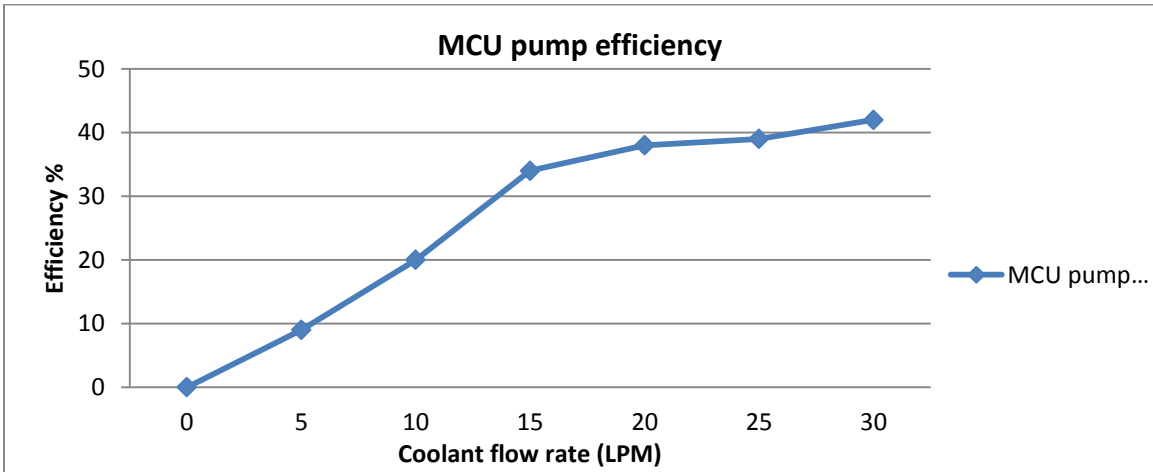
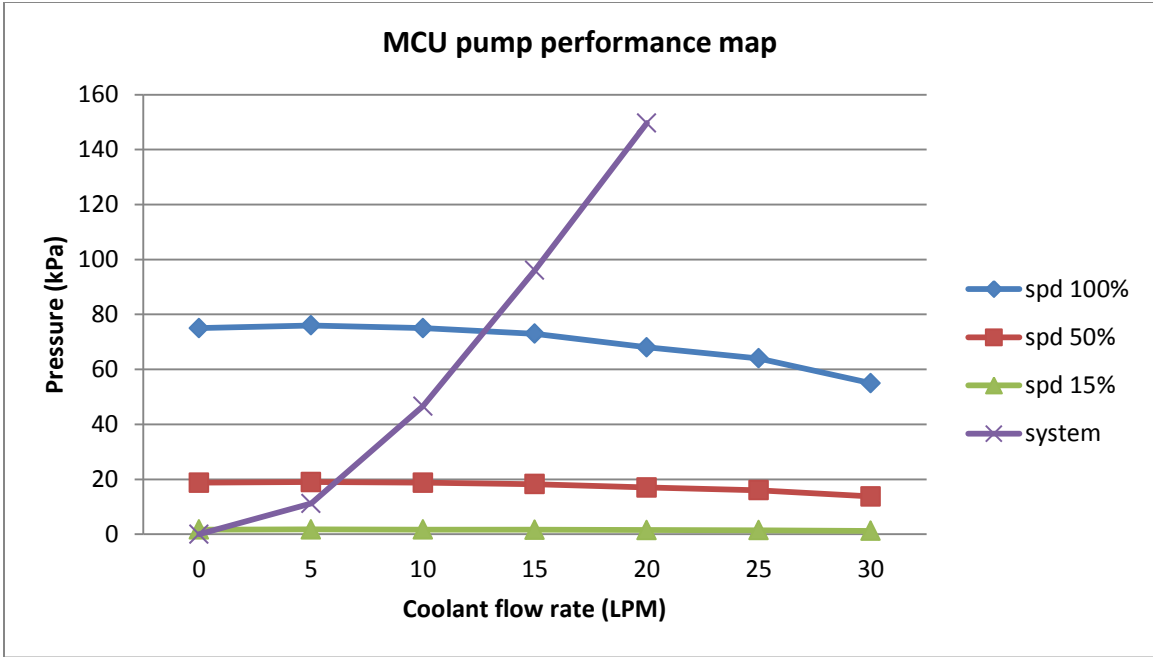
MCU Water Pump

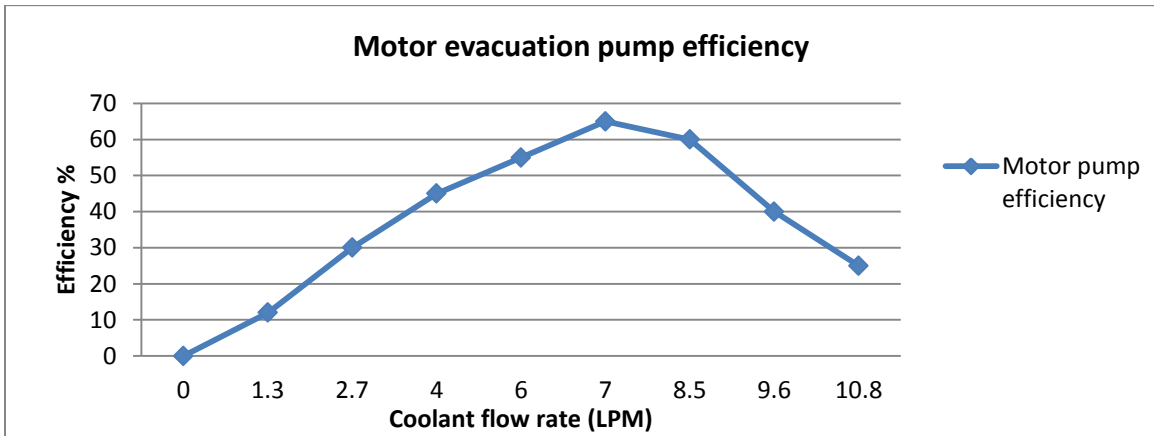
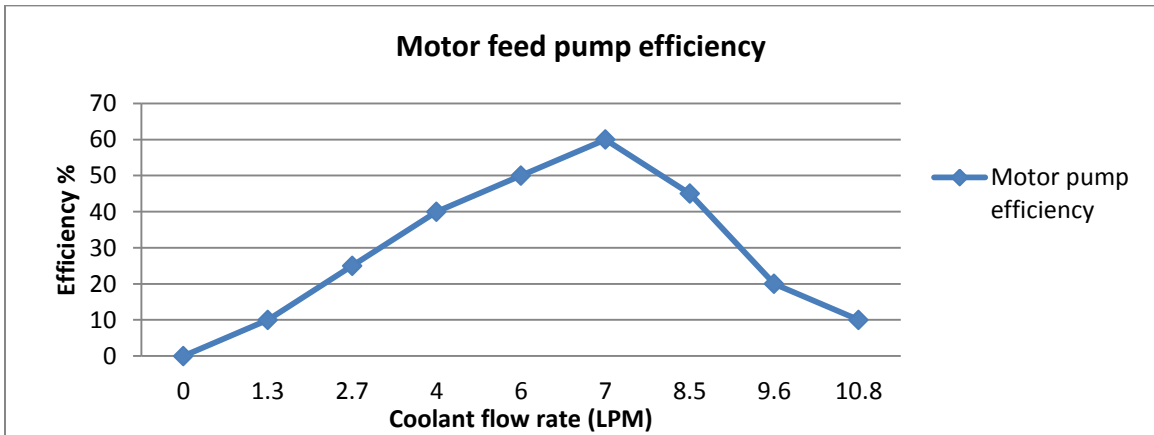
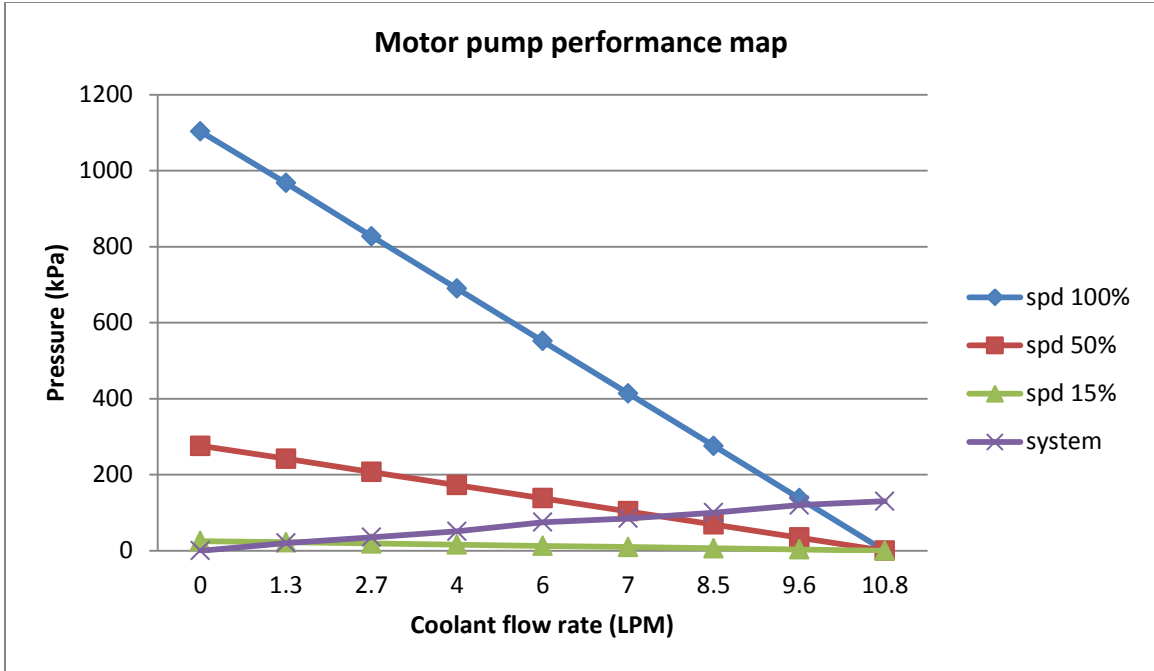


| | |
|-------------------|-----------------|
| Part Name | Pierburg CWA 50 |
| Operating point | 25LPM @ 0.6 bar |
| Voltage | 12.5V |
| Temperature Range | -40 °C -140°C |

APPENDIX B. PUMPS PERFORMANCE CHARACTERISTICS







REFERENCES

1. Regev, I.D., et al., *Parallel-Through-The-Road Plug-In Hybrid Vehicle Design Development Process*, 2012, SAE International.
2. Gao, D.W., C. Mi, and A. Emadi, *Modeling and simulation of electric and hybrid vehicles*. Proceedings of the IEEE, 2007. **95**(4): p. 729-745.
3. Park, S., *A Comprehensive Thermal Management System Model for Hybrid Electric Vehicles*, 2011, The University of Michigan.
4. Lang, G., F. Kitanoski, and C. Kussmann, *Principal Aspects and Simulation of a Hybrid Demonstrator Vehicle's Cooling System*, 2007, SAE International.
5. Pesaran, A.A., *Battery thermal models for hybrid vehicle simulations*. Journal of Power Sources, 2002. **110**(2): p. 377-382.
6. Pesaran, A.A., *Battery Thermal Management in EV and HEVs: Issues and Solutions*. Battery Man, 2001. **43**(5): p. 34-49.
7. Hu, X., et al., *A foster network thermal model for HEV/EV battery modeling*. Industry Applications, IEEE Transactions on, 2011. **47**(4): p. 1692-1699.
8. Saxena, A. and A. Leyland, *Analytical Modeling and Simulation of Auxiliary Cooling System of Hybrid Electric Vehicle for Improving System Performance*. Lubricating Oil. **2013**: p. 09-09.
9. Yoo, I.K., et al., *An engine coolant temperature model and application for cooling system diagnosis*. SAE transactions, 2000. **109**(3): p. 950-960.
10. Arici, O., J.H. Johnson, and A.J. Kulkarni, *The vehicle engine cooling system simulation part I—model development*. SAE, 1999: p. 01-0240.

11. Cortona, E. and C.H. Onder, *Engine thermal management with electric cooling pump*, 2000, SAE Technical Paper.
12. Jawad, B., K. Zellner, and C. Riedel, *Small engine cooling and the electric water pump*. Training, 2004. **2014**: p. 09-18.
13. Wagner, J.R., et al., *Coolant flow control strategies for automotive thermal management systems*. Training, 2002. **2013**: p. 11-12.
14. Kovent, I. and J. Ku, *Developing Modeling and Simulation Tools in Class to Prepare Engineering Students for the Automotive Industry*. SAE Technical Paper, 2014.
15. Markel, T., et al., *ADVISOR: a systems analysis tool for advanced vehicle modeling*. Journal of power sources, 2002. **110**(2): p. 255-266.
16. Lor, L., *Supervisory Controller Validation for a Plug-in Parallel-through-the-Road by Software-in-the-Loop Testing*. MS Thesis, Wayne State University, 2013.
17. Rutkowski, B., *EcoCar Battery Sub-System Design Specification Interface Control Document*. A123 Systems, 2009.
18. gm-volt.com, "*The Chevrolet Volt Cooling/Heating Systems Explained*" <http://gm-volt.com/2010/12/09/the-chevrolet-volt-coolingheating-systems-explained/>. 2010.
19. Boglietti, A., et al., *Evolution and modern approaches for thermal analysis of electrical machines*. Industrial Electronics, IEEE Transactions on, 2009. **56**(3): p. 871-882.
20. Ng, E., P. Johnson, and S. Watkins, *An analytical study on heat transfer performance of radiators with non-uniform airflow distribution*. Proceedings of the Institution of Mechanical Engineers, Part D: Journal of Automobile Engineering, 2005. **219**(12): p. 1451-1467.
21. Kays, W.M. and A.L. London, *Compact heat exchangers*. 1984.

22. Jung, D. and D. Assanis, *Numerical modeling of cross flow compact heat exchanger with louvered fins using thermal resistance concept*. SAE Paper, 2006: p. 01-0726.
23. Olsson, C.-O. and B. Sunden, *Heat transfer and pressure drop characteristics of ten radiator tubes*. International journal of heat and mass transfer, 1996. **39**(15): p. 3211-3220.
24. Oliet, C., et al., *Parametric studies on automotive radiators*. Applied thermal engineering, 2007. **27**(11): p. 2033-2043.
25. Gnielinski, V., *New equations for heat and mass-transfer in turbulent pipe and channel flow*. International Chemical Engineering, 1976. **16**(2): p. 359-368.
26. Sieder, E.N. and G.E. Tate, *Heat transfer and pressure drop of liquids in tubes*. Industrial & Engineering Chemistry, 1936. **28**(12): p. 1429-1435.
27. Quaiyum, M.A., *Experimental Investigation of Automatic Transmission Fluid (ATF) in an Air Cooled Minichannel Heat Exchanger*, 2012, MA Sc. Thesis, University of Windsor, Canada.
28. Waterloo, U.o., "*Fluid Properties Calculator*"
<http://www.mhtl.uwaterloo.ca/old/onlinetools/airprop/airprop.html>.

ABSTRACT**THERMAL AND COOLING SYSTEMS MODELING OF POWERTRAIN FOR A PLUG
-IN PARALLEL-THROUGH-THE ROAD HYBRID ELECTRIC VEHICLE**

by

MENGJIA CAO**May 2014****Advisors:** Dr. Jerry Ku**Major:** Electric-drive Vehicle Engineering**Degree:** Master of Science

Thermal modeling and control play an ever increasing role with hybrid electric vehicle (HEV) design and development for improving overall vehicle energy efficiency, and to account for additional thermal loading from electric powertrain components such as electric motor, motor controller and battery pack.

This thesis presents a complete development process for an efficient modeling approach with integrated control strategy for the thermal management of plug-in HEV in a parallel-through-the road (PTTR) architecture, adopted by Wayne State University Hybrid Warriors for their Department of Energy's EcoCAR2 Plugging in to the Future Competition.

The frameworks of this project include simulating the thermal behavior of major HEV powertrain components using system oriented models suitable for real-time vehicle operation. A comprehensive control algorithm is established in a Thermal Manager, as part of vehicle supervisory controller. Finally, the proposed model is tested through realistic driving conditions to demonstrate reliability.

AUTOBIOGRAPHICAL STATEMENT

As my career goal to engage in the emerging EV/PHEV engineering and development field, I decided to relocate across the sea to pursuit a MS degree in Electric-drive Vehicle Engineering at Wayne State University.

There are 2 major reasons why I believe EVE MS program is the best choice for me: first, EVE courses program is coupled with EcoCAR2 competition, it can provide invaluable hands-on experience and training. Second, staying at the capital of automotive industry means easier access to job market. Fortunately, the vision becomes true with 2 year's practice, hardworking and persistence. With knowledge of modeling/controls of hybrid system, skill of Matlab/Simulink, experience with CAN communication I gained through EcoCAR2 work, I finally land a career at Chrysler LLC as hybrid system engineer. Beyond that, the confidence and the friendship I earned throughout the process will continue to enrich the rest of my life.

It was a life-changing journey that contributed to my personal and academic growth. I look forward to the new opportunities and challenges that await me as new chapter begins.